US009791551B1

(12) **United States Patent**
Eshraghi et al.

(10) **Patent No.: US 9,791,551 B1**
(45) **Date of Patent: Oct. 17, 2017**

(54) **VEHICULAR RADAR SYSTEM WITH SELF-INTERFERENCE CANCELLATION**

(71) Applicant: **UHNDER, INC.**, Austin, TX (US)

(72) Inventors: **Aria Eshraghi**, Austin, TX (US); **Jean P. Bordes**, St. Charles, MO (US); **Curtis Davis**, St. Louis, MO (US); **Raghunath K. Rao**, Austin, TX (US); **Murtaza Ali**, Cedar Park, TX (US); **Paul W. Dent**, Pittsboro, NC (US)

(73) Assignee: **UHNDER, INC.**, Austin, TX (US)

(*) Notice: Subject to any disclaimer, the term of this patent is extended or adjusted under 35 U.S.C. 154(b) by 0 days.

(21) Appl. No.: **15/496,314**

(22) Filed: **Apr. 25, 2017**

Related U.S. Application Data

(63) Continuation-in-part of application No. 15/492,159, filed on Apr. 20, 2017.

(Continued)

(51) **Int. Cl.**
G01S 7/35 (2006.01)
G01S 13/93 (2006.01)
(Continued)

(52) **U.S. Cl.**
CPC ***G01S 7/354*** (2013.01); ***G01S 7/038*** (2013.01); ***G01S 7/4021*** (2013.01); ***G01S 13/931*** (2013.01); *G01S 7/292* (2013.01)

(58) **Field of Classification Search**
CPC G01S 7/038; G01S 7/292; G01S 7/2921; G01S 7/354; G01S 7/40; G01S 7/4021;
(Continued)

(56) **References Cited**

U.S. PATENT DOCUMENTS

1,882,128	A	10/1932	Fearing
3,374,478	A	3/1968	Blau

(Continued)

FOREIGN PATENT DOCUMENTS

EP	0725480	11/2011
EP	2821808	1/2015

(Continued)

OTHER PUBLICATIONS

Chambers et al., An article entitled "Real-Time Vehicle Mounted Multistatic Ground Penetrating Radar Imaging System for Buried Object Detection," Lawrence Livermore National Laboratory Reports (LLNL-TR-615452), Feb. 4, 2013; Retrieved from the Internet from https://e-reports-ext.llnl.gov/pdf/711892.pdf.

(Continued)

Primary Examiner — Peter M Bythrow
(74) *Attorney, Agent, or Firm* — Gardner, Linn, Burkhart & Flory

(57) **ABSTRACT**

A digital FMCW radar is described that simultaneously transmits and receives digitally frequency modulated signals using multiple transmitters and multiple receivers and associated antennas. Several sources of nearby spillover from transmitters to receivers that would otherwise degrade receiver performance are subtracted by a cancellation system in the analog radio frequency domain that adaptively synthesizes an analog subtraction signal based on residual spillover measured by a correlator operating in the receivers' digital signal processing domains and based on knowledge of the transmitted waveforms. The first adaptive cancellation system achieves a sufficient reduction of transmit-receive spillover to avoid receiver saturation or other non-linear effects, but is then added back in to the signal path in the digital domain after analog-to-digital conversion so that spillover cancellation can also operate in the digital signal

(Continued)

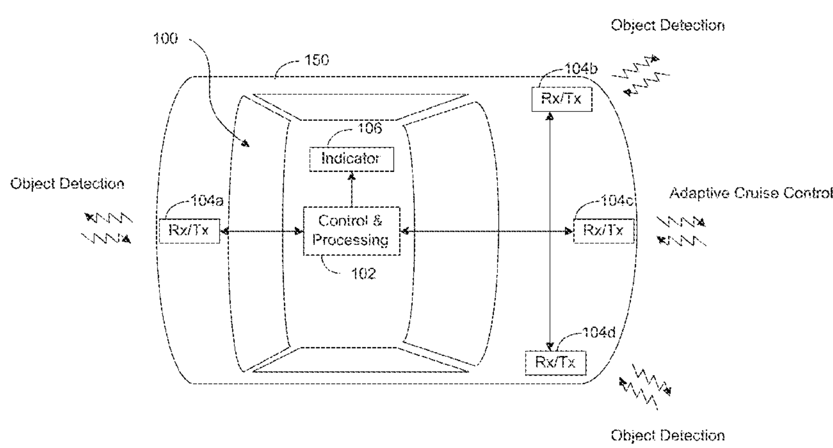

processing domain to remove deleterious spillover components.

20 Claims, 46 Drawing Sheets

Related U.S. Application Data

(60) Provisional application No. 62/327,003, filed on Apr. 25, 2016, provisional application No. 62/469,165, filed on Mar. 9, 2017, provisional application No. 62/382,857, filed on Sep. 2, 2016.

(51) **Int. Cl.**
G01S 7/40 (2006.01)
G01S 7/03 (2006.01)
G01S 7/292 (2006.01)

(58) **Field of Classification Search**
CPC G01S 7/4052; G01S 2007/406–2007/4073; G01S 13/284; G01S 13/325; G01S 13/34; G01S 13/931
See application file for complete search history.

(56) **References Cited**

U.S. PATENT DOCUMENTS

3,735,395	A	5/1973	Ross	
3,750,169	A	7/1973	Strenglein	
3,896,434	A	7/1975	Sirven	
4,939,685	A	7/1990	Feintuch	
5,034,906	A	7/1991	Chang	
5,151,702	A	9/1992	Urkowitz	
5,175,710	A	12/1992	Hutson	
5,218,619	A	6/1993	Dent	
5,280,288	A	1/1994	Sherry et al.	
5,341,141	A	8/1994	Frazier et al.	
5,345,470	A	9/1994	Alexander	
5,657,023	A *	8/1997	Lewis	H01Q 3/2652 342/174
5,892,477	A	4/1999	Wehling	
5,917,430	A	6/1999	Greneker, III et al.	
5,920,285	A *	7/1999	Benjamin	G01S 13/89 342/22
5,931,893	A	8/1999	Dent et al.	
5,959,571	A	9/1999	Aoyagi et al.	
6,067,314	A	5/2000	Azuma	
6,069,581	A	5/2000	Bell et al.	
6,121,918	A	9/2000	Tullsson	
6,184,829	B1	2/2001	Stilp	
6,191,726	B1	2/2001	Tullsson	
6,288,672	B1	9/2001	Asano et al.	
6,347,264	B2	2/2002	Nicosia et al.	
6,400,308	B1	6/2002	Bell et al.	
6,411,250	B1	6/2002	Oswald et al.	
6,417,796	B1	7/2002	Bowlds	
6,614,387	B1	9/2003	Deadman	
6,624,784	B1	9/2003	Yamaguchi	
6,674,908	B1	1/2004	Aronov	
6,714,956	B1	3/2004	Liu et al.	
6,747,595	B2 *	6/2004	Hirabe	H01Q 3/267 342/174
6,768,391	B1	7/2004	Dent et al.	
7,119,739	B1	10/2006	Struckman	
7,289,058	B2	10/2007	Shima	
7,299,251	B2	11/2007	Skidmore et al.	
7,338,450	B2	3/2008	Kristoffersen et al.	
7,545,310	B2	6/2009	Matsuoka	
7,545,321	B2	6/2009	Kawasaki	
7,564,400	B2	7/2009	Fukuda	
7,609,198	B2	10/2009	Chang	
7,663,533	B2	2/2010	Toennesen	
7,728,762	B2 *	6/2010	Sakamoto	G01S 7/35 342/109
7,791,528	B2	9/2010	Klotzbuecher	
7,847,731	B2	12/2010	Wiesbeck	
8,019,352	B2	9/2011	Rappaport et al.	
8,049,663	B2	11/2011	Frank et al.	
8,154,436	B2	4/2012	Szajnowski	
8,330,650	B2	12/2012	Goldman	
8,390,507	B2	3/2013	Wintermantel	
8,532,159	B2	9/2013	Kagawa et al.	
8,547,988	B2	10/2013	Hadani et al.	
8,686,894	B2	4/2014	Fukuda et al.	
8,694,306	B1	4/2014	Short et al.	
9,121,943	B2	9/2015	Stirling-Gallacher et al.	
9,239,378	B2	1/2016	Kishigami et al.	
9,239,379	B2	1/2016	Burgio et al.	
9,282,945	B2	3/2016	Smith et al.	
9,335,402	B2 *	5/2016	Maeno	G01S 7/2813
9,541,639	B2	1/2017	Searcy et al.	
9,568,600	B2	2/2017	Alland	
9,575,160	B1	2/2017	Davis et al.	
9,599,702	B1	3/2017	Bordes et al.	
2002/0004692	A1	1/2002	Nicosia et al.	
2002/0075178	A1	6/2002	Woodington et al.	
2002/0155811	A1	10/2002	Prismantas	
2003/0058166	A1	3/2003	Hirabe	
2003/0235244	A1	12/2003	Pessoa et al.	
2004/0012516	A1	1/2004	Schiffmann	
2004/0015529	A1	1/2004	Tanrikulu et al.	
2004/0066323	A1	4/2004	Richter	
2004/0138802	A1	7/2004	Kuragaki et al.	
2005/0069162	A1	3/2005	Haykin	
2005/0201457	A1	9/2005	Allred et al.	
2005/0225476	A1	10/2005	Hoetzel et al.	
2006/0036353	A1	2/2006	Wintermantel	
2006/0109170	A1	5/2006	Voigtlaender et al.	
2006/0109931	A1	5/2006	Asai	
2006/0114324	A1	6/2006	Farmer et al.	
2006/0181448	A1	8/2006	Natsume et al.	
2006/0262007	A1	11/2006	Bonthron	
2007/0018884	A1	1/2007	Adams	
2007/0018886	A1	1/2007	Watanabe et al.	
2007/0109175	A1	5/2007	Fukuda	
2007/0132633	A1	6/2007	Uchino	
2007/0152870	A1	7/2007	Woodington et al.	
2007/0152871	A1	7/2007	Puglia	
2007/0152872	A1	7/2007	Woodington	
2007/0164896	A1	7/2007	Suzuki et al.	
2007/0182623	A1	8/2007	Zeng	
2007/0188373	A1	8/2007	Shirakawa et al.	
2007/0200747	A1	8/2007	Okai	
2008/0208472	A1	8/2008	Morcom	
2009/0015459	A1	1/2009	Mahler et al.	
2009/0015464	A1	1/2009	Fukuda	
2009/0079617	A1	3/2009	Shirakawa et al.	
2009/0121918	A1 *	5/2009	Shirai	G01S 7/023 342/159
2009/0212998	A1	8/2009	Szajnowski	
2009/0237293	A1	9/2009	Sakuma	
2009/0295623	A1	12/2009	Falk	
2010/0116365	A1	5/2010	McCarty	
2010/0156690	A1	6/2010	Kim et al.	
2010/0198513	A1	8/2010	Zeng et al.	
2011/0006944	A1	1/2011	Goldman	
2011/0187600	A1	8/2011	Landt	
2011/0196568	A1	8/2011	Nickolaou	
2011/0279307	A1	11/2011	Song	
2011/0285576	A1	11/2011	Lynam	
2011/0291874	A1	12/2011	De Mersseman	
2011/0292971	A1	12/2011	Hadani et al.	
2012/0001791	A1 *	1/2012	Wintermantel	G01S 7/023 342/109
2012/0112957	A1	5/2012	Nguyen et al.	
2012/0257643	A1	10/2012	Wu et al.	
2013/0016761	A1	1/2013	Nentwig	
2013/0027240	A1	1/2013	Chowdhury	
2013/0069818	A1	3/2013	Shirakawa et al.	
2013/0102254	A1 *	4/2013	Cyzs	H04B 1/126 455/63.1

(56) **References Cited**

U.S. PATENT DOCUMENTS

2013/0113653	A1	5/2013	Kishigami et al.	
2013/0135140	A1*	5/2013	Kishigami	G01S 7/282 342/189
2013/0169485	A1	7/2013	Lynch	
2013/0176154	A1	7/2013	Bonaccio et al.	
2013/0229301	A1	9/2013	Kanamoto	
2013/0244710	A1	9/2013	Nguyen et al.	
2013/0314271	A1	11/2013	Braswell et al.	
2014/0028491	A1*	1/2014	Ferguson	G01S 7/023 342/122
2014/0035774	A1	2/2014	Khlifi	
2014/0085128	A1	3/2014	Kishigami et al.	
2014/0111372	A1	4/2014	Wu	
2014/0159948	A1*	6/2014	Ishimori	G01S 7/41 342/200
2014/0220903	A1	8/2014	Schulz et al.	
2014/0253345	A1	9/2014	Breed	
2014/0348253	A1	11/2014	Mobasher et al.	
2015/0035662	A1	2/2015	Bowers et al.	
2015/0061922	A1	3/2015	Kishigami	
2015/0198709	A1	7/2015	Inoue	
2015/0204966	A1	7/2015	Kishigami	
2015/0226848	A1	8/2015	Park	
2015/0234045	A1	8/2015	Rosenblum	
2015/0247924	A1	9/2015	Kishigami	
2015/0301172	A1	10/2015	Ossowska	
2015/0323660	A1	11/2015	Hampikian	
2016/0003939	A1	1/2016	Stainvas et al.	
2016/0018511	A1	1/2016	Nayyar et al.	
2016/0041260	A1*	2/2016	Cao	G01S 7/282 342/129
2016/0061935	A1	3/2016	McCloskey et al.	
2016/0084941	A1	3/2016	Arage	
2016/0084943	A1	3/2016	Arage	
2016/0139254	A1	5/2016	Wittenberg	
2016/0238694	A1*	8/2016	Kishigami	G01S 7/023
2017/0023661	A1	1/2017	Richert	

FOREIGN PATENT DOCUMENTS

FR	2751086	1/1998
WO	WO2015175078	11/2015
WO	WO2015185058	12/2015
WO	WO2016011407	1/2016
WO	WO2016030656	3/2016

OTHER PUBLICATIONS

Fraser, “Design and simulation of a coded sequence ground penetrating radar,” In: Diss. University of British Columbia, Dec. 3, 2015.

Zhou et al., “Linear extractors for extracting randomness from noisy sources,” In: Information Theory Proceedings (ISIT), 2011 IEEE International Symposium on Oct. 3, 2011.

* cited by examiner

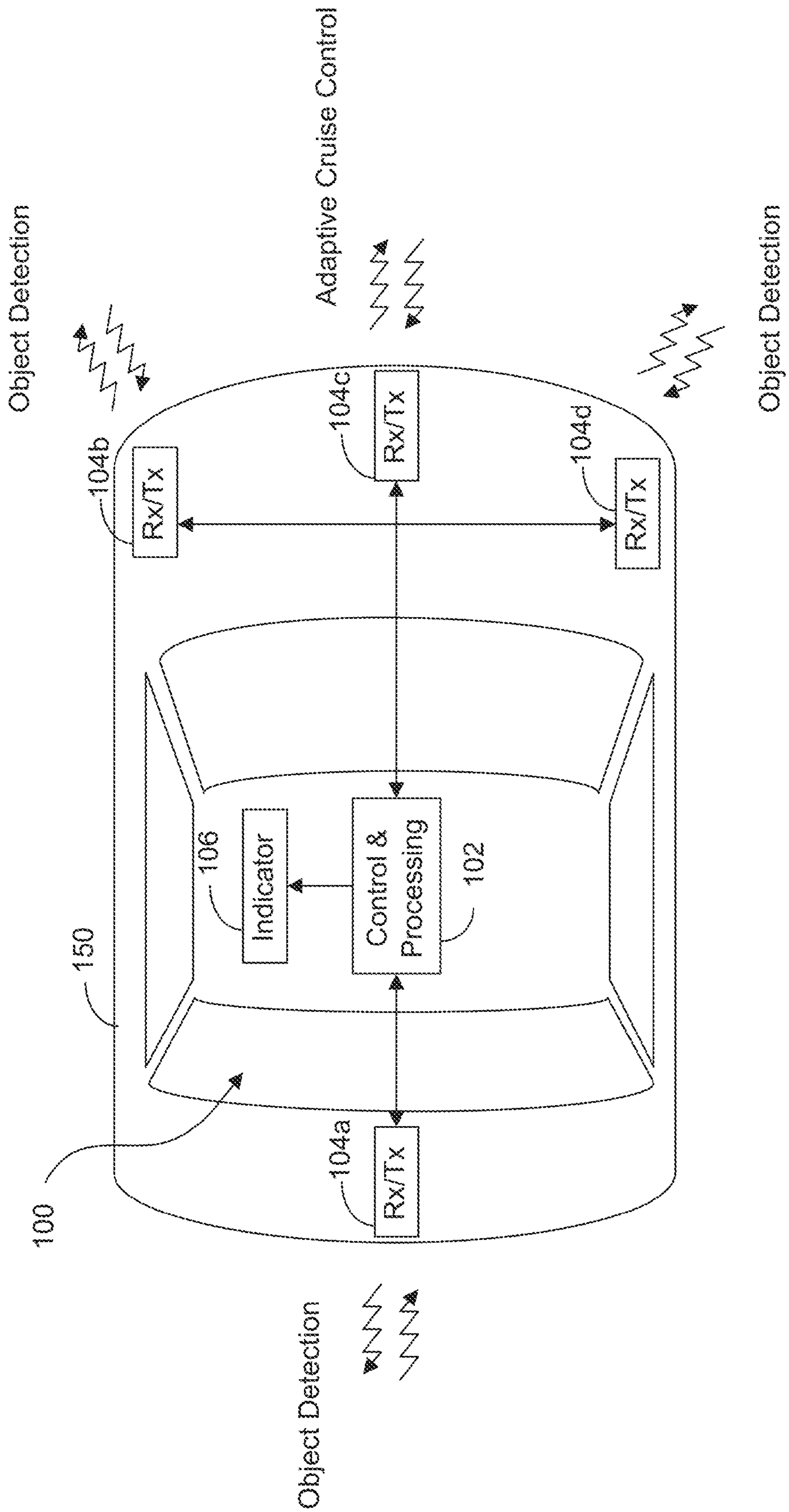

Adaptive Cruise Control
Object Detection
Object Detection
Object Detection
Rx/Tx
104a
Rx/Tx
104b
Rx/Tx
104c
Rx/Tx
104d
Control & Processing
102
Indicator
106
150
100

FIG. 1

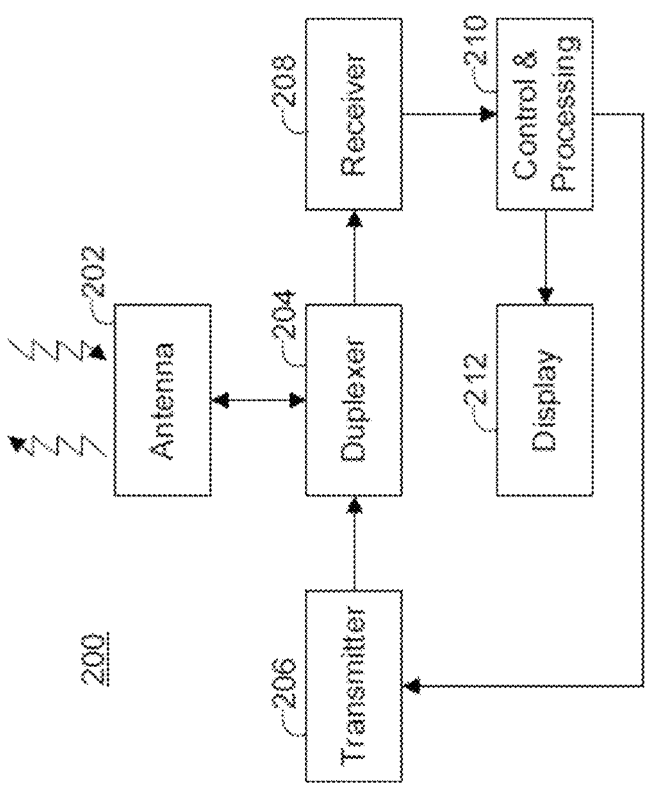
200
Antenna
202
Duplexer
204
Transmitter
206
Receiver
208
Control & Processing
210
Display
212

FIG. 2A

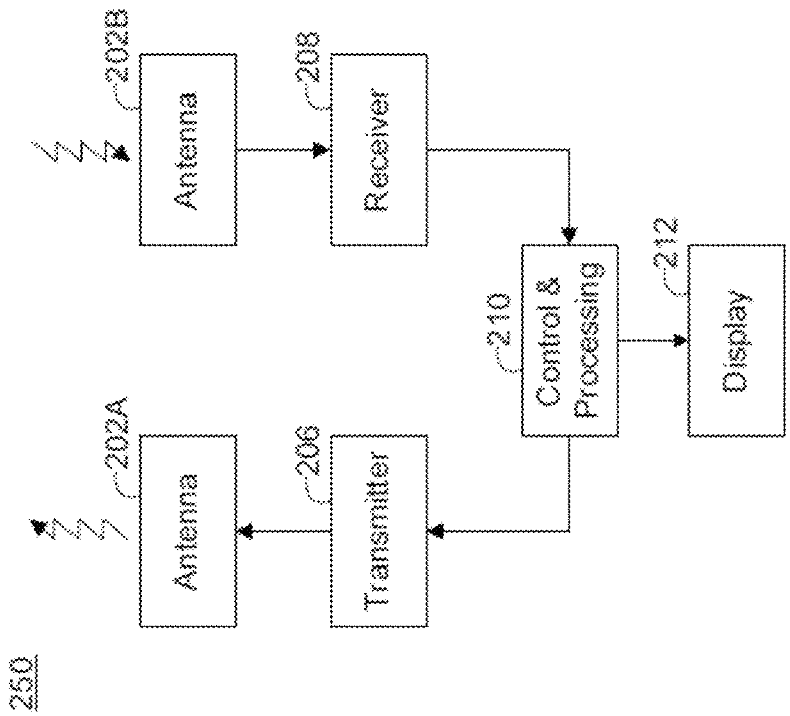
250
Antenna
202A
Antenna
202B
Transmitter
206
Receiver
208
Control & Processing
210
Display
212

FIG. 2B

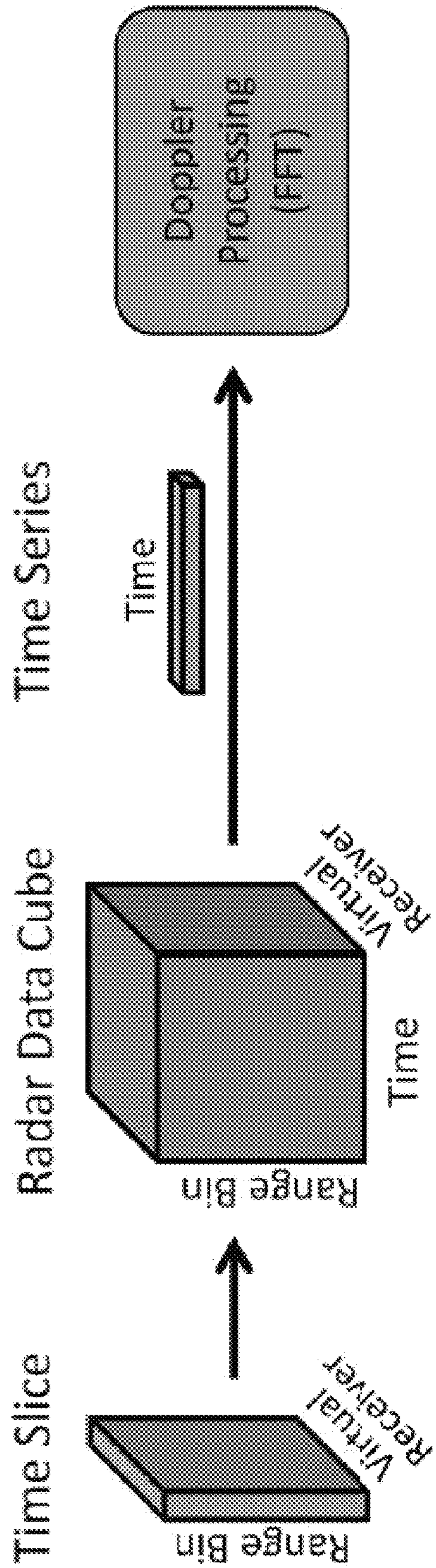
Time Slice
Range Bin
Virtual Receiver
Radar Data Cube
Range Bin
Time
Virtual Receiver
Time Series
Time
Doppler Processing (FFT)

FIG. 3

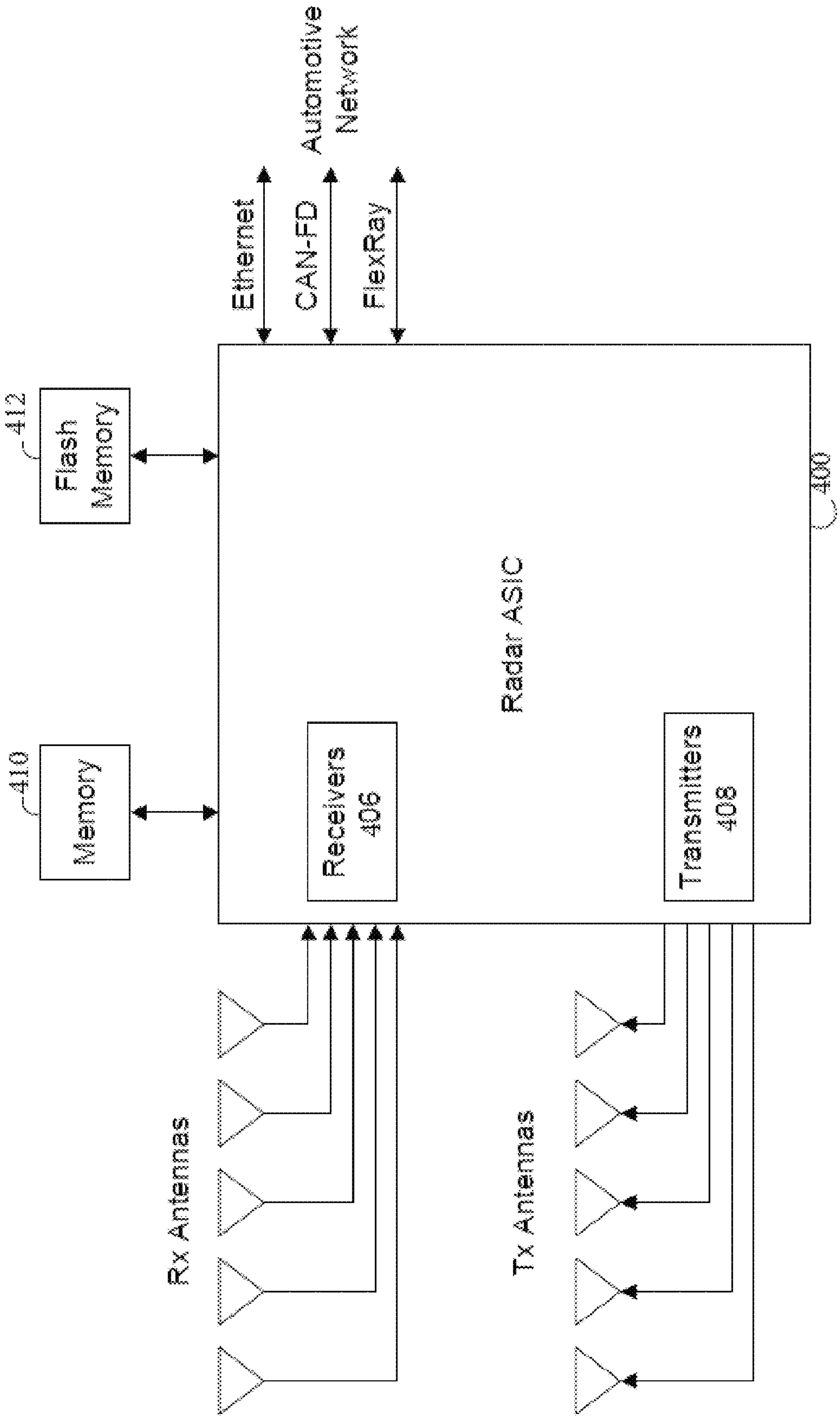
Automotive Network
Ethernet
CAN-FD
FlexRay
412
Flash Memory
410
Memory
Radar ASIC
400
Receivers 406
Transmitters 408
Rx Antennas
Tx Antennas

FIG. 4

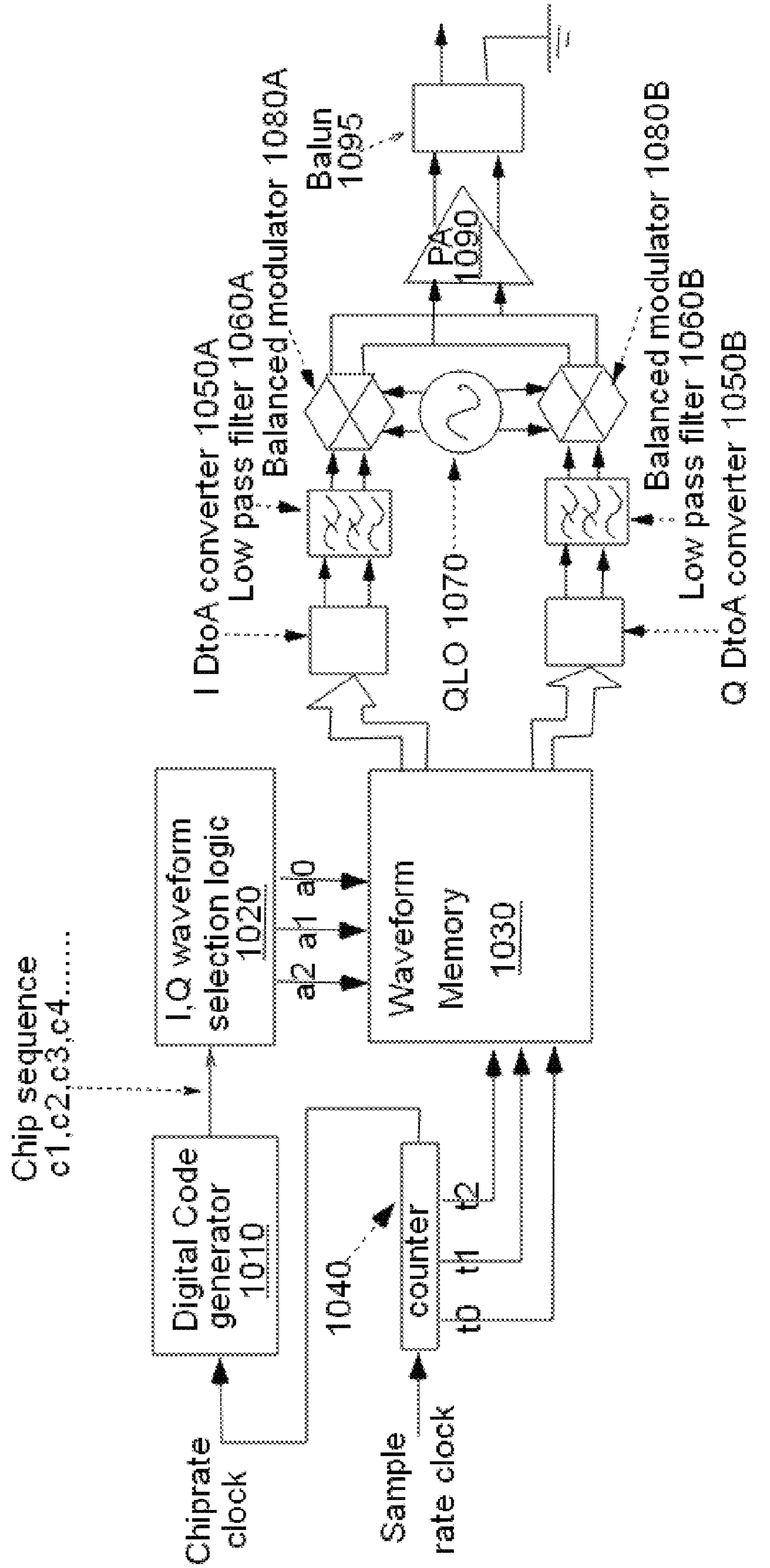

FIGURE 5: Transmitter Architecture for implementing the invention

FIG. 5

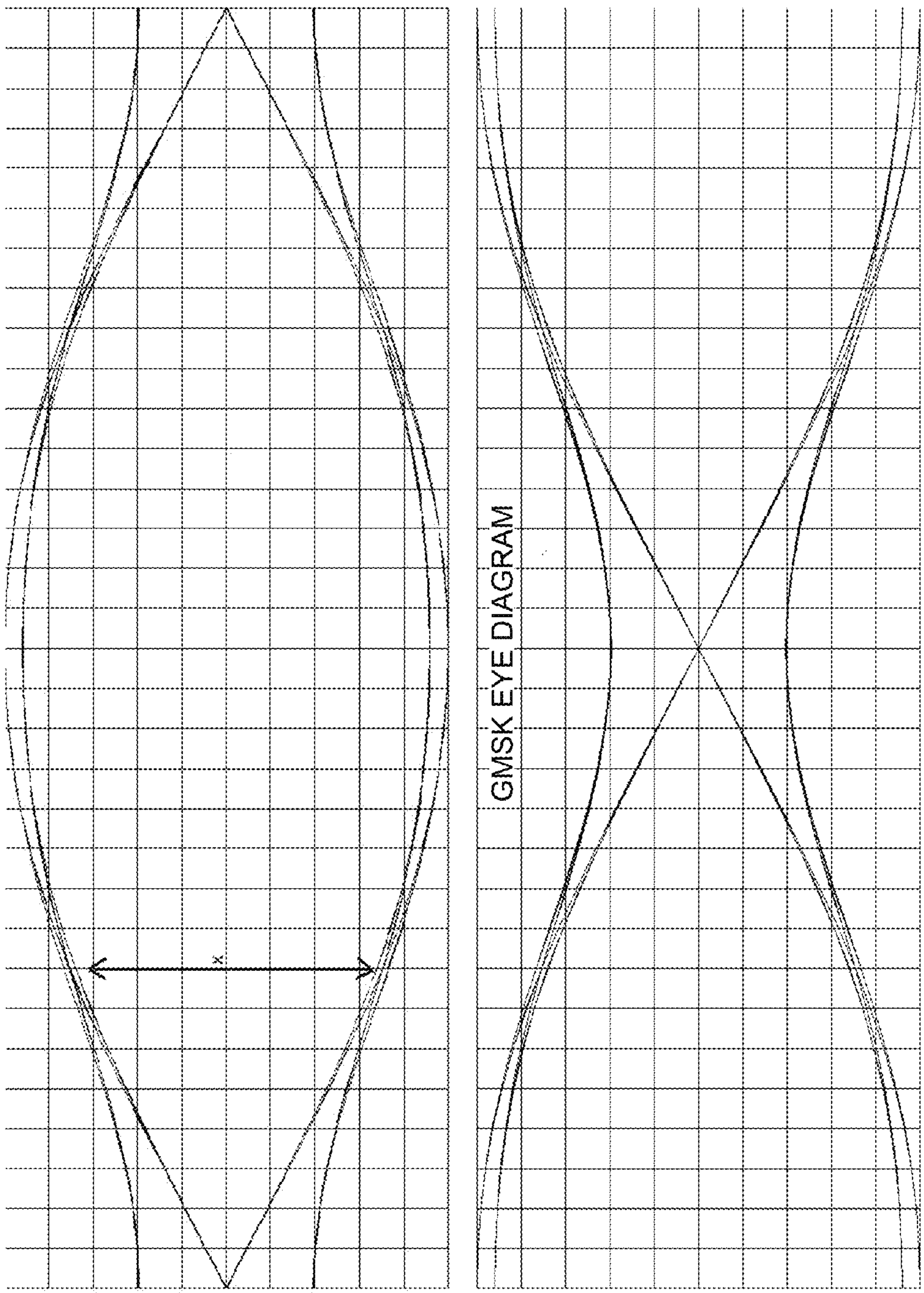

I,Q Eye Diagram for GMSK with a Gaussian BT = 0.3

FIG. 6

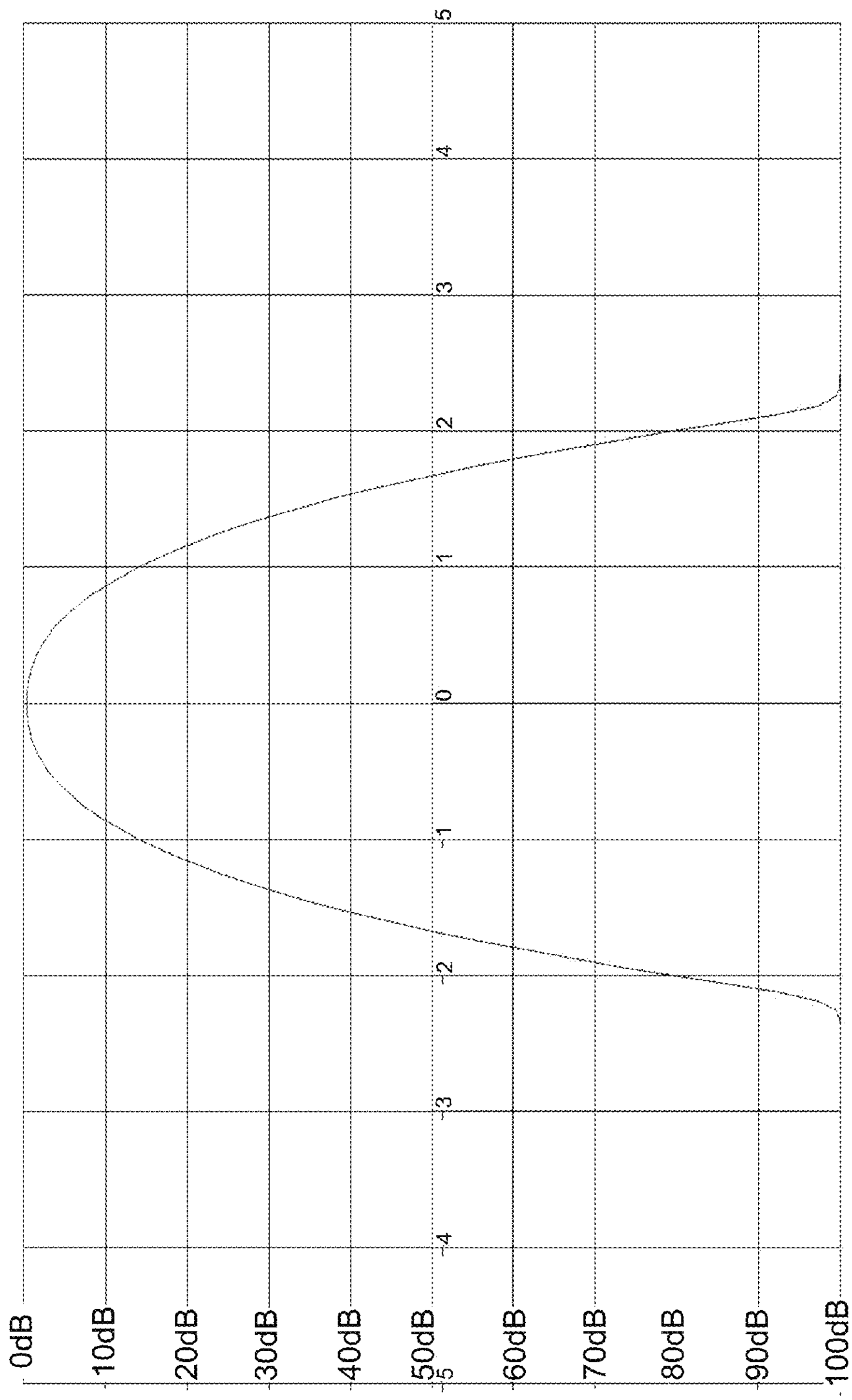

Correlation of the transmitted signal with the transmitted code

FIG. 7

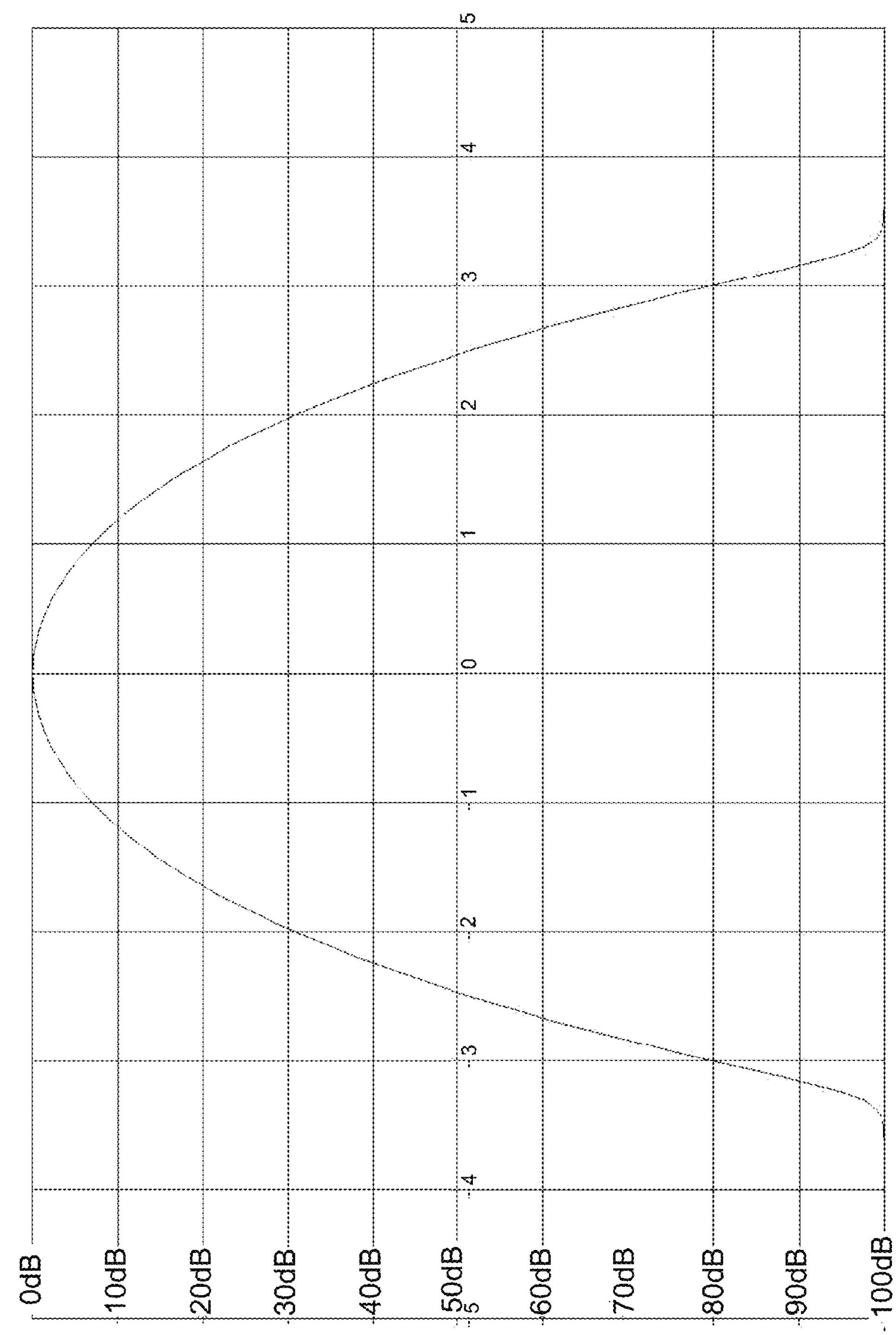

Autocorrelation function for GMSK with BT=0.3

FIG. 8

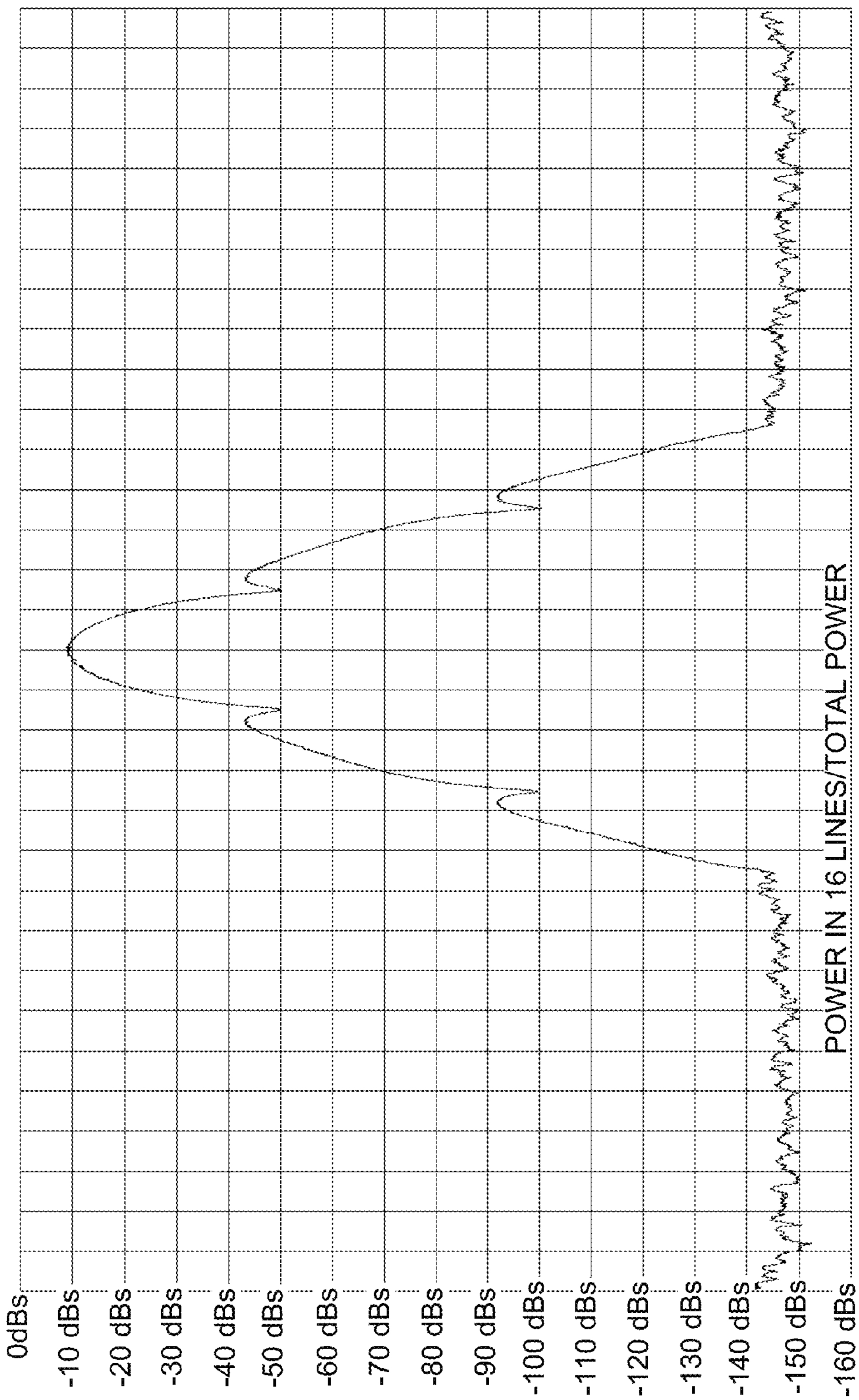

Power spectrum of GMSK with BT=0.3

FIG. 9

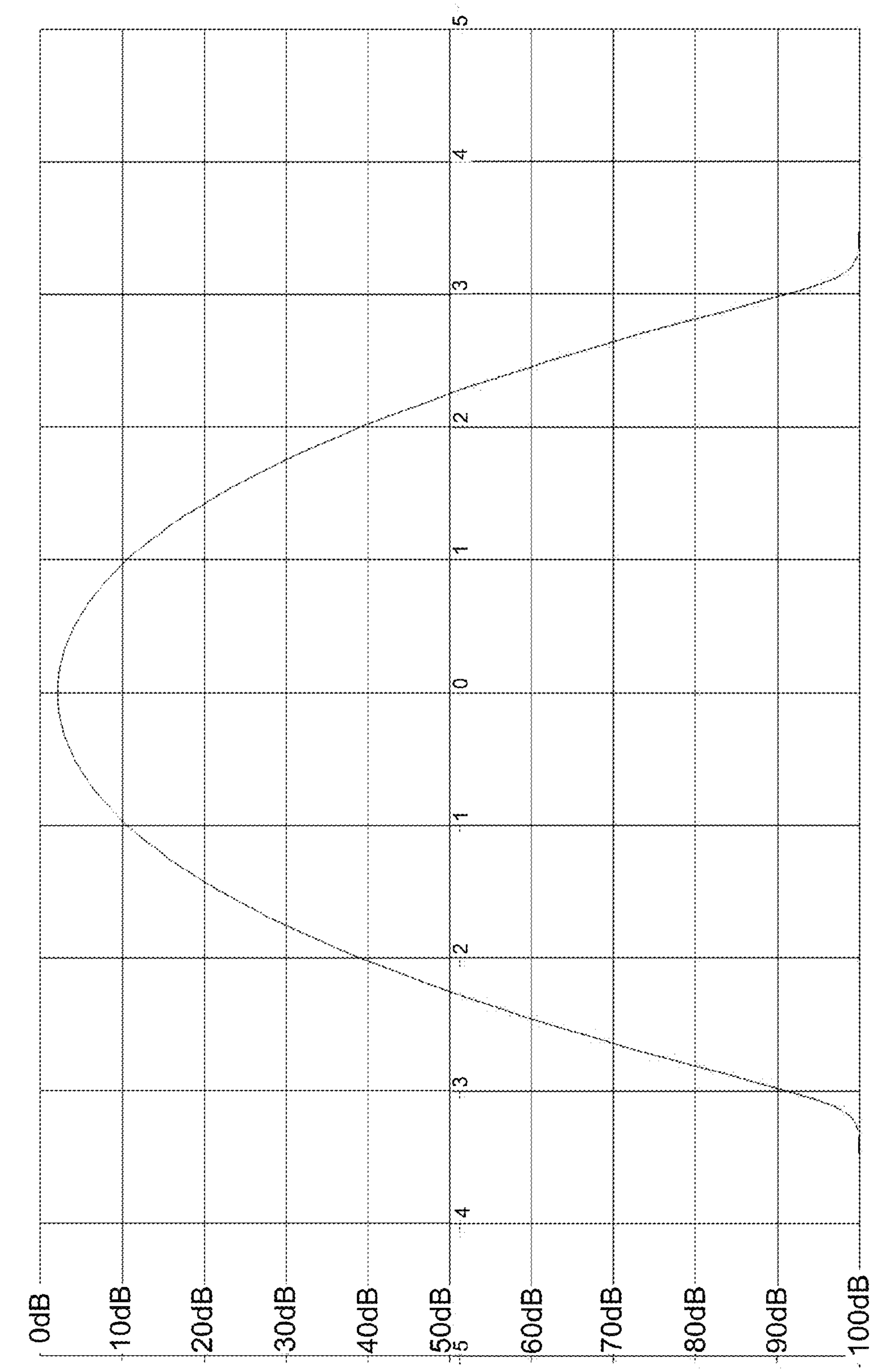

Correlation sidelobes for Gaussian receiver filter; with BT=0.3

FIG. 10

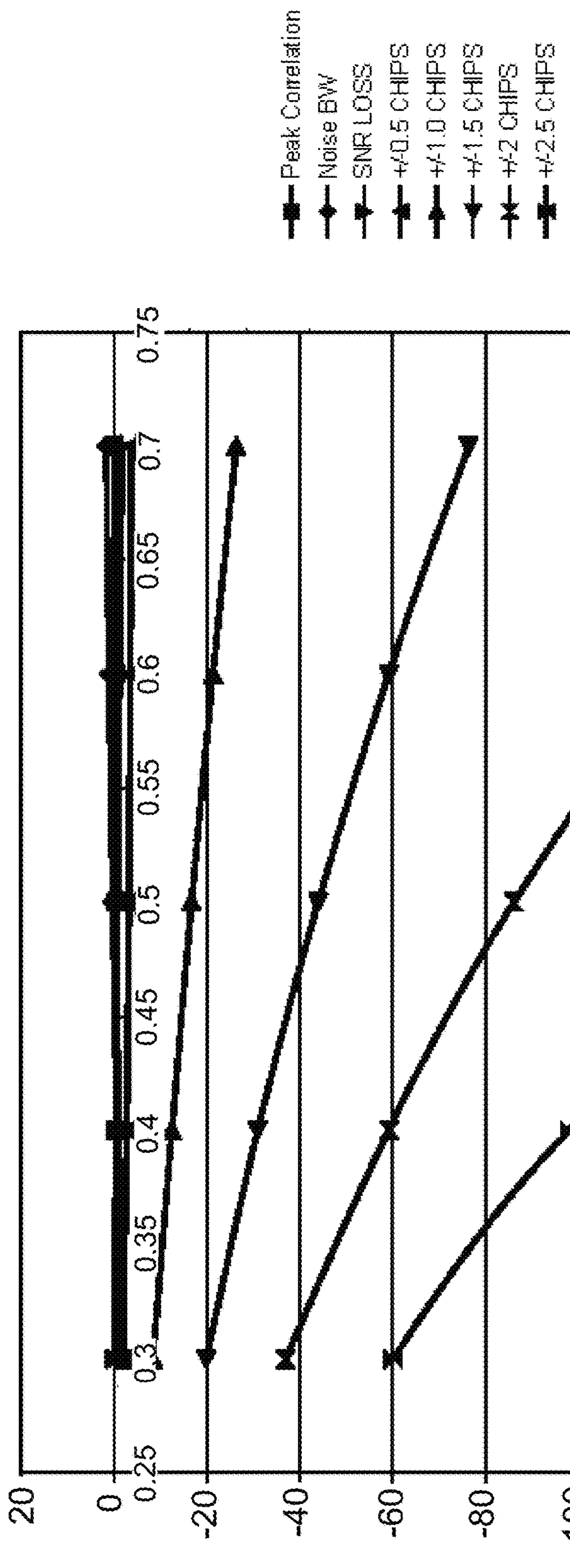

Variation of the indicated parameters in dB v. Receiver filter BT

FIG. 11

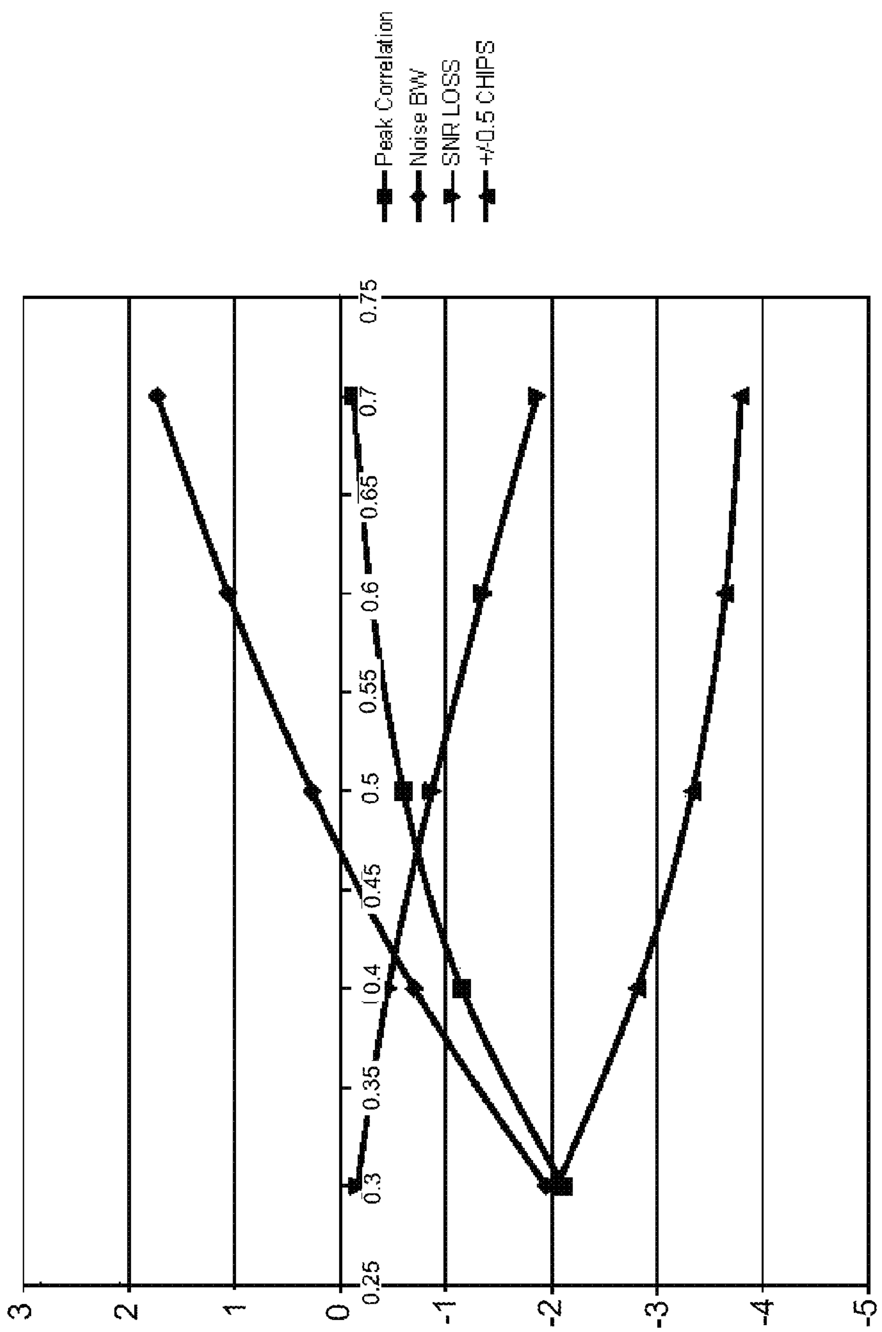

Parameter variation with receiver BT on a finer dB scale

FIG. 12

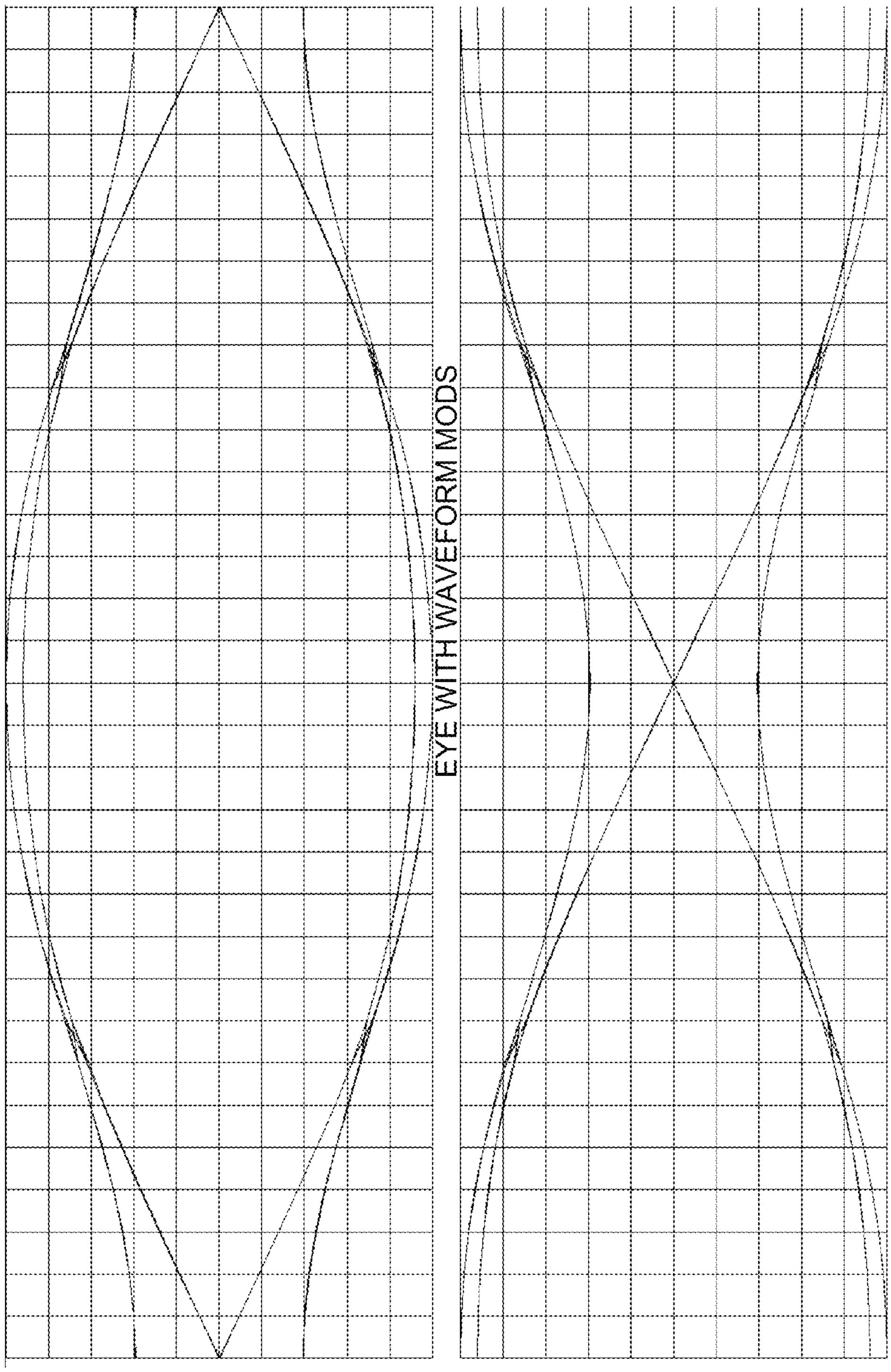

GMSK (BT=0.3) constrained to depend on only 3 successive chips

FIG. 13

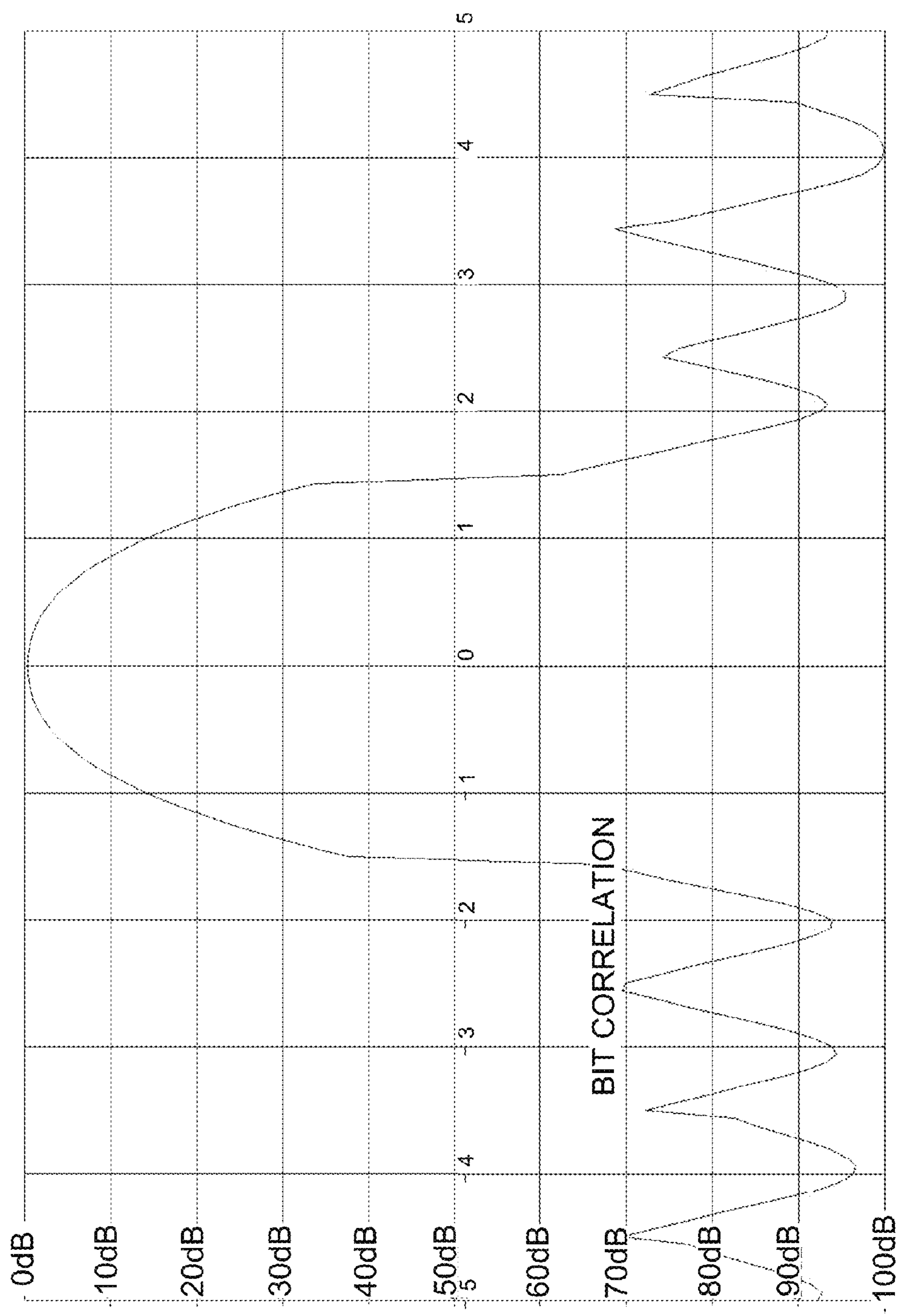

Correlation function of the waveform of figure 13

FIG. 14

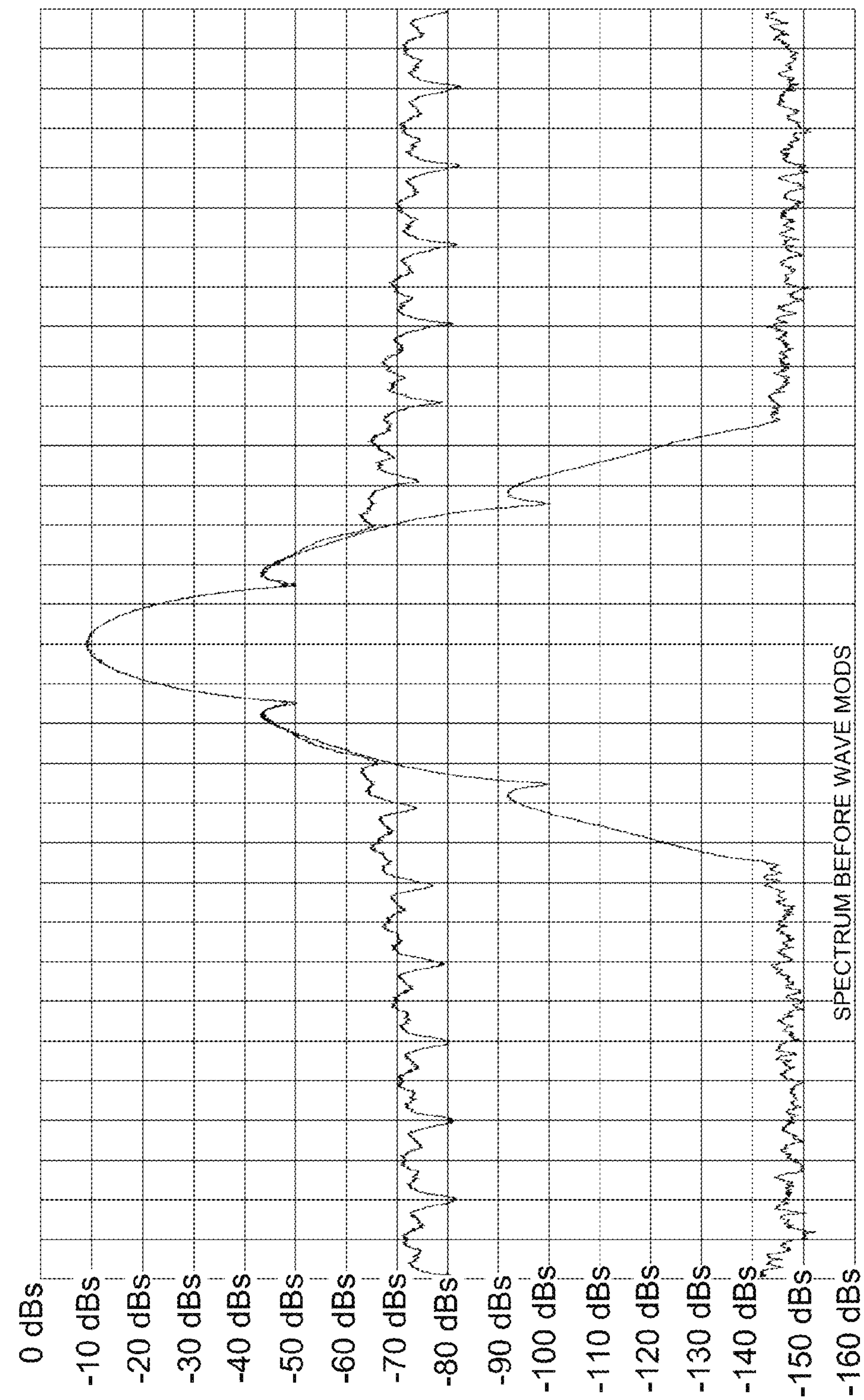

Comparison of the spectrum of the waveforms of 6 and 13

FIG. 15

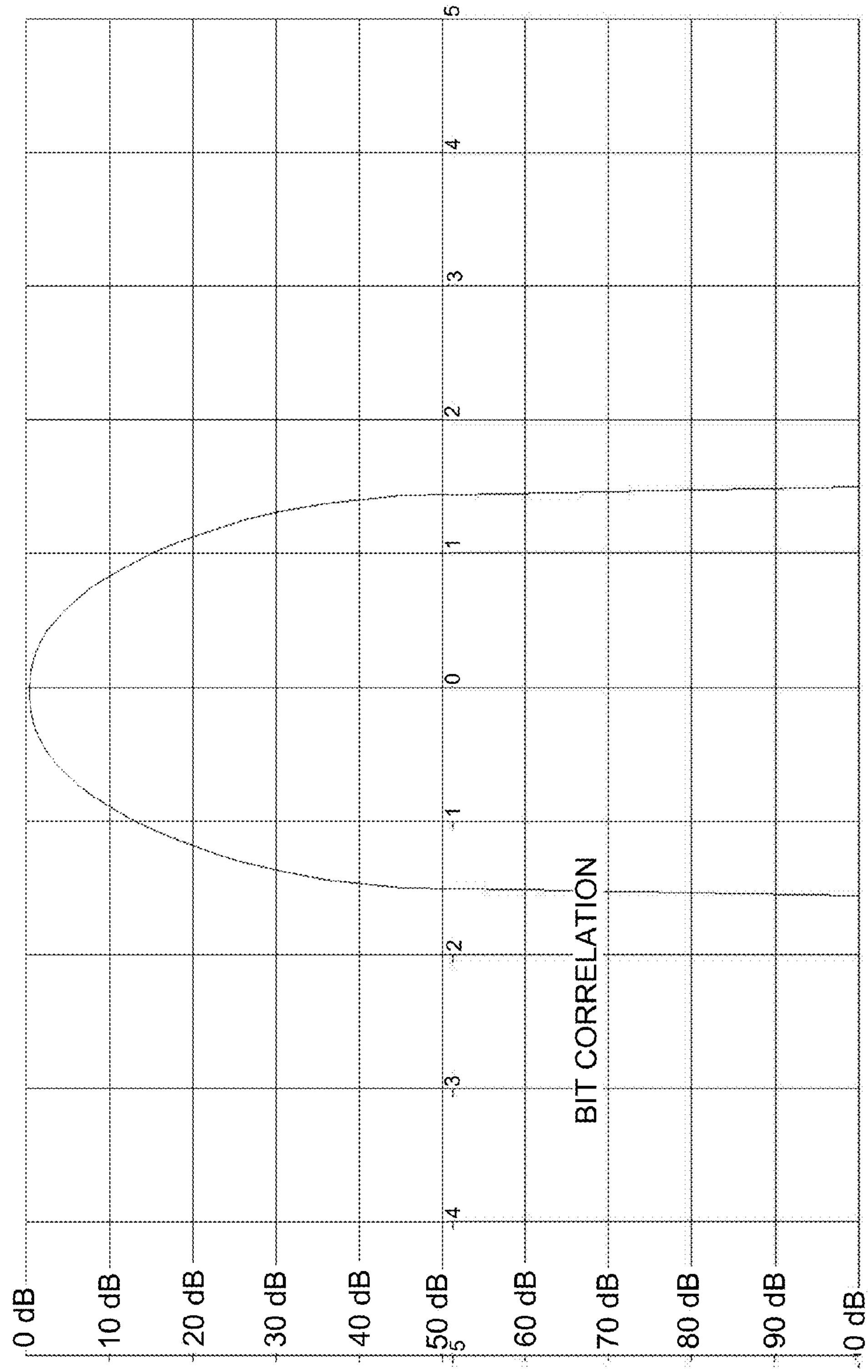

Correlation of the handcrafted waveform of figure 17

FIG. 16

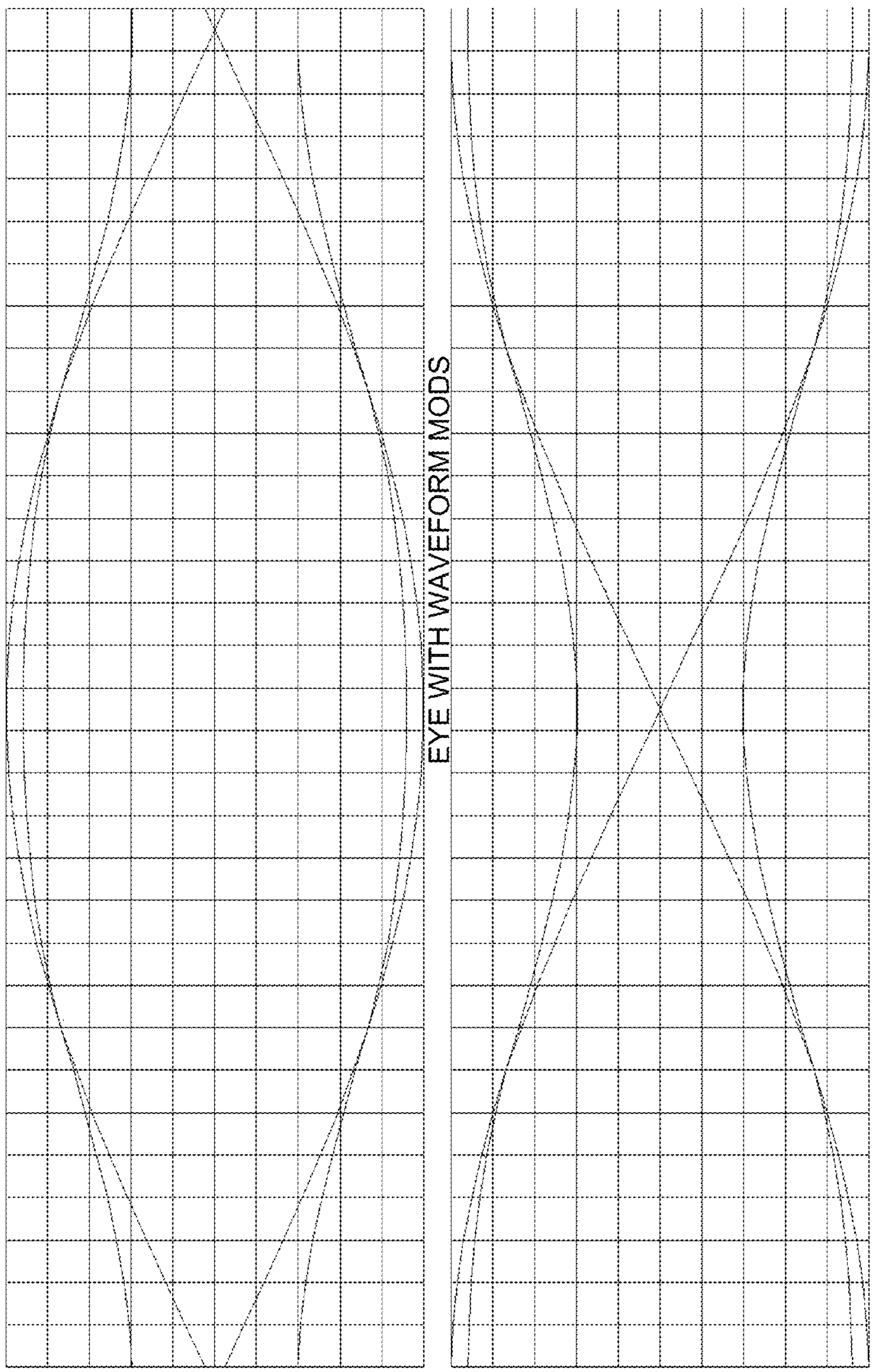

Eye diagram after waveform handcrafting

FIG. 17

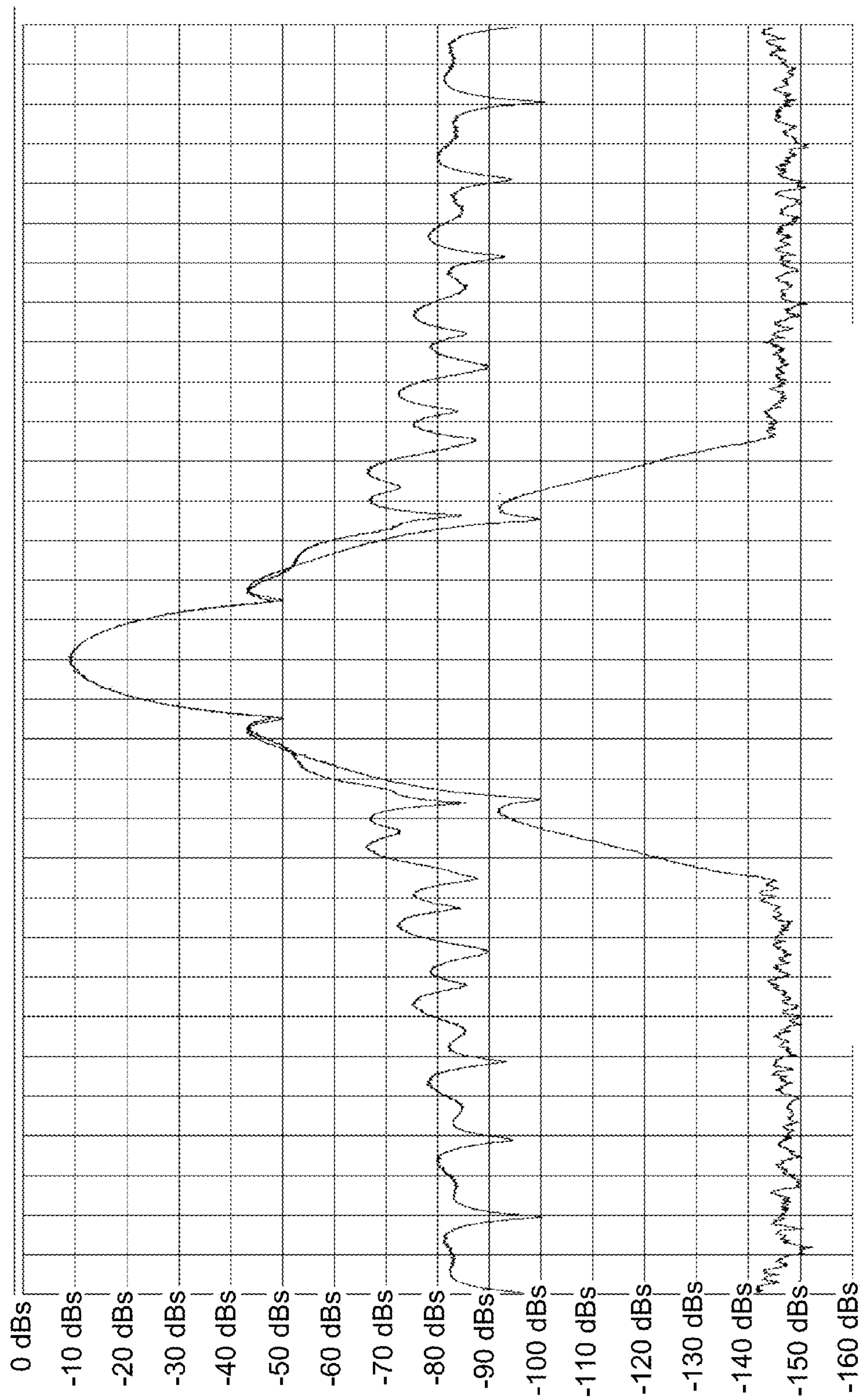

Improved spectrum of the handcrafted waveform of figure 17

FIG. 18

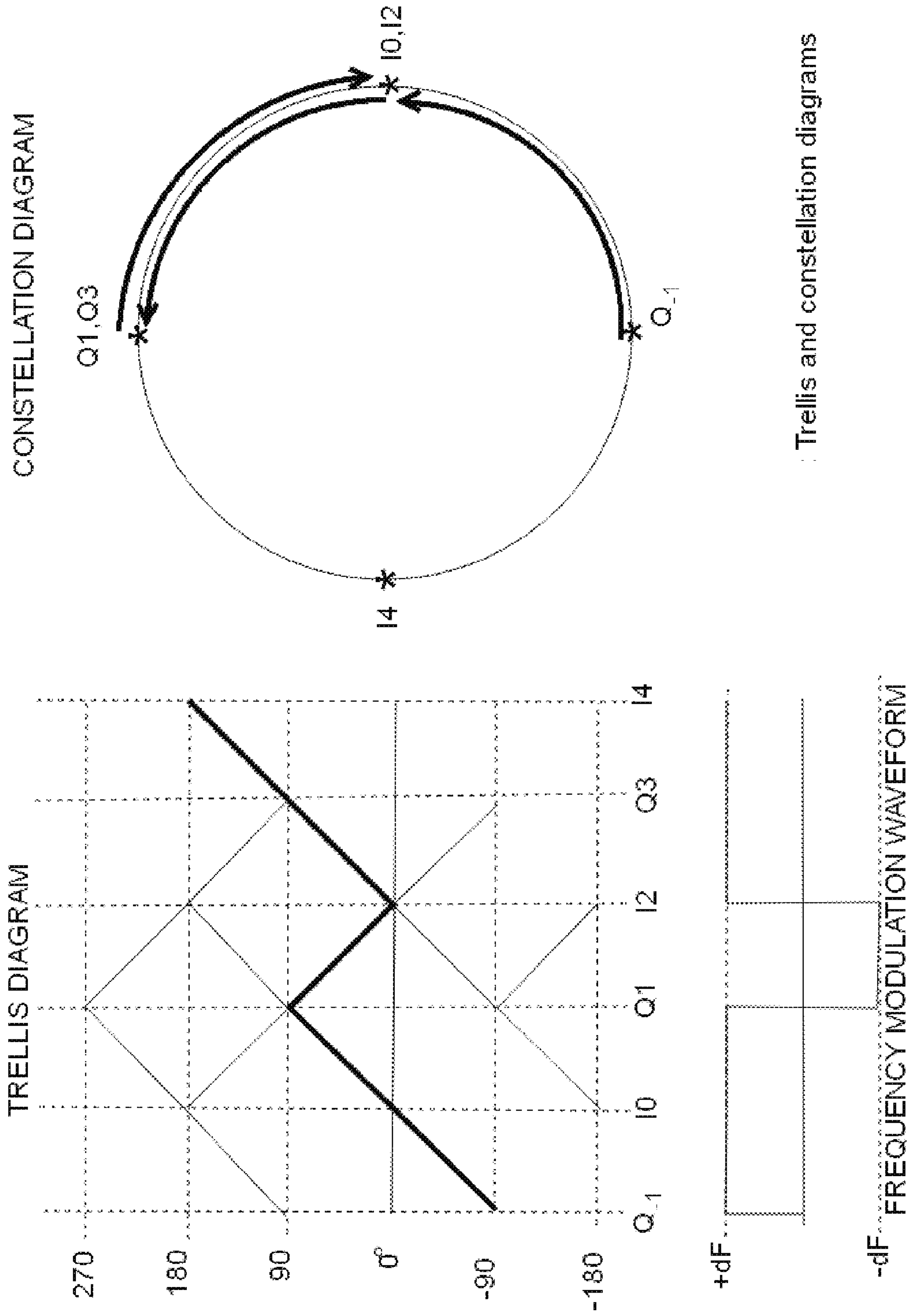
TRELLIS DIAGRAM
270
180
90
0°
-90
-180
Q_{-1}
I0
Q1
I2
Q3
I4
+dF
-dF
FREQUENCY MODULATION WAVEFORM
CONSTELLATION DIAGRAM
Q1,Q3
I0,I2
Q_{-1}
I4
Trellis and constellation diagrams

FIG. 19

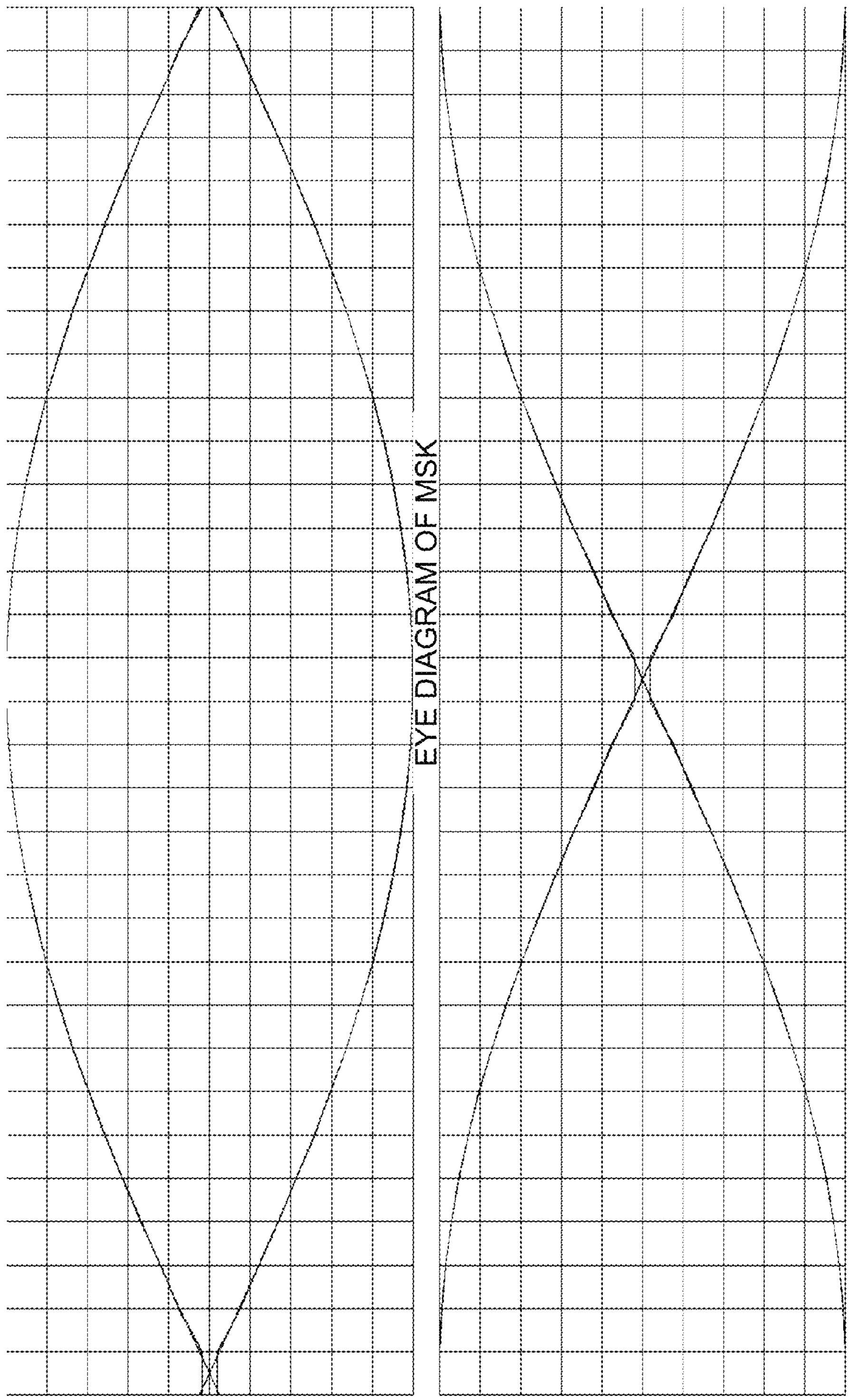

Eye diagram of MSK computed using 16 samples per chip

FIG. 20

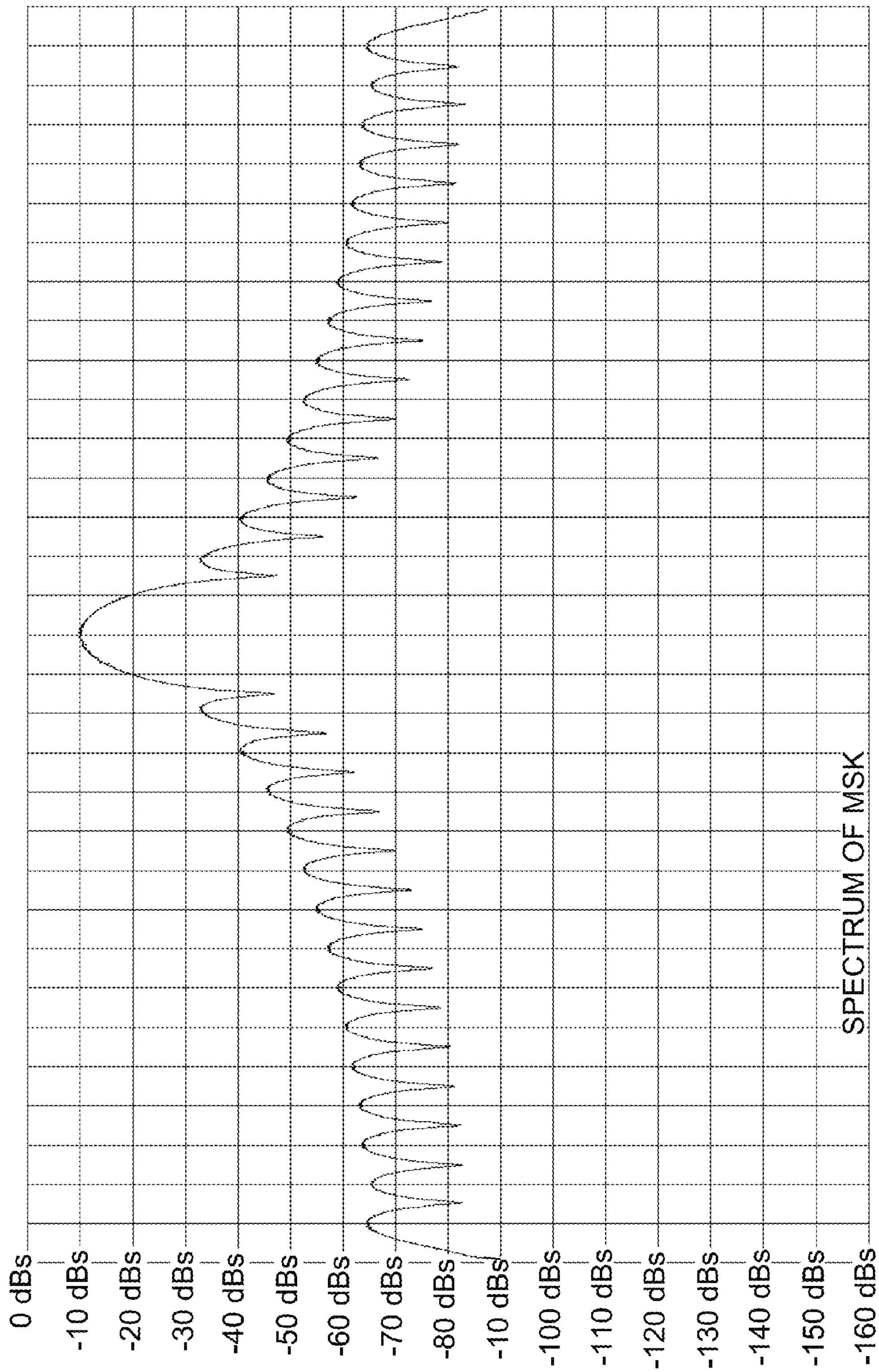

Spectrum of unfiltered MSK

FIG. 21

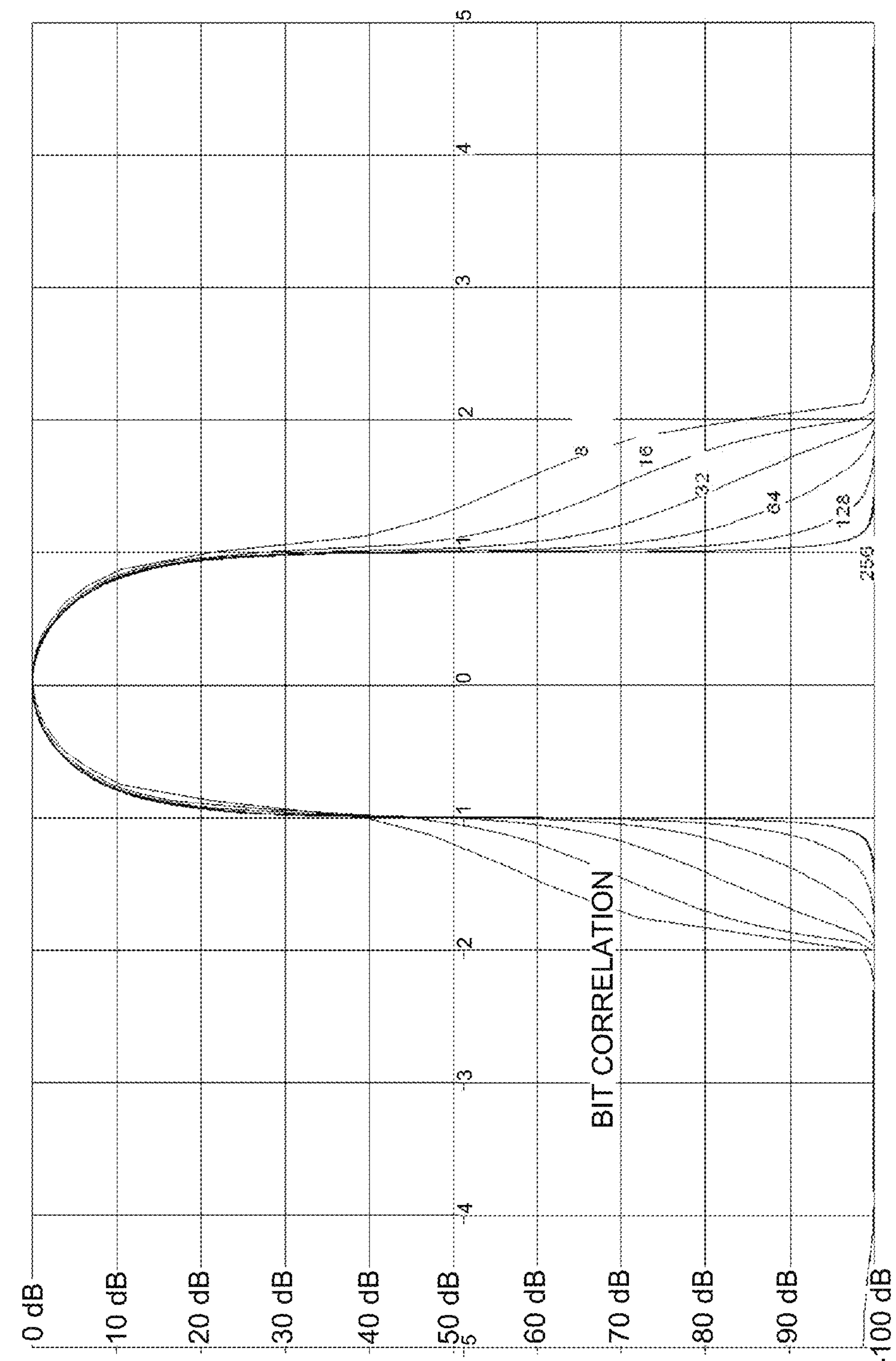

Correlation function of MSK versus the number samples per chip

FIG. 22

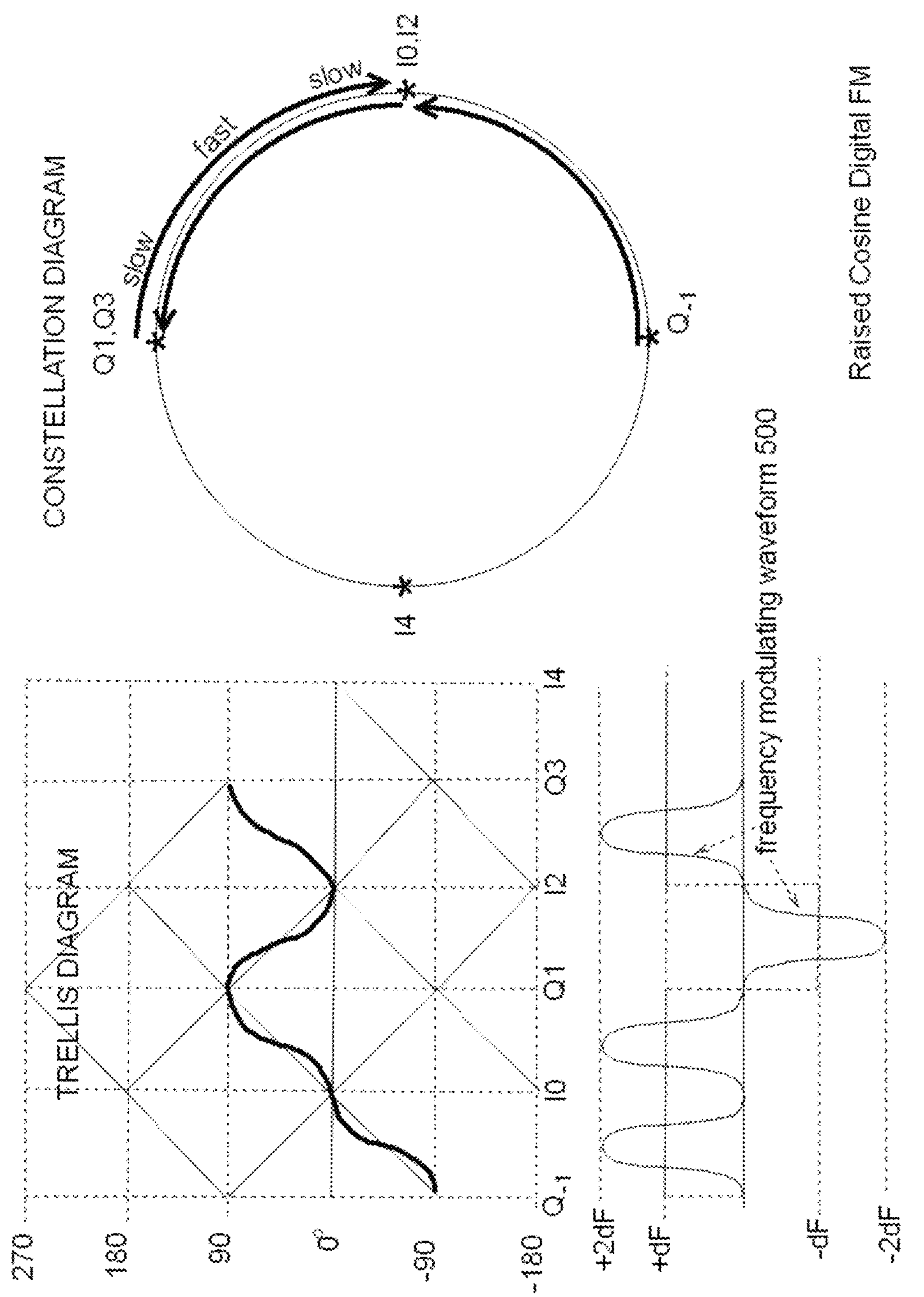
CONSTELLATION DIAGRAM
Q1,Q3
slow
fast
slow
I0,I2
Q-1
I4
Raised Cosine Digital FM
TRELLIS DIAGRAM
270
180
90
0°
-90
-180
Q-1
I0
Q1
I2
Q3
I4
+2dF
+dF
-dF
-2dF
frequency modulating waveform 500

FIG. 23

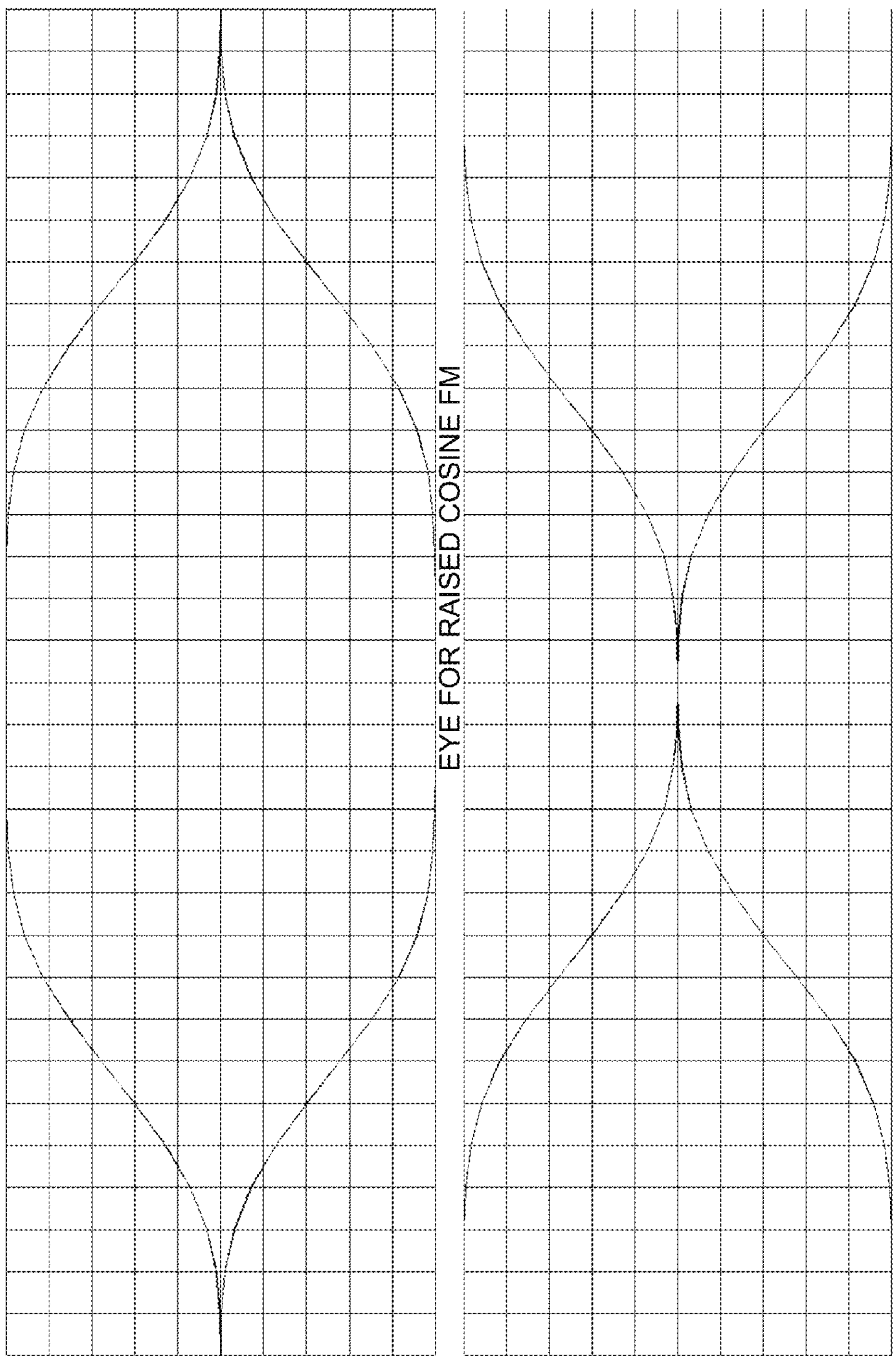

Eye Diagram for Raised Cosine Digital FM

FIG. 24

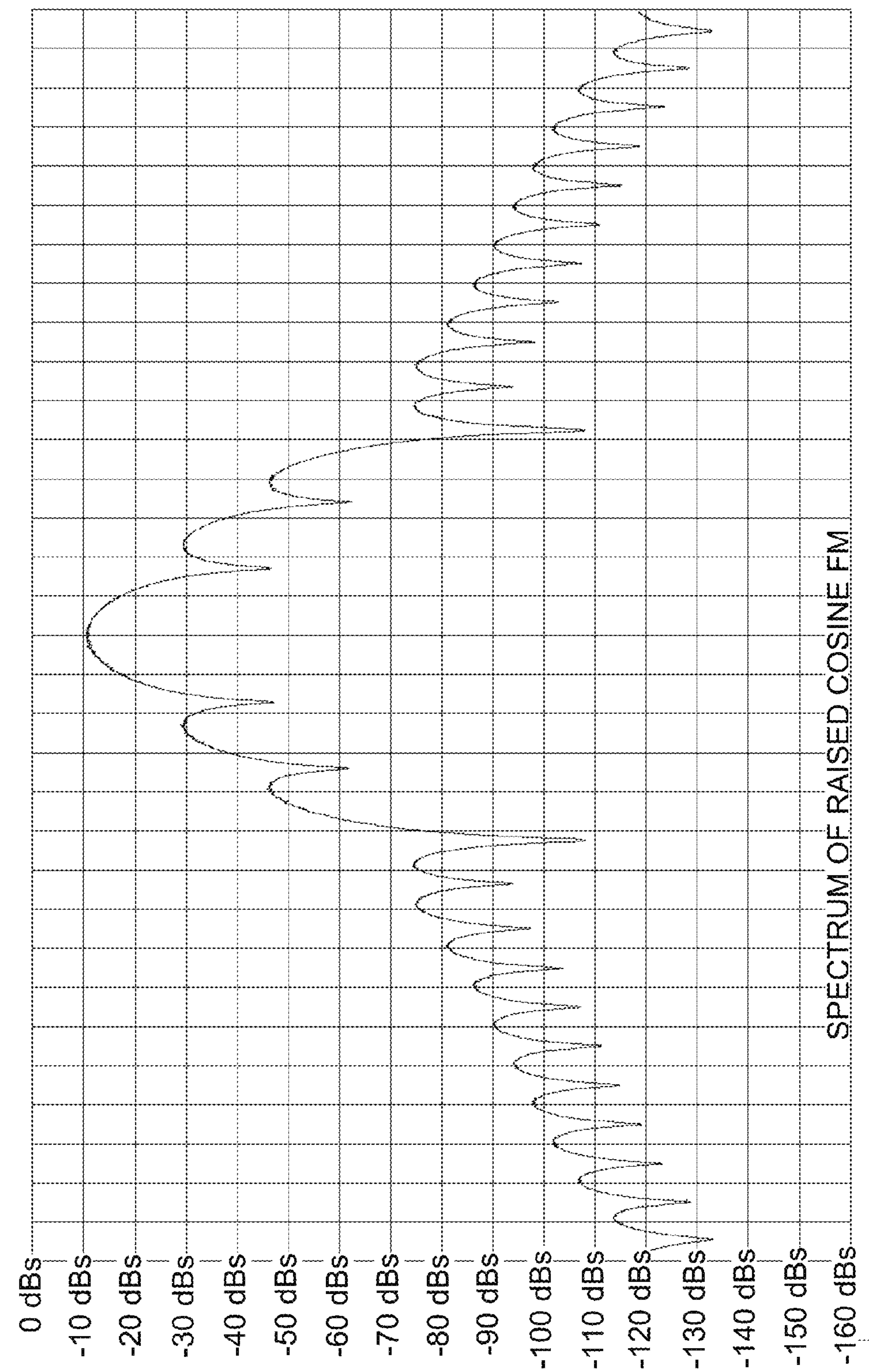

Spectrum of Raised Cosine Digital FM

FIG. 25

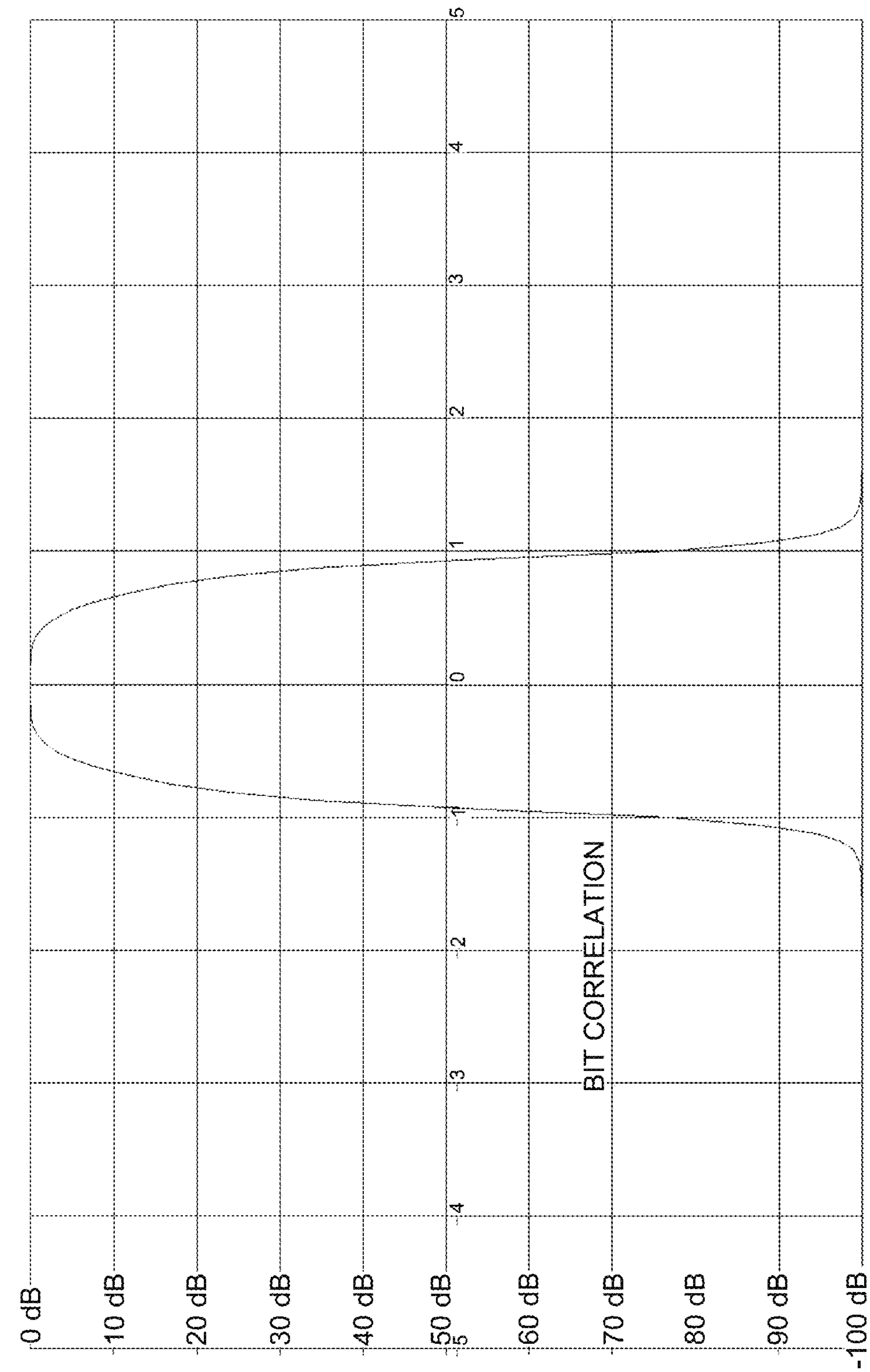

Correlation function of Raised Cosine FM at 16 samples/bit

FIG. 26

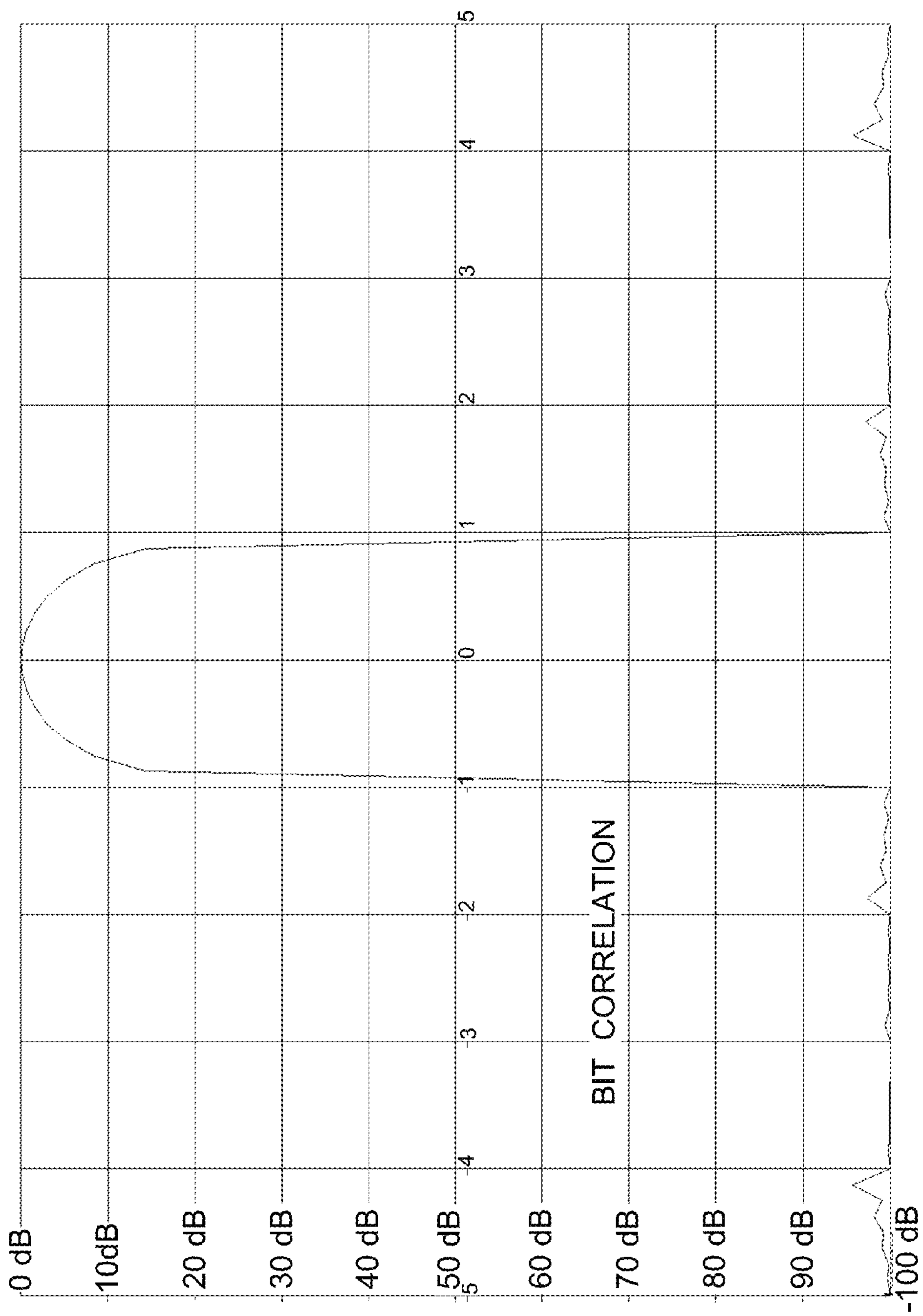

Eradicated sidelobe skirts by waveform handcrafting
(MSK with 8 samples/chip)

FIG. 27

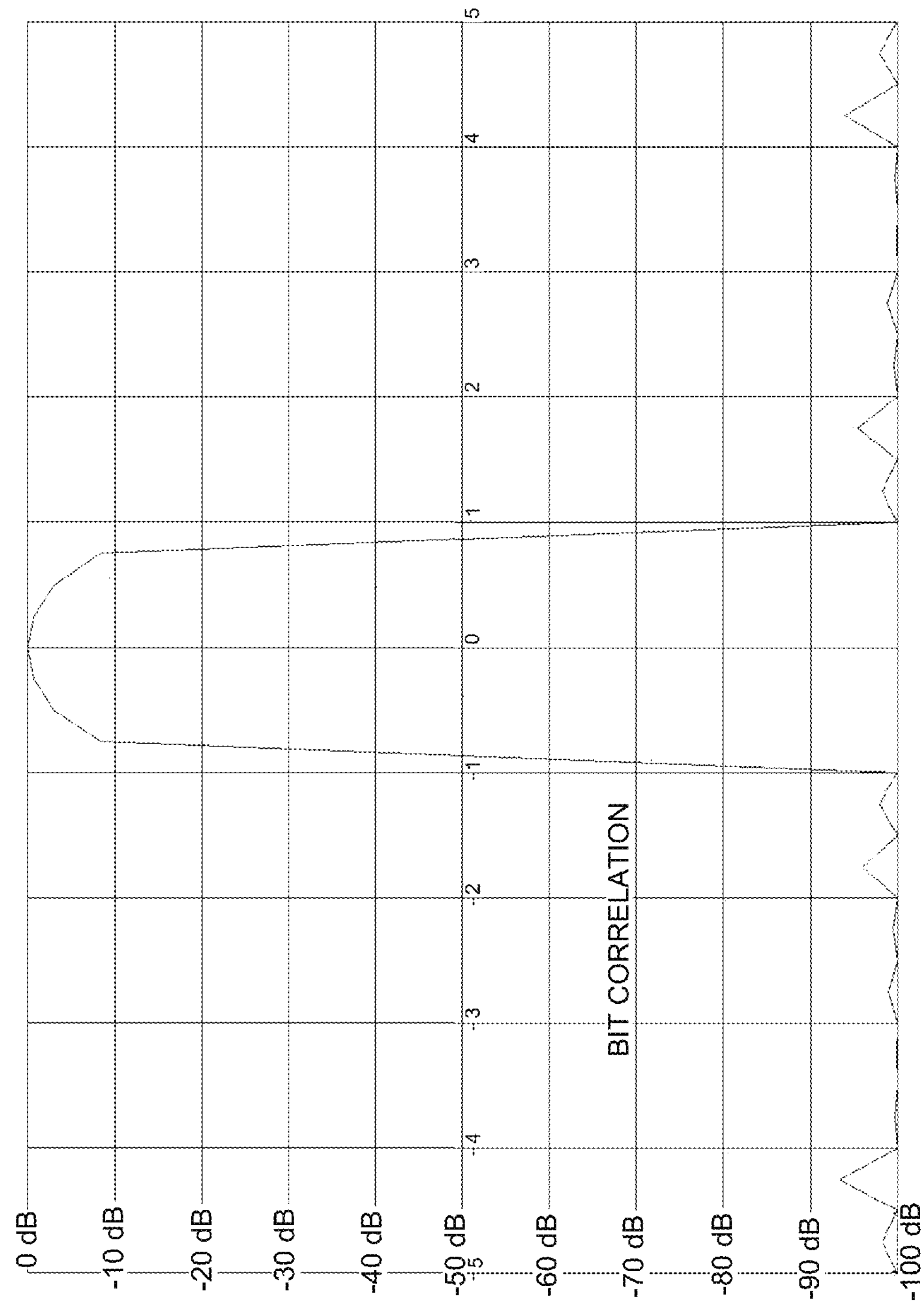

Correlation function of handcrafted MSK at 4 samples/chip

FIG. 28

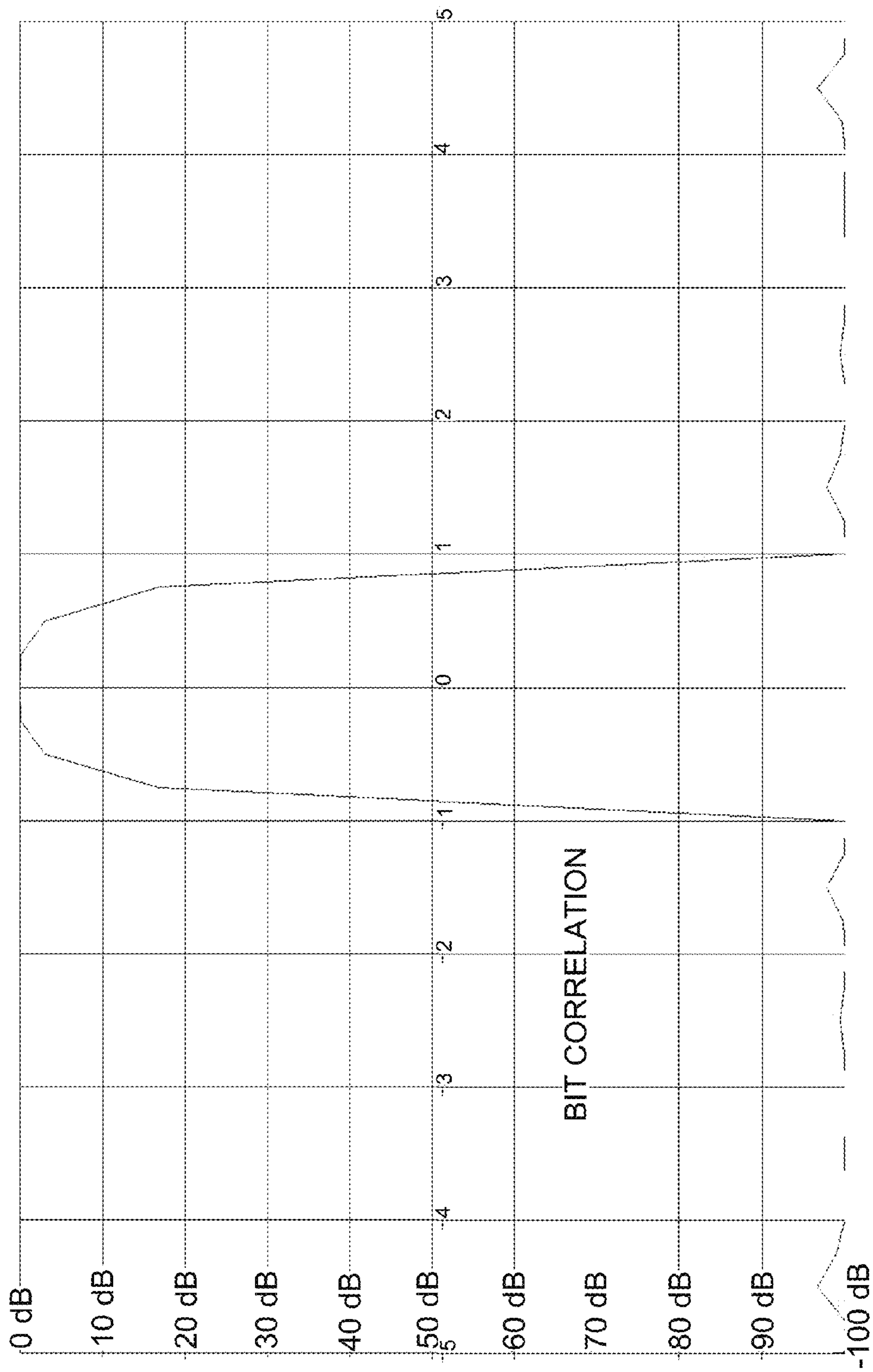

Correlation function for raised cosine digital FM after handcrafting (4 samples per bit)

FIG. 29

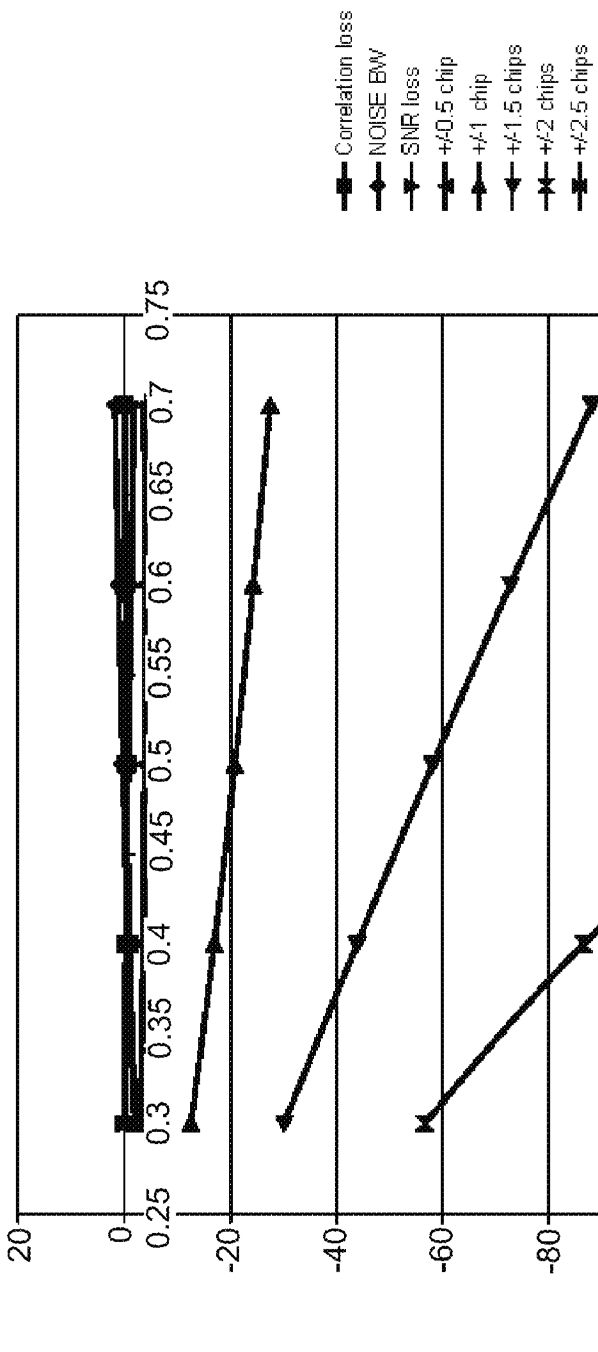

Variation of parameters with receiver BT for Raised Cosine transmitter modulation

FIG. 30

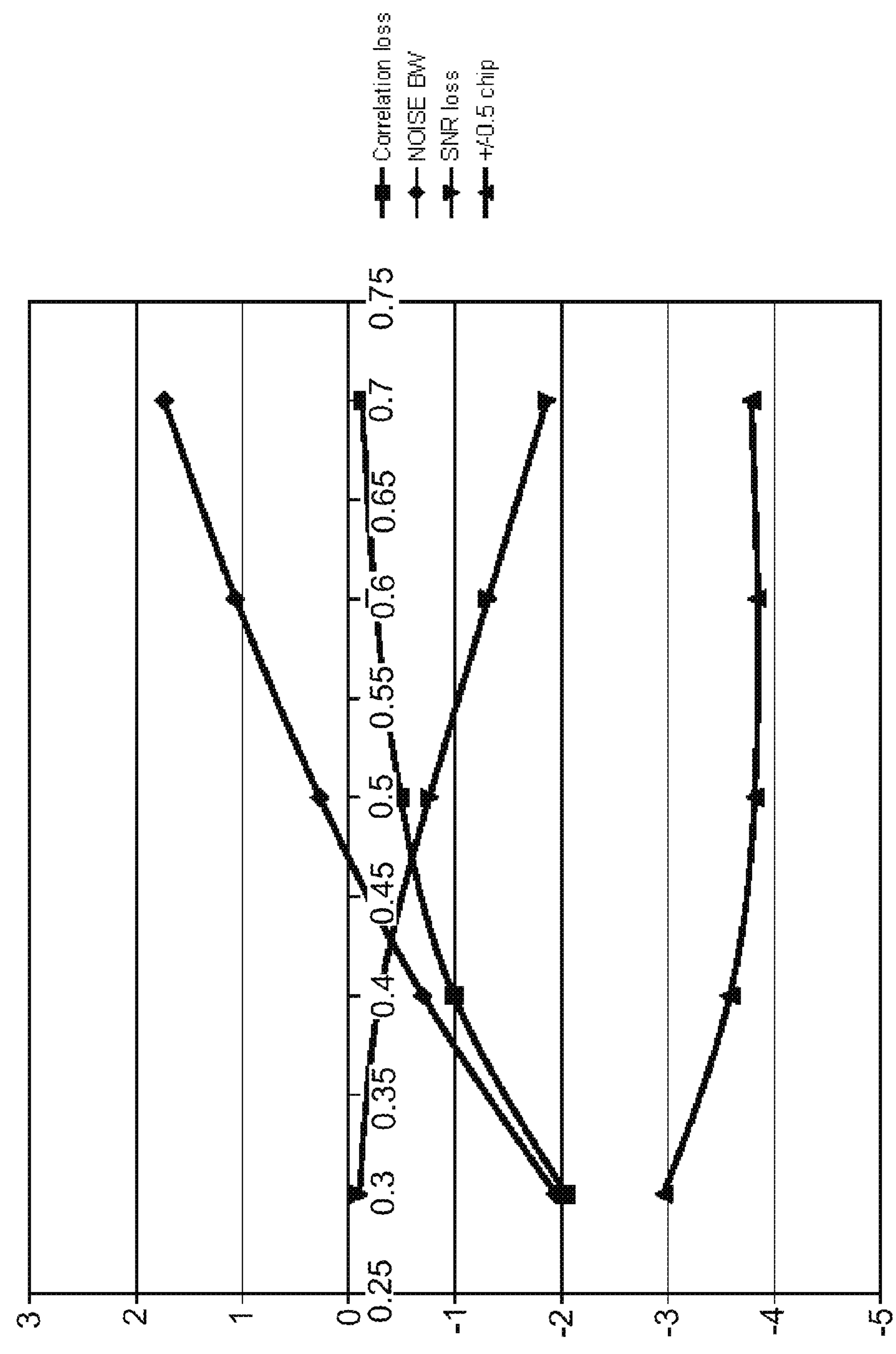

Parameters of figure 30 on a finer dB scale

FIG. 31

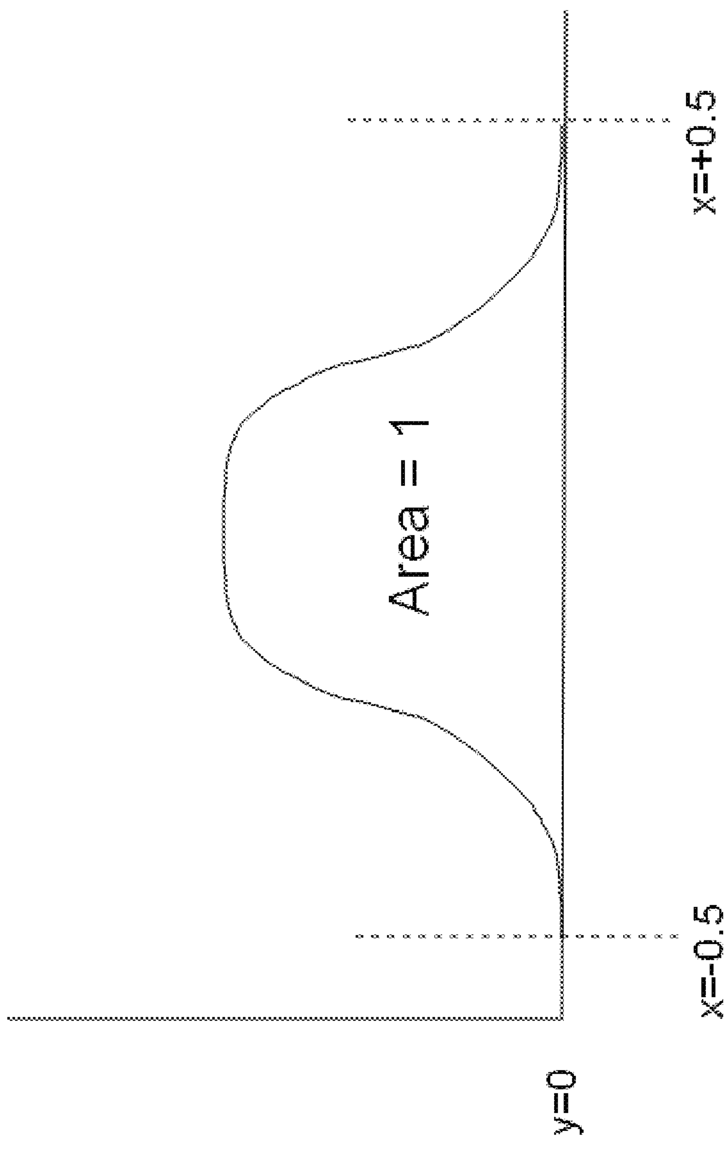

Class of functions to be investigated

FIG. 32

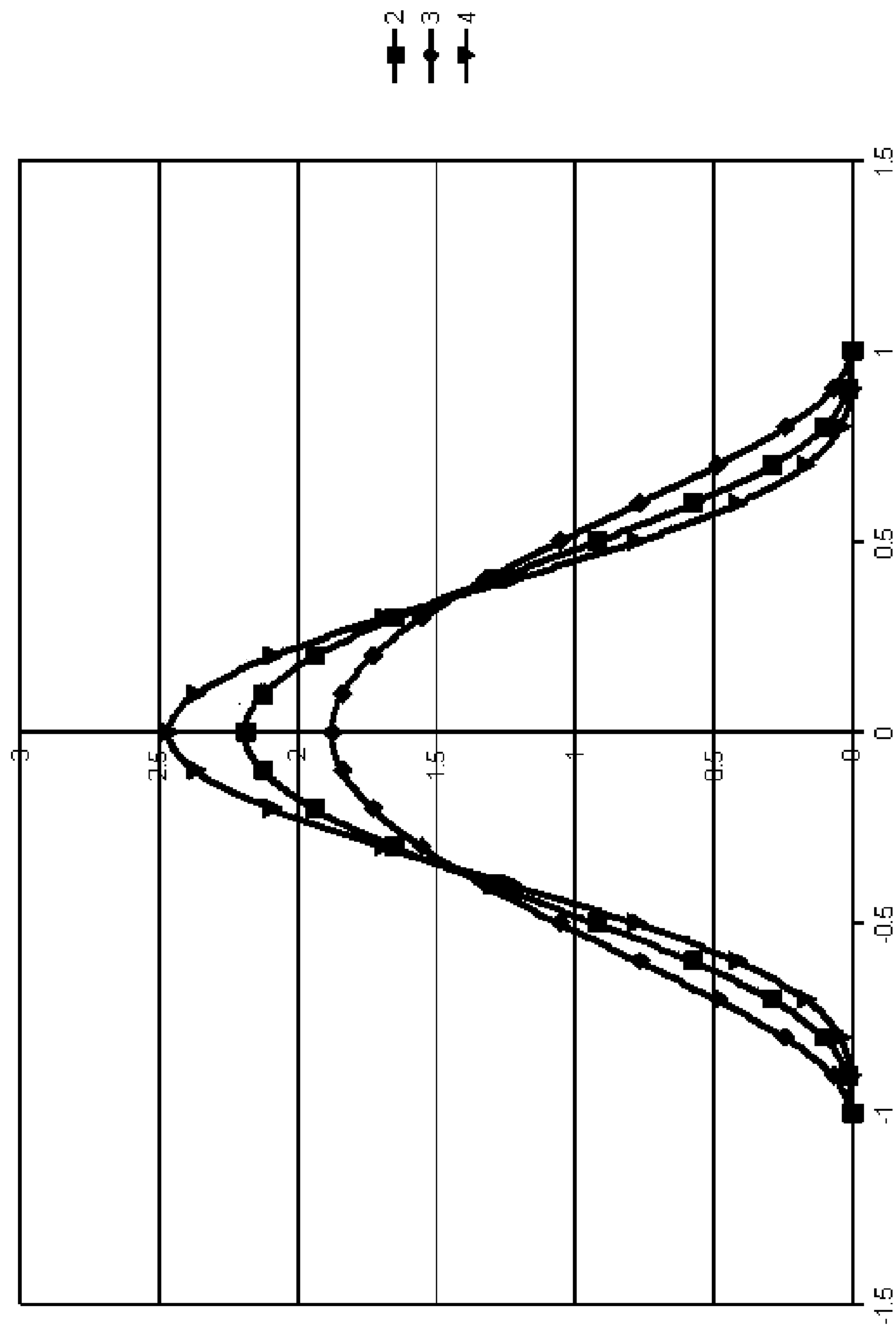

Other polynomial based frequency-pulse shaping functions

FIG. 33

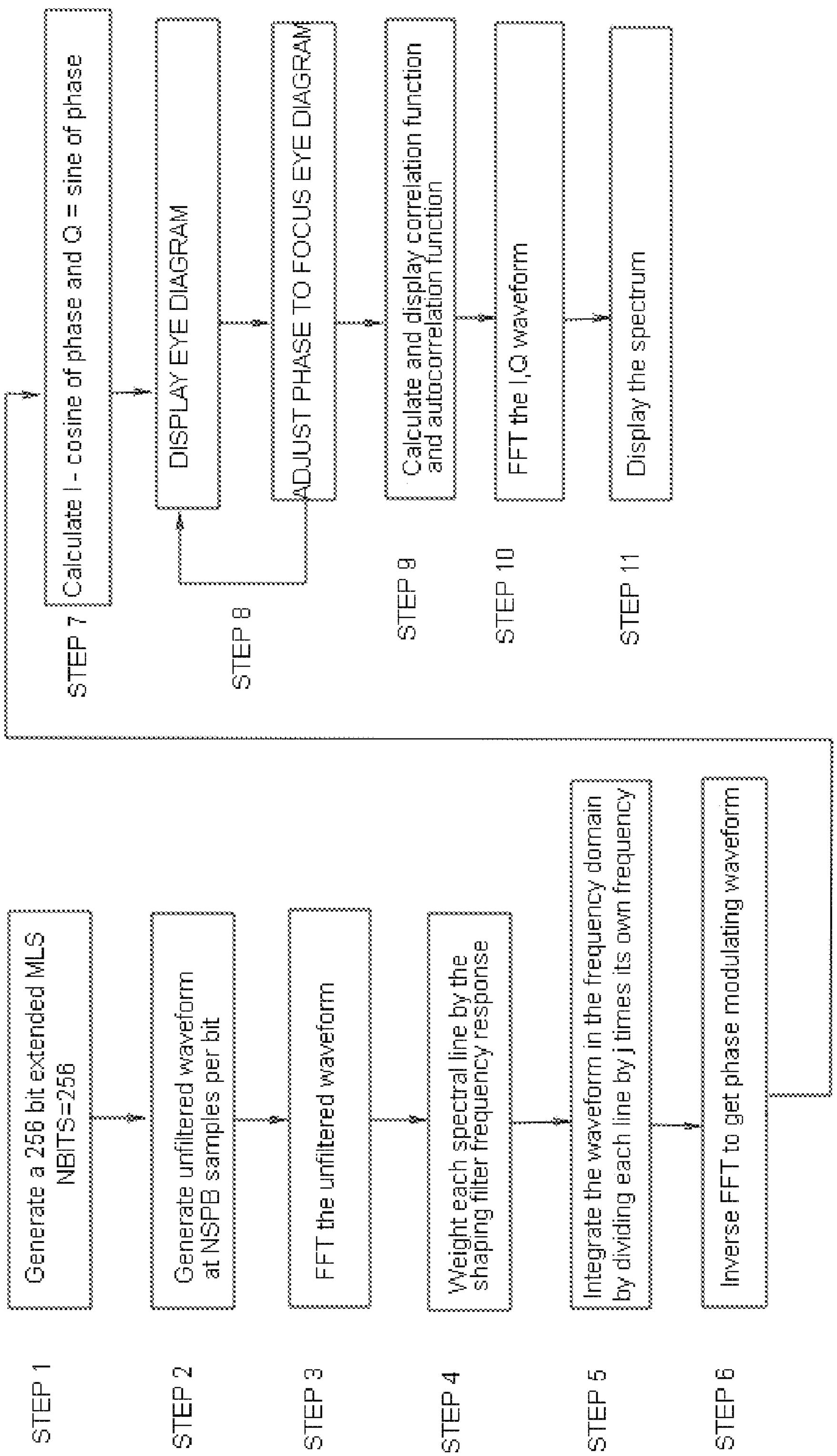

: Flow chart for simulating the modulation

FIG. 34

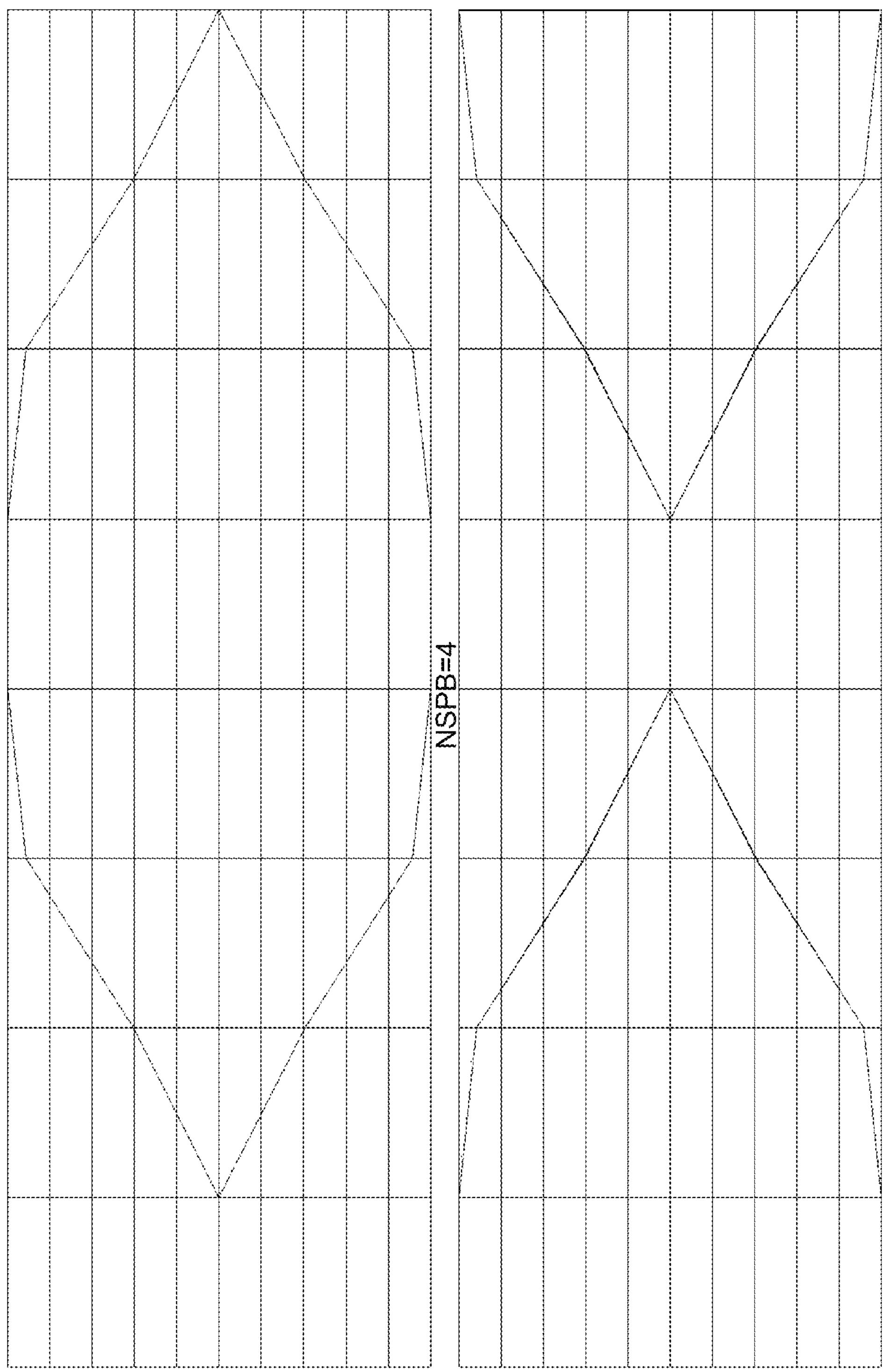

One possible Eye Diagram for 4 samples per bit

FIG. 35

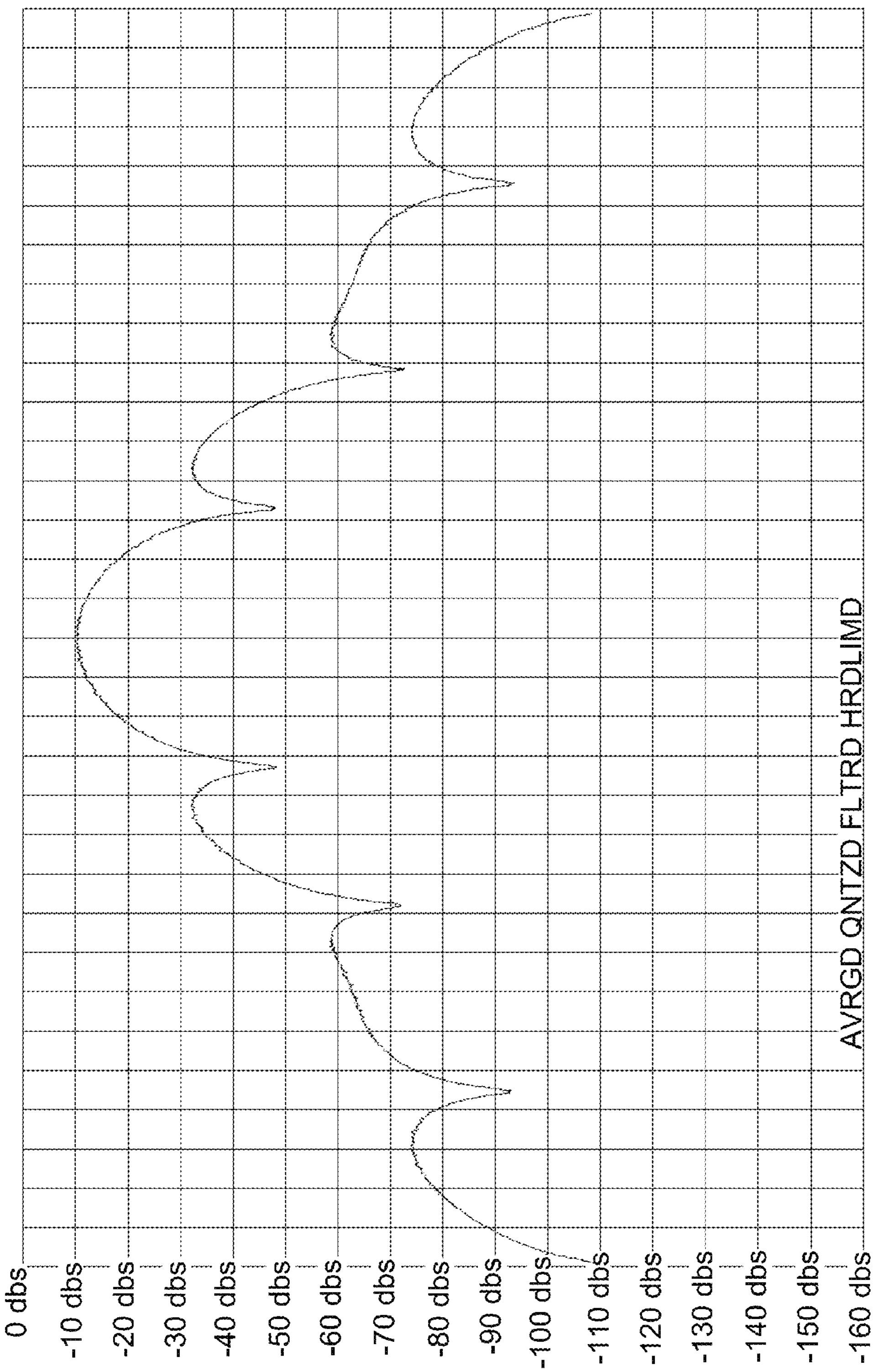

Spectrum of Fig. 35 with Gaussian post DtoA filter BT=0.8

FIG. 36

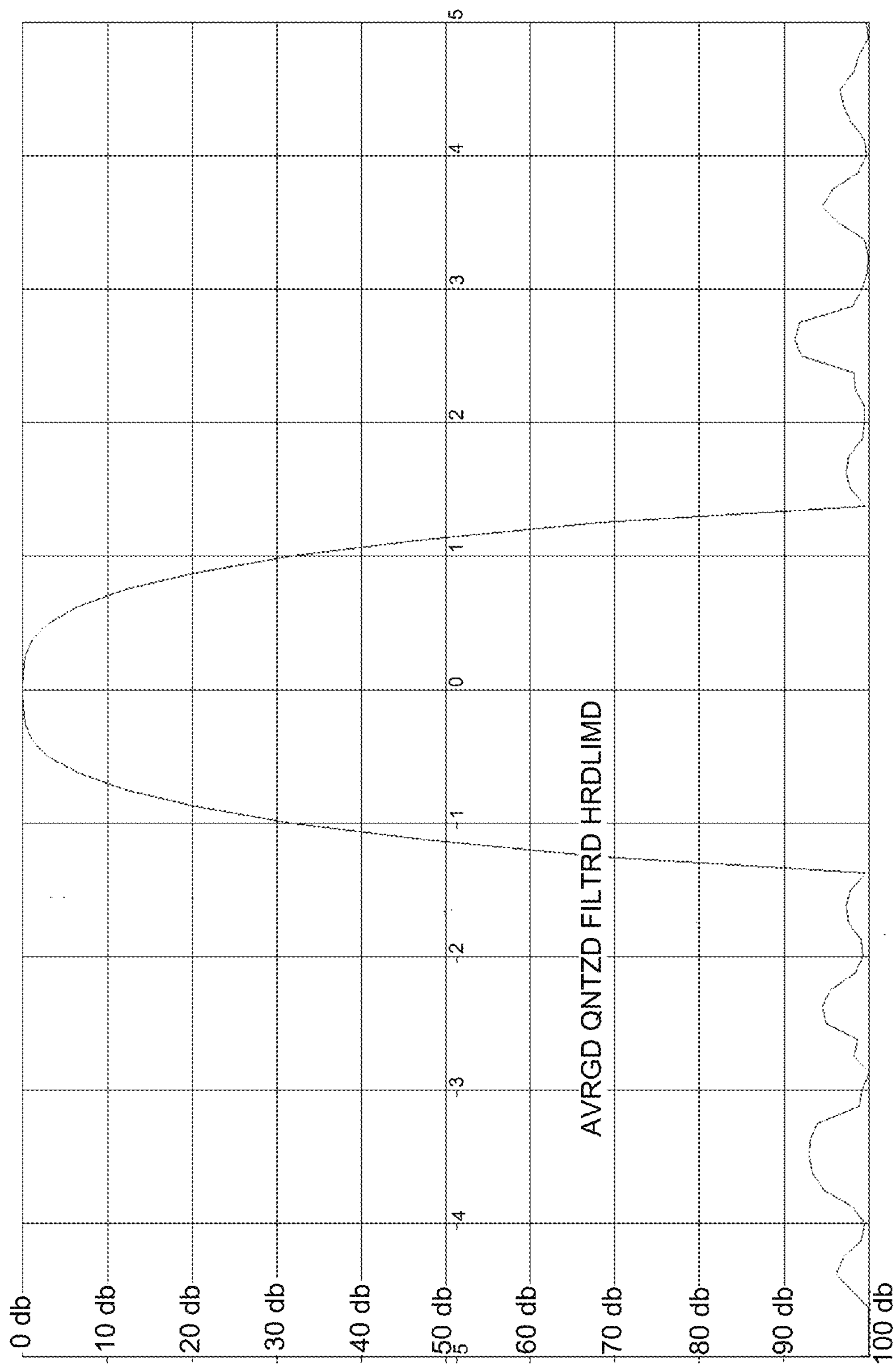

Correlation sidelobes for the signals of figures 35 and 36

FIG. 37

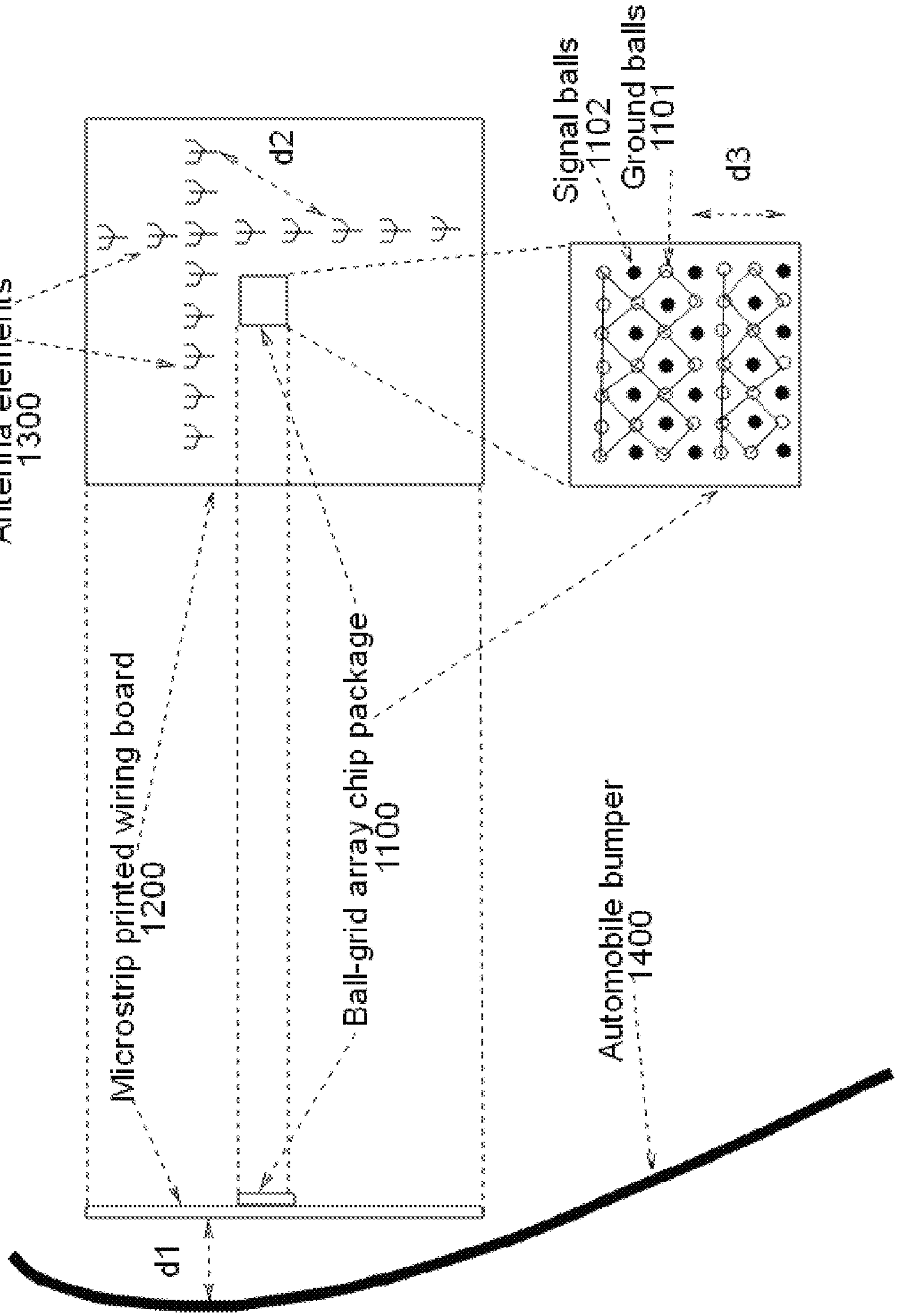

FIGURE 38: Physical Arrangement of an automotive Digital FMCW Radar

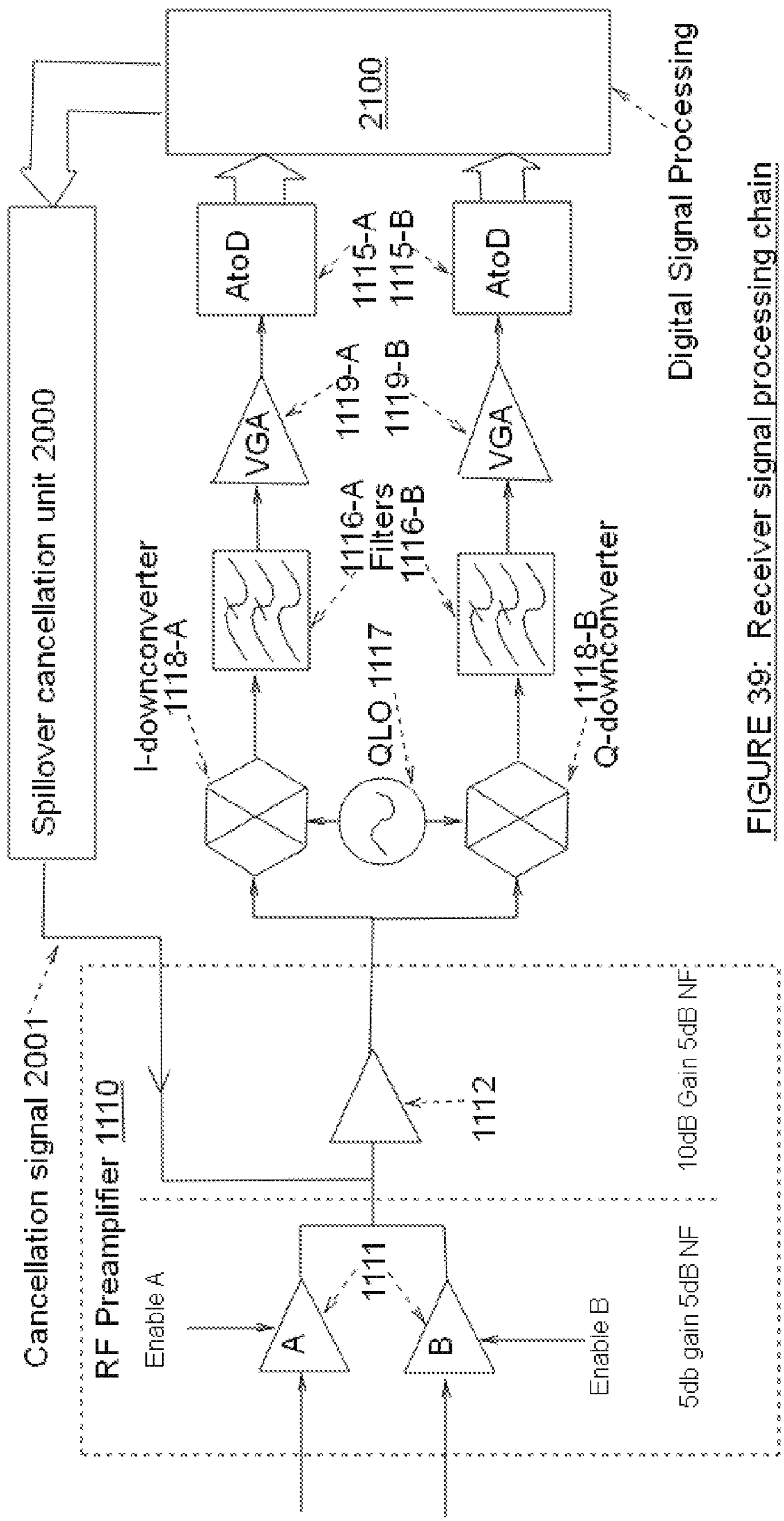

FIGURE 39: Receiver signal processing chain

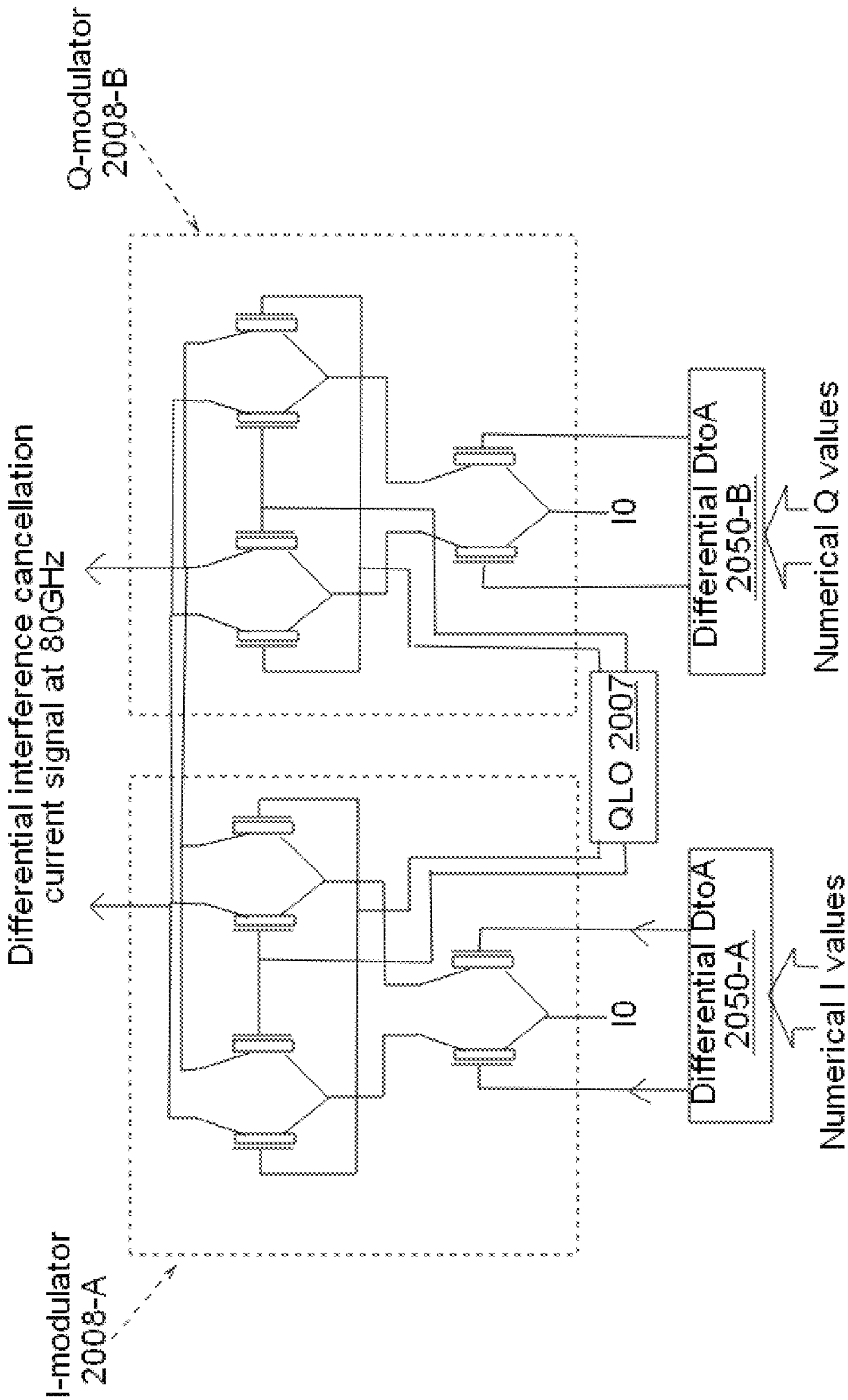

Figure 40: Balanced I,Q modulators based on MOSFET Gilbert cells

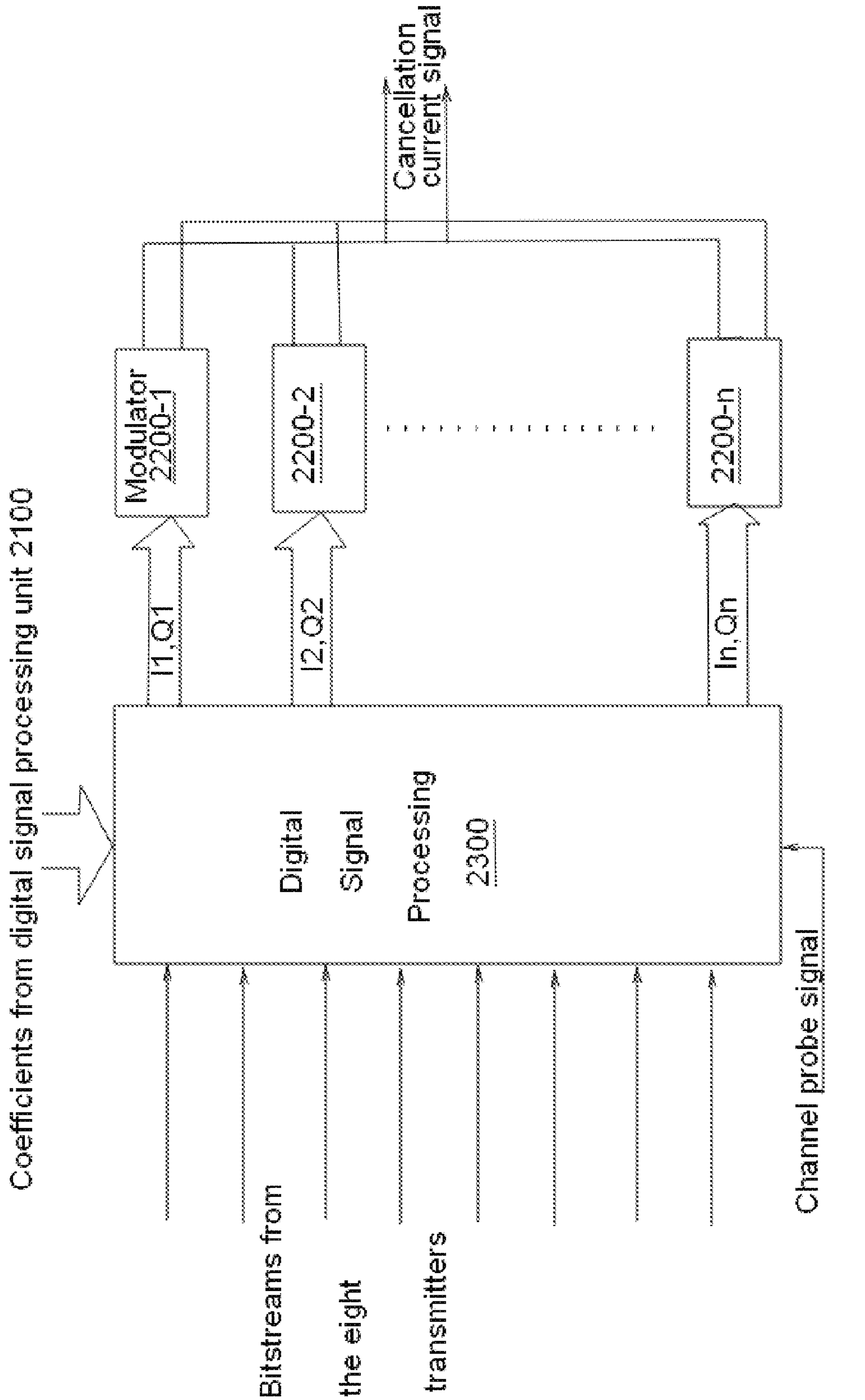

Figure 41: More detail of Spillover Cancellation unit 2000

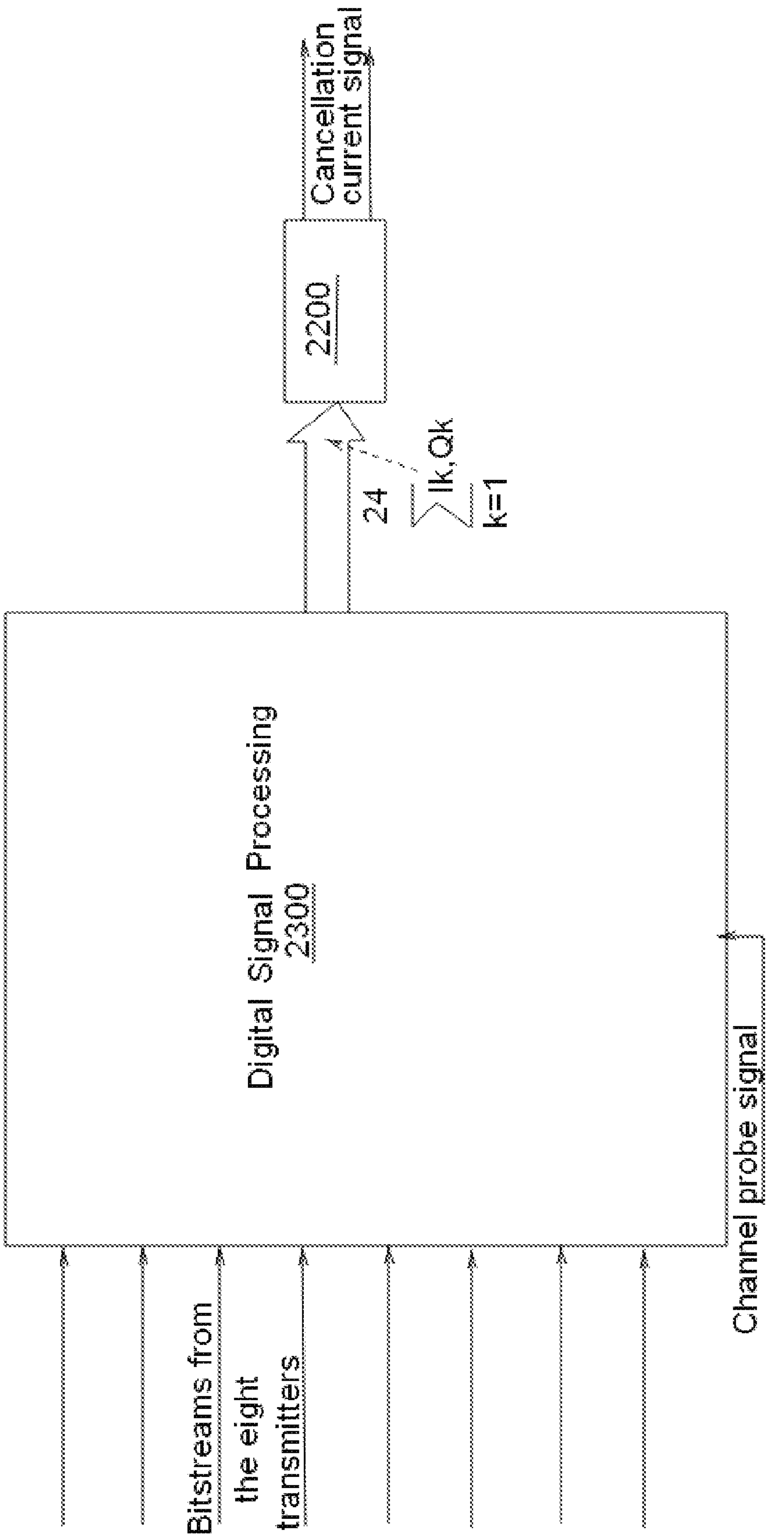

Figure 42: Alternative Spillover Cancellation unit 2000

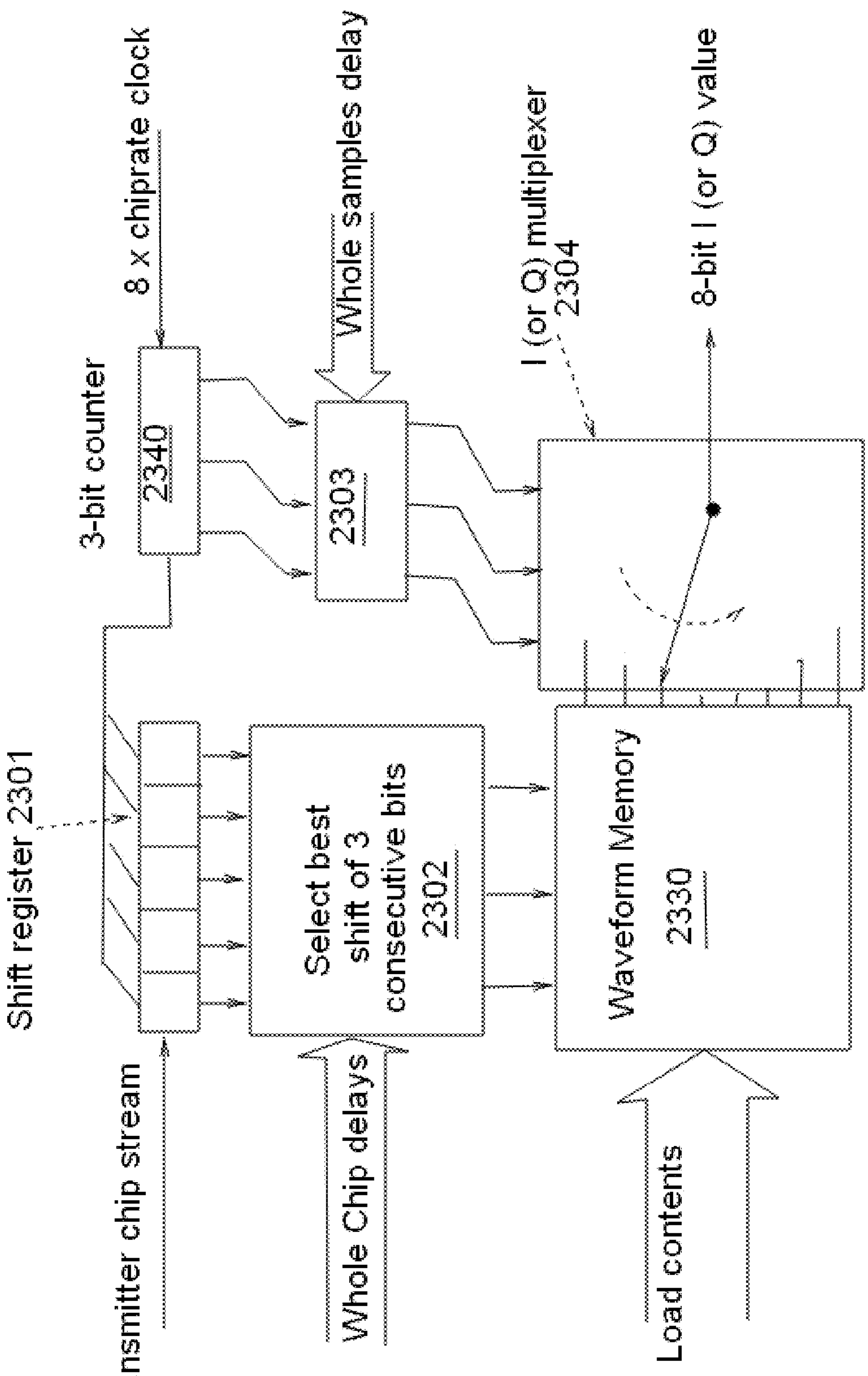

Figure 43: Spillover cancellation signal generator for one transmitter and one path

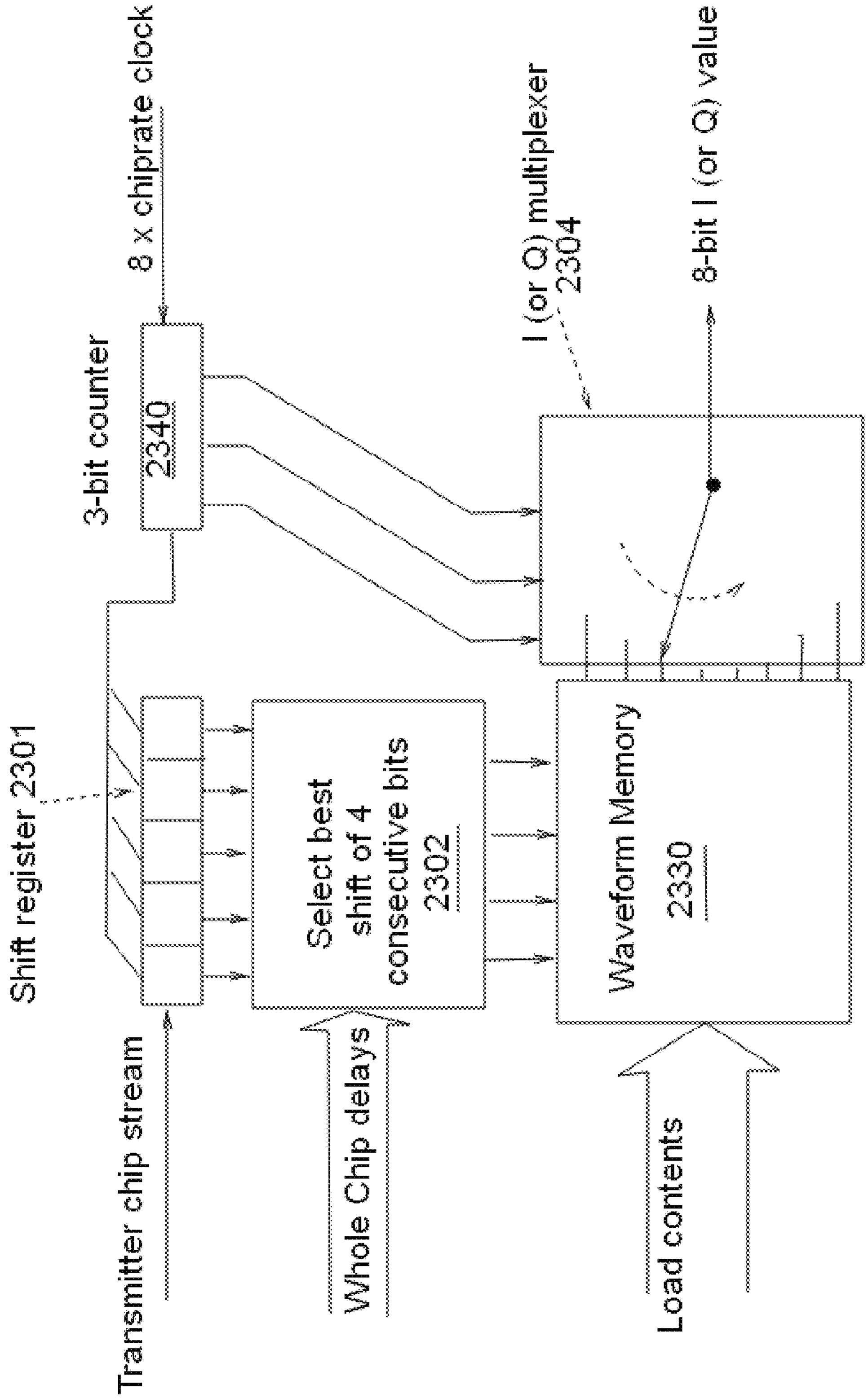

Figure 44: Spillover cancellation signal generator for all paths of one transmitter

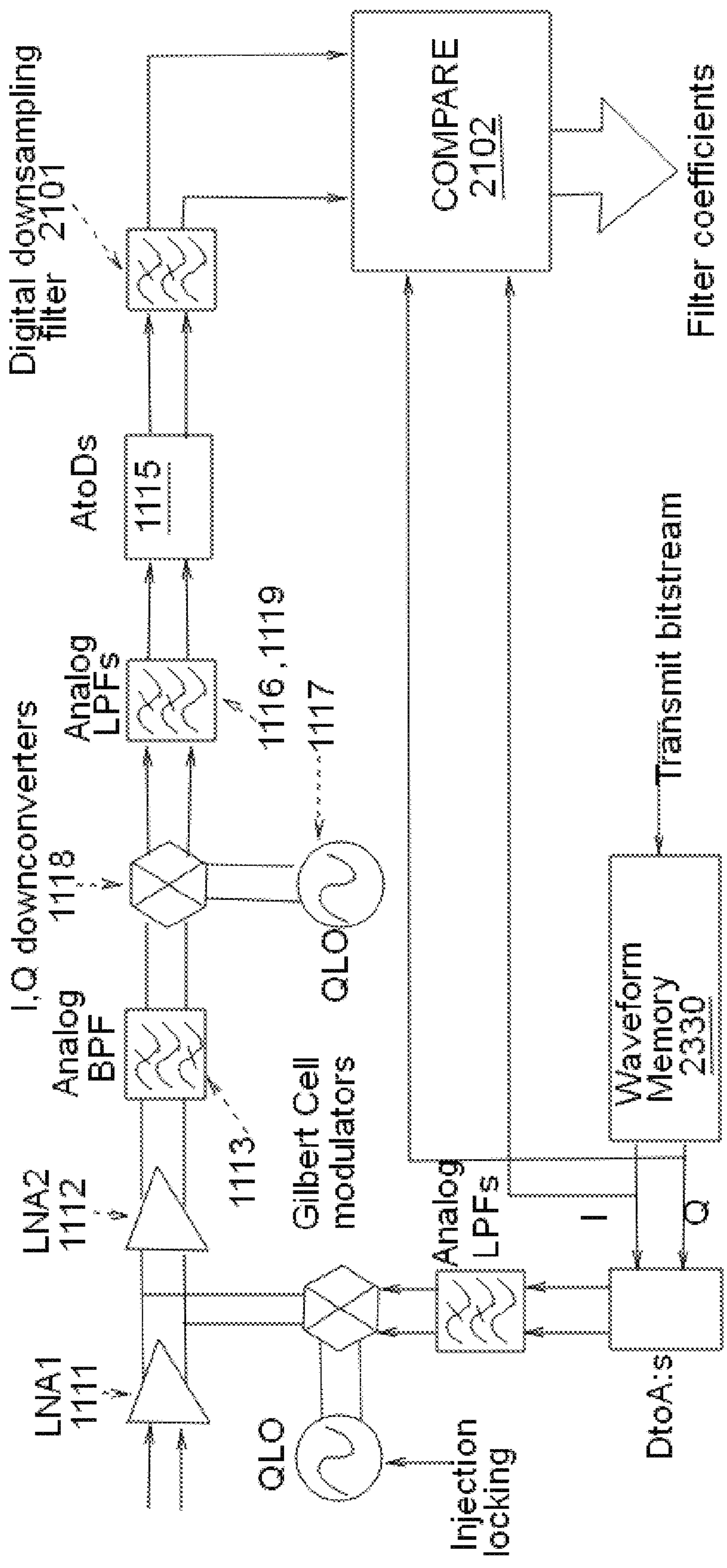

Figure 45: Block Diagram for Forward Channel Determination

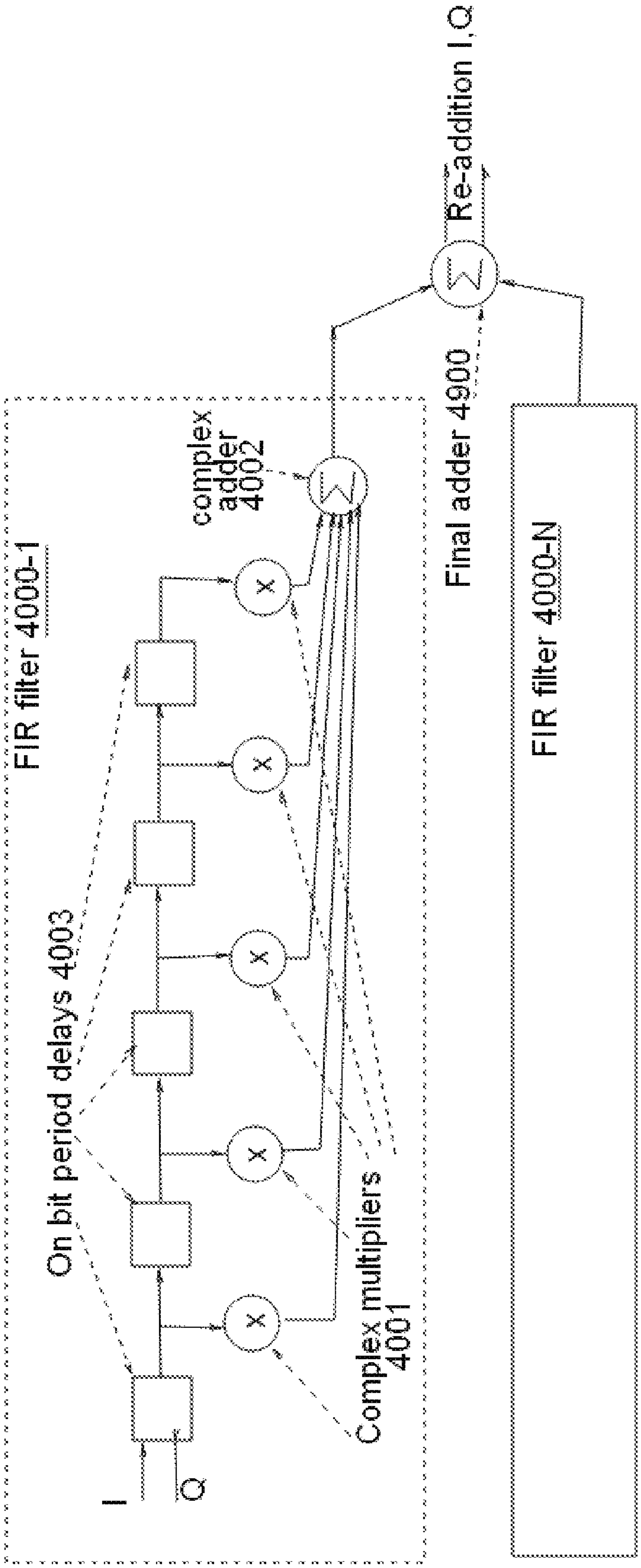

Figure 46: FIR filters for developing the re-addition signal

VEHICULAR RADAR SYSTEM WITH SELF-INTERFERENCE CANCELLATION

CROSS REFERENCE TO RELATED APPLICATIONS

The present application claims the filing benefits of U.S. provisional application Ser. No. 62/327,003, filed Apr. 25, 2016, and is a continuation-in-part of U.S. patent application Ser. No. 15/492,159, filed Apr. 20, 2017, which claims the filing benefits of U.S. provisional applications, Ser. No. 62/469,165, filed Mar. 9, 2017, Ser. No. 62/382,857, filed Sep. 2, 2016, and Ser. No. 62/327,003, filed Apr. 25, 2016, which are all hereby incorporated by reference herein in their entireties.

FIELD OF THE INVENTION

The present invention is directed to radar systems, and more particularly to radar systems for vehicles.

BACKGROUND

The use of radar to determine range and velocity of objects in an environment is important in a number of applications including automotive radar and gesture detection. A radar system typically transmits a signal and listens for the reflection of the signal from objects in the environment. By comparing the transmitted signal with the received signal, a radar system can determine the distance to an object. Using multiple transmissions, the velocity of the object can be determined. Moreover, using multiple transmitters and receivers, the location (angle) of the object can also be determined.

There are several types of waveforms used in different types of radar systems. One type of waveform or radar signal is known as a frequency-modulated continuous waveform (FMCW). In an FMCW-type radar system, the transmitter of the radar system sends a continuous signal in which the frequency of the signal varies. This is sometimes called a chirp radar system. Mixing (multiplying) a waveform reflected from an object (also known as a target) with a replica of the transmitted signal results in a CW signal with a frequency that represents the distance between the radar transmitter/receiver and the target. By sweeping up in frequency and then down in frequency, the Doppler frequency can also be determined.

There is a continuous need for improved radar techniques that achieve good range performance without excessive transmitter power, which permit multiple users to share the spectrum, and which achieve an improved tradeoff between instantaneous bandwidth occupancy and range resolution.

SUMMARY

An FMCW radar system comprises one or more constant envelope transmitters for transmitting radio signals that are frequency modulated. The frequency modulation uses codes to deviate the frequency from a mean or center frequency according to one of a limited number of shaped frequency transitions associated with a limited number of successive codes. The codes of each transmitter are different and preferably exhibit low cross-correlation. In one exemplary implementation, for each transmitter, the frequency modulated signal may be produced by expressing the frequency modulation as a sequence of generated I and Q baseband vectors that are dependent on the limited number of successive codes and which have a constant envelope property where I^2+Q^2 is a constant, for example, unity. The values are modulated on to a microwave carrier frequency for transmission by the radar transmitting antenna, for example by using an I,Q modulator. The I and Q waveforms are precomputed to depend on a limited number (N) of successive bits of a code, for example, 2 or 3 bits, and the precomputed waveforms are stored in a memory as numerical values. A plurality of I,Q values are stored in memory for each possible pattern of the N successive bits and a state variable indicative of the phase quadrant. The plurality of values are read from the memory sequentially for each new value of a code bit, the memory being addressed by the new bit, N−1 previous bits and the state variable. Each plurality of the I,Q values is engineered to obtain an optimum compromise between a number of often conflicting criteria, including compliance with a spectral mask, range resolution, the ease or difficulty of discriminating weak targets from close by strong targets, and correlation loss with target echo delays of a non-integral number of bit periods.

For operating at very high digital code rates, the memory is organized as a plurality of N memories that are read at the code rate divided by N. Each pair of read I,Q values is digital to analog converted using a D to A converter that shapes the quantizing noise to reduce its spectral density near the microwave carrier frequency, and low-pass filtered to obtain analog I,Q signals that are applied to the I,Q modulator.

In an aspect of the present invention, a radar system for a vehicle includes a transmitter and a receiver. The transmitter transmits an amplified and frequency modulated radio signal. Each transmitter comprises a frequency generator, a code generator, a modulator, a constant-envelop power amplifier, and an antenna. The frequency generator is operable to or configured to generate the radio signal with a desired mean or center frequency. The code generator is operable to or configured to generate a sequence of chips at a selected chiprate. A modulation interval between successive chips is a reciprocal of the chiprate. The modulator frequency is operable to or configured to modulate the radio signal such that the frequency modulation comprises shaped frequency pulses. The shaped frequency pulses correspond to a first signal, the frequency of which deviates from the desired mean or center frequency during each of the modulation intervals according to a selected pulse shape. The constant-envelope power amplifier amplifies the frequency modulated radio signal at a desired transmit power level. The antenna transmits the radio signal.

These and other objects, advantages, purposes and features of the present invention will become apparent upon review of the following specification in conjunction with the drawings.

BRIEF DESCRIPTION OF THE DRAWINGS

FIG. **1** is a plan view of an automobile equipped with one or more radar systems in accordance with the present invention;

FIG. **2**A and FIG. **2**B are block diagrams of radar systems in accordance with the present invention;

FIG. **3** is a block diagram illustrating a flow of data structures through a radar system in accordance with the present invention;

FIG. **4** is a block diagram illustrating a radar system with a plurality of receivers and a plurality of transmitters (MIMO radar) for producing the data structures of FIG. **3**, in accordance with the present invention;

FIG. **5** illustrates an exemplary transmitter architecture in accordance with the present invention;

FIG. **6** illustrates an exemplary eye diagram for Gaussian minimum shift keying (GMSK) with a BT factor of 0.3 in accordance with the present invention;

FIG. **7** is a graph illustrating the correlation of a transmitted signal with a transmitted code in accordance with the present invention;

FIG. **8** is a graph illustrating an autocorrelation function for GMSK with BT=0.3 in accordance with the present invention;

FIG. **9** is a graph illustrating a power spectrum for GMSK with BT=0.3 in accordance with the present invention;

FIG. **10** is a graph illustrating correlation sidelobes using a Gaussian receiver filter with BT=0.3 in accordance with the present invention;

FIG. **11** is a graph illustrating variation of sidelobe levels with receiver filter BT in accordance with the present invention;

FIG. **12** is a graph illustrating variation of noise bandwidth and SNR with receiver filter BT in accordance with the present invention;

FIG. **13** is a graph illustrating an eye diagram of modulation engineered to depend on 3 chips in accordance with the present invention;

FIG. **14** is a graph illustrating the correlation function of the modulation of FIG. **13** in accordance with the present invention;

FIG. **15** is a graph illustrating a comparison of the spectrum of regular GMSK with that of FIG. **14** in accordance with the present invention;

FIG. **16** is a graph illustrating the correlation function of a more handcrafted waveform in accordance with the present invention;

FIG. **17** is a graph illustrating an eye diagram of the handcrafted waveform in accordance with the present invention;

FIG. **18** is a graph illustrating the spectrum of the handcrafted waveform in accordance with the present invention;

FIG. **19** is a set of graphs illustrating trellis and constellation diagrams in accordance with the present invention;

FIG. **20** is a graph illustrating the eye diagram of MSK computed using 16 samples per chip in accordance with the present invention;

FIG. **21** is a graph illustrating the spectrum of unfiltered MSK in accordance with the present invention;

FIG. **22** is a graph illustrating the correlation function of MSK versus the number samples per chip in accordance with the present invention;

FIG. **23** is a graph illustrating raised cosine digital FM in accordance with the present invention;

FIG. **24** is a graph illustrating the eye diagram for raised cosine digital FM in accordance with the present invention;

FIG. **25** is a graph illustrating the spectrum of raised cosine digital FM in accordance with the present invention;

FIG. **26** is a graph illustrating the correlation function for raised cosine digital FM in accordance with the present invention;

FIG. **27** is a graph illustrating the eradication of correlation sidelobe skirts of MSK with 8 samples/chip by waveform handcrafting in accordance with the present invention;

FIG. **28** is a graph illustrating the correlation function of handcrafted MSK at 4 samples/chip in accordance with the present invention;

FIG. **29** is a graph illustrating the correlation function for raised cosine digital FM at 4 samples/bit after handcrafting in accordance with the present invention;

FIG. **30** is a graph illustrating the variation of parameters with receiver BT for raised cosine transmitter modulation in accordance with the present invention;

FIG. **31** is a graph illustrating the parameters of FIG. **30** on a finer dB scale in accordance with the present invention;

FIG. **32** is a graph illustrating a class of shaping functions to be investigated in accordance with the present invention;

FIG. **33** is a graph illustrating other polynomial-based frequency-pulse shaping functions in accordance with the present invention;

FIG. **34** is a flow diagram of a processing for simulating modulation in accordance with the present invention;

FIG. **35** is a graph illustrating one possible eye diagram optimized for four (4) samples per bit in accordance with the present invention;

FIG. **36** is a graph illustrating the spectrum of the waveform of FIG. **35** with Gaussian post D to A filter BT=0.8 in accordance with the present invention;

FIG. **37** is a graph illustrating the correlation sidelobes for the signals of FIGS. **35** and **36**;

FIG. **38** is a diagram illustrating a physical arrangement of an automotive radar installation in accordance with the present invention;

FIG. **39** is a block diagram illustrating an exemplary receiving processing chain with spillover cancellation in accordance with the present invention;

FIG. **40** is a block diagram illustrating exemplary balanced I, Q modulators in accordance with the present invention;

FIG. **41** is a block diagram illustrating an exemplary implementation of a spillover cancellation unit in accordance with the present invention;

FIG. **42** is a block diagram illustrating an exemplary alternative implementation of a spillover cancellation unit in accordance with the present invention;

FIG. **43** is a block diagram illustrating an exemplary spillover cancellation signal generator for one transmitter and one spillover path at a time in accordance with the present invention;

FIG. **44** is a block diagram illustrating an exemplary spillover cancellation unit configured to cancel all spillover paths of one transmitter at a time in accordance with the present invention;

FIG. **45** is a block diagram illustrating channel determination for spillover cancellation signals to receiver output signals in accordance with the present invention; and

FIG. **46** is a block diagram illustrating an exemplary signal development for re-addition of the subtracted Q interference signal in accordance with the present invention.

DETAILED DESCRIPTION

The present invention will now be described with reference to the accompanying figures, wherein numbered elements in the following written description correspond to like-numbered elements in the figures. Methods and systems of the present invention may achieve a good performance range without excessive transmitter power requires and provide improved tradeoffs between instantaneous bandwidth occupancy and range resolution, through the use of constant envelope transmitter amplifiers and frequency modulation using smoothly shaped frequency deviation pulses.

Small, low-cost radar systems are increasingly becoming of interest for motor vehicle collision avoidance applications. National frequency management authorities such as the FCC in the USA have made available certain frequency bands in the millimeter wave region for this purpose, for example the frequency band 76 to 77 GHz and the band 81 to 86 GHz.

Automobile radar systems become of greater utility the greater the object resolution achieved in ultimately the three dimensions of range, azimuth and elevation, as well as in Doppler shift, which indicates relative velocity of a target object. An ultimate goal is object recognition and hazard detection using the radar data, possibly in fusion with video data, map databases, and GPS positioning.

As with communications systems such as cellular phones, the frequency band has to be shared by many users without unacceptable mutual interference, so the same concerns of multiple access efficiency, spectral efficiency and capacity arise, in terms of the number of devices per square kilometer that can be simultaneously operated. Through generations 1, 2, 3 and 4 of mobile phone systems, many different techniques of modulation and coding have been explored to optimize capacity, including Frequency Division Multiple Access (FDMA), Time Division Multiple Access (TDMA), Code Division Multiple Access (CDMA) also known as Direct Sequence Spread Spectrum (DSSS) and Frequency Hopping Spread Spectrum (FHSS). Many different modulation methods have also been explored, including Analog Frequency Modulation (FM), Digital frequency modulation, such as GSM's Gaussian Minimum Shift Keying (GMSK), and all the usual digital phase modulation schemes such as Quadrature Phase Shift Keying (QPSK), Offset QPSK (OQPSK), Quadrature Amplitude modulation (QAM, 16QAM, etc.), and latterly Orthogonal Frequency Division Multiplexing (OFDM).

In communications systems operating in the lower microwave frequencies (900 MHz to L-band) and higher (S-band to 2400 MHz), multipath propagation has increasingly become a problem. For example, transistor frequency performances have increased to the point where radio devices can be made economically at much higher frequencies than before. However, signals at shorter wavelengths are reflected by smaller objects, and such delayed reflections distort digital transmission, causing intersymbol interference (ISI). Higher frequency digital cellular communication only became possible through the use of advanced digital signal processing algorithms that could correctly decode information distorted by ISI. Research into such techniques remains the dominant subject of wireless communications and resulted in the most recent shift to OFDM.

Unlike communications systems where multiple, differently-delayed reflections are a nuisance, in radar systems, the delayed reflections are the wanted information. Also in contrast with communications systems, except in bistatic radar systems, the signal reflected from an object or target and processed by a radar receiver has originated in the radar's own transmitter, which may be in intimate proximity to the receiver. Thus, the receiver can use information on exactly what was transmitted, and when, to aid in analyzing the received signal, and to determine the delays of target echoes which indicate their range.

There are several different types of radar systems. The most well-known is pulse radar, in which a very short pulse of very high power microwave energy is transmitted during which time the receiver is blanked to prevent overload or damage; then the receiver is unblanked and listens for echoes received with various delays. The length of time the receiver can listen before the next transmitter pulse equates to the maximum range. The antenna may rotate between pulses to test for reflecting objects at different azimuths or elevations or both.

A less common variation of the above is the bistatic radar system in which the transmitter is not co-located with the receiver and uses a totally different antenna. The receiver thereby does not need to be blanked during the transmit pulse.

In pulse radar systems, the transmitter duty factor and therefore the mean power is small; therefore, to achieve enough sensitivity for long range performance a high peak pulse power must be used. To overcome that, another type of radar called continuous wave (CW) radar is used. A CW radar transmits and receives all the time. The transmitted signal has features in its waveform that enable the receiver to determine the delay of a received signal by determining the time difference between the transmitted feature and the received feature. In FMCW-type radar systems, the feature used is the instantaneous frequency. The transmitter frequency is changed linearly and very rapidly from a starting value to an ending value to create what is known as a chirp. A delayed signal will be received at an earlier value of the chirp frequency. By forming a beat between the transmit frequency and the received frequency in the receive mixer, and determining the beat frequency, which is the transmit-receive frequency difference, the delay of the reflected chirp can be calculated. Because such a frequency difference cannot be distinguished from Doppler, a forward and backward chirp may be used alternately, producing a sawtooth frequency modulation. Any Doppler has opposite effect on interpreting the forward chirp compared to the backward chirp, thus allowing range and Doppler to be separated. In FMCW radar systems, one issue is the extreme accuracy and linearity needed for the chirp signal. The greatest issue in CW radar is receiving at the same time as transmitting. The transmitted signal is much stronger than any received echo and can overload the receiver's limited dynamic range.

Another version of CW radar called pulse-CW radar aims to reduce the difficulty of receiving weak echoes from distant objects in the presence of the strong own transmitter signal. This is similar to pulse radar except that the transmitter duty factor is much higher, for example 50%. A modulated transmit pulse is transmitted for a duration that fills up the time to the furthest object and then switches off. Meanwhile, the receiver attempts to receive strong echoes from nearby objects while the transmitter is transmitting, but when receiving weak later echoes from distant objects, the transmitter has already switched off, facilitating their detection. Improving near-far performance in radar systems is described in detail in U.S. patent application Ser. No. 15/292,755, filed Oct. 13, 2016 ("the '755 patent application"), which is hereby incorporated by reference herein in its entirety.

In the following disclosure, digital codes are sometimes referred to as comprising a bit sequence and sometimes as comprising a chip sequence. The terms "chips" and "bits" are used interchangeably herein, and mean binary valued quantities. The binary values are 0 or 1 in Boolean notation or +1 and −1 in numerical notation. They may also be abbreviated to just + and − signs. The term "symbols" is also known, and may apply to binary values or multi-valued quantities selected from a finite alphabet. When a multi-valued quantity can exhibit 2^N different values, it can also be equated with N binary values or bits. Therefore, it should be understood that grouping a number of bits into a multi-valued symbol and describing a system in terms of symbols rather than bits or chips does not represent a significant technical departure from the teachings herein. Also, while the invention is described in terms of waveforms that have four principal constellation points of +/−90 degrees and

0/180 degrees, a person of normal skill in the art would be able to produce variations using the teachings herein that used higher order constellations such as 8-PSK or MFSK. Hereinafter, the invention shall be described in terms of binary bits or chips, but the scope of the invention encompasses all such variations as may be made by a person of normal skill in the art and described by the attached claims.

The invention is described primarily for use in a digital FMCW radar in which transmission and reception occur simultaneously at a same site. However, the modulation is also useful in digital FM radars that do not necessarily transmit and receive at the same time, but rather alternately. Hybrid radars can also be made in which transmission and reception are simultaneous for a first period and then the transmitter switches off to allow the receiver to receive weak, late echoes without strong interference from the local transmitter, as discussed in the '755 patent application.

All such references to digital FMCW radar therefore, especially in the claims, shall also be interpreted to encompass the above variations, unless explicitly limited by appropriate wording.

In all radar systems, the distance resolution is ultimately related to the width of the autocorrelation function of the transmitted signal. Advanced algorithms such as Multiple Signal Classification (MUSIC) allow resolution less than, but still related to the width of the autocorrelation function.

The power spectrum is the Fourier transform of the autocorrelation function and so has a spectral occupancy inversely proportional to the range resolution. When a signal with certain spectrum S(jw) is transmitted and received with a matched filter H(jw) that has the conjugate frequency response to that of the transmit spectral shaping, namely H(j(w)=S(−jw), the output has a spectrum that is shaped by the product of the transmit shaping and its conjugate at the receiver, namely by $S(jw)S(-jw)=|S(jw)|^2$, which is the power spectrum shape, and thus has a correlation function equal to the autocorrelation function of the transmitted signal. However, in a practical realization, the receiver does not necessarily receive the transmitted signal with a matched filter, so deviations in the relationship between range resolution and signal autocorrelation function may arise. In that case, the correlation curve exhibited when the receiver correlates a received signal with a transmitted chip sequence that is received with various delays must be computed versus the delay for each case, and is herein termed the correlation function. With small delays of plus or minus two or three chips, the shape of the correlation function mimics the impulse response of the entire channel that exists between the transmitter's code generator and the point at which the received signal is extracted into the correlator. For large relative shifts of many chips or bits, the correlation function will exhibit the autocorrelation function of the digital code chosen. It is well known that Maximum Length Sequences exhibit autocorrelation functions that only have one large peak, and all sidelobes are at a level relative to the peak of −1/N, where N is the length of the code. If they can be used, this autocorrelation property is a desirable one for radar systems.

As noted above, FMCW radar typically used chirp signals to determine range and Doppler.

A digital FMCW radar on the other hand transmits an RF signal which is frequency modulated with a digital code sequence to produce a transmitted signal that has good autocorrelation properties that facilitate range resolution while exhibiting good spectral containment. One type of frequency modulation that appears to have interesting properties in this regard is minimum shift keying (MSK). In MSK, the frequency is changed between two values spaced at plus and minus one quarter (¼) the chiprate (=bitrate) from the carrier, with the result that the phase, which is the integral of frequency deviation, changes by +/−quarter (¼) of a cycle over each bit or chip. Thus, at the end of each chip, the signal vector lies at one of two diametrically opposite points along a line at right angles to the prior signal vector position. MSK is related to Offset QPSK in that the signal vector for even bits ends up at +/−1 while the signal vector for odd bits ends up at +/−j. The difference however is, that when the 1<-->0 transitions of the digital code are filtered or shaped to contain the spectrum, the MSK signal remains at a constant amplitude while an OQPSK signal acquires amplitude modulation, requiring a linear transmit power amplifier to preserve it. Such linear power amplifiers have lower efficiency than constant envelope amplifiers because they do not operate at the optimum power point 100% of the time. At low microwave frequencies such as L-band and S-band, a solid state constant envelope transmitter may achieve 60% efficiency while a linear power amplifier may achieve only 30% efficiency. Since even class-C constant envelope solid-state transmit power amplifiers operating at millimeter wave frequencies only have efficiencies of the order of 15% at the present state of the art, the extra loss of efficiency of a linear power amplifier is to be avoided. Thus, constant amplitude phase modulations such as MSK are of great interest for digital FMCW radar use.

The bandwidth of the transmitted RF signal using digital FM is proportional to the chiprate of the digital modulating code, while the rate at which the spectrum falls off outside of the main spectral lobe depends on the shaping applied to the frequency modulation. It is well known that filtering an MSK modulating waveform using a Gaussian filter produces, for some coincidental reason, the greatest ultimate rate of spectral fall-off outside the main occupied bandwidth. This was particularly exploited for the GSM digital cellular phone system which employed this modulation, termed Gaussian minimum shift keying (GMSK). In this application, versions of such modulations are described that are particularly optimized to meet criteria important in the radar application, rather than criteria important in the communications application, and other advantageous frequency modulation pulse shapes are disclosed.

Radars with a single transmitter and a single receiver can determine distance to a target but cannot accurately determine a direction or an angle of a target from the radar sensor or system unless the antenna pattern is steered between pulses either mechanically or electronically using a phased-array. To acquire angular information for each radar pulse period, which in the case of the exemplary radar system described herein comprises a sequence of frequency modulating bits with which the receiver performs correlation, either multiple transmitter antennas or multiple receiver antennas or both are needed, and which are operative in all directions all the time. Each receiver receives and separates each echoed transmitter signal, thus resulting in N×M received results, where N is the number of transmitters and M is the number of receivers. With proper design, these N×M results can be post-combined in any number of ways according to a plurality of beamforming vectors, thereby achieving elevation and azimuth location of each signal as well as range and Doppler information.

The larger the number of transmitter antennas and receiver antennas, the better the resolution possible. Each transmission antenna is connected to a separate transmitter, and each receiver antenna is connected to a separate receiver. As discussed herein, such a radar system is known as a multiple-input, multiple-output (MIMO) radar system.

An exemplary MIMO radar system is illustrated in FIG. **4**. With MIMO radar systems, each transmitter signal is rendered distinguishable from every other transmitter by using appropriate differences in the modulation, for example, different digital code sequences. Each receiver correlates with each transmitter signal, producing a number of correlated outputs equal to the product of the number of receivers with the number of transmitters. The outputs are deemed to have been produced by a number of virtual receivers, which can exceed the number of physical receivers. A receiver may be referred to as a virtual receiver even when there is only a single transmitter, in order to avoid changing the terminology. The output of a given receiver receiving a transmitted signal from a given transmitter has a phase that depends on the loop distance from the transmitting antenna to the receiving antenna. Each transmit-receive combination produces a different loop phase due to the separation of their antennas. By combining the outputs for each transmitter/receiver combination while correcting for these different loop phase shifts, a combined output is obtained that only constructively adds for a target at a unique point in space. By repeating the combination using the precomputed loop phase shifts for many different points in space, signals may be resolved in the three dimensions of range, azimuth and elevation. The focusing effect of the above phase coherent combining is effective for resolution in azimuth and elevation but only contributes to range resolution at very short ranges, and the range resolution at long ranges is principally determined by the round-trip delay of the digital modulation. An exemplary radar system according to the invention therefore determines the range of a target or the distance to a target principally by determining how long it takes an echo of transmitted RF signals to be heard back at the receivers. From this measured time-delay and knowing that the electromagnetic RF signals travel at the speed of light (or ultrasonic signals traveling at the speed of sound), the distance can be determined.

In digital FMCW radar, the method of determining the time delay is by correlating a received RF signal with multiple time-shifts of the digital modulating code to produce correlations which are stored in range bins. The length of time over which coherent correlations can be performed is limited by the phase rotation caused by Doppler shift. To continue cumulative correlation for longer times than this, partial correlations are combined while compensating for the Doppler-induced phase drift. The partial correlations may be stored for each virtual receiver and range in a 3-dimensional array called a radar data cube, as illustrated in FIG. **3**, in which the three dimensions are virtual receiver number, range, and time or index of the partial correlation. Partial correlations for the same receiver and range are then submitted to an FFT, which combines them in a computationally efficient manner with many different hypotheses of the rate-of-change of phase, thus producing long correlations for each of a number of Doppler bins. The result is then stored in a radar data cube having the dimensions of virtual receiver number, range and Doppler shift. Thus, the radar data cube time dimension has been converted into a Doppler shift dimension which is more meaningful for characterizing a reflecting target or object as stationary or moving. Then, for the same range and Doppler bin, the results across different virtual receivers may be combined by using beamforming matrices as mentioned above in order to achieve angular resolution in azimuth, elevation or both.

Because there can be multiple objects in the environment, there will be multiple bins in the radar cube for which there will be a high correlation. While a virtual receiver/radar could correlate the received RF signal with all possible delays, generally there is a finite set of delays with which the virtual receiver/radar will correlate, that is, a finite set of range bins over the range of interest. Likewise, there will be a finite set of Doppler bins up to the maximum conceivable relative velocity between the radar and an oncoming vehicle. Because the transmission and return range changes at twice the relative velocity of the target to the radar, the maximum Doppler shift may be based on four times the maximum speed of any one vehicle. For a maximum vehicle speed of 250 km/hr, which can be reached on the German Autobahn for example, the maximum Doppler shift can be that of a 1000 km/hr object, which is 74 KHz at 80 GHz. If a radar system's own velocity, which is presumed to be known, is digitally removed by applying a systematic phase de-twisting to the received data, the maximum Doppler shift drops to 37 KHz.

The radar sensing system of the present invention may utilize aspects of the radar systems described in U.S. Pat. Nos. 9,599,702 and/or 9,575,160, and/or U.S. patent application Ser. No. 15/481,648, filed Apr. 7, 2017, Ser. No. 15/416,219, filed Jan. 26, 2017, and/or Ser. No. 15/292,755, filed Oct. 13, 2016, and/or U.S. provisional applications, Ser. No. 62/381,808, filed Aug. 31, 2016, Ser. No. 62/327,004, filed Apr. 25, 2016, Ser. No. 62/327,005, filed Apr. 25, 2016, Ser. No. 62/327,006, filed Apr. 25, 2016, Ser. No. 62/327,015, filed Apr. 25, 2016, Ser. No. 62/327,016, filed Apr. 25, 2016, Ser. No. 62/327,017, filed Apr. 25, 2016, Ser. No. 62/327,018, filed Apr. 25, 2016, which are all hereby incorporated by reference herein in their entireties.

FIG. **1** illustrates an exemplary radar system **100** configured for use in a vehicle **150**. A vehicle **150** may be an automobile, truck, or bus, etc. As illustrated in FIG. **1**, the radar system **100** may comprise one or more transmitters and one or more receivers **104***a*-**104***d* which can be used jointly to realize a plurality of virtual radars. Other configurations are also possible. FIG. **1** illustrates a radar system **100** comprising one or more receivers/transmitters **104***a*-**104***d*, control and processing module **102** and indicator **106**. The receivers/transmitters **104***a*-**104***d* are placed to acquire and provide data for object detection and adaptive cruise control. The radar system **100** (providing such object detection and adaptive cruise control or the like) may be part of an Advanced Driver Assistance System (ADAS) for the automobile **150**.

FIG. **2**A illustrates an exemplary radar system **200** with an antenna **202** that is time-shared between a transmitter **206** and a receiver **208** via a duplexer **204**. As also illustrated in FIG. **2**A, output from the receiver **208** is received by a control and processing module **210** that processes the output from the receiver **208** to produce display data for the display **212**. The control and processing module **210** is also operable to produce a radar data output that is provided to other control units. The control and processing module **210** is also operable to control the transmitter **206**.

FIG. **2**B illustrates an alternative exemplary radar system **250** with a pair of antennas **202***a*, **202***b*: an antenna **202***a* for the transmitter **206** and another antenna **202***b* for the receiver **208**. While pulse radar systems may use shared or separate antennas, continuous-wave radars (discussed herein) will use separate antennas (for transmitting and receiving) because of their continuous operation. Despite using different antennas, local spillover from transmitter to receiver is a huge signal having a short delay. A critical issue in CW radar is the removal by subtraction of this large local spillover signal, for the success of which an accurately defined modulation, as is disclosed herein, is essential.

FIG. **4** illustrates an exemplary digitally-modulated continuous-wave radar system **400**. Radar system **400** comprises a plurality of receivers and their respective antennas **406** and a plurality of transmitters and their respective antennas **408**. The radar system **400** also includes a flash memory **412**, and optionally a random access memory **410**. The random access memory **410**, for example, an external DRAM, may be used to store radar data cube(s) instead of using the limited internal (on-chip) memory (e.g., SRAM), and may also be used to store selected range bins from a greater number of radar data cubes for post processing to improve Doppler resolution or range resolution by tracking objects using Kalman filtering. The radar system may also include a variety of interconnections to an automotive network, e.g., Ethernet, CAN-FD, and/or Flexray.

As was indicated above, range resolution is related to the width of the autocorrelation function of the transmitted signal. A practical autocorrelation function width cannot be too small, otherwise it will have to be computed from the received signal with a sufficiently high sampling density to avoid missing the peak, and the results have to be stored in memory for further analysis, e.g., Doppler analysis. Therefore, computational power and on chip memory limitations, or, in the case of off-chip memory, I/O bandwidth limitations, limit the narrowness of the autocorrelation function that can be contemplated. In a digital FMCW radar system based on transmitting digital codes, one possible sampling density is one sample per chip period, obtained by correlating the transmitted sequence with different whole-chip shifts of the received signal. It could be contemplated to correlate with half-chip shifts of the received signal, but if sufficient memory is available to store that double number of results, then the chiprate may as well be doubled to reduce the width of the autocorrelation function, if bandwidth is available. In the present application, bandwidth in the 80 GHz range is not the limitation. Therefore, the practical solution is to determine how many correlations per second can be computed and stored, and to equate that with the chip rate, such that correlations are to be computed only for whole-shifts of the received signal. Therefore, the characteristics of the autocorrelation functions, computed at whole-chip shifts, need to be investigated for digital code frequency-modulated signals. Several known algorithms exist for computing many correlations between one or more codes and multiple shifts of a received signal; for example, a technique using FFTs for performing circular convolution is known.

FIG. **5** illustrates an exemplary transmitter block diagram. A digital code generator **1010** is fed with a chiprate clock to produce a pseudorandom code for modulating the transmitter. The pseudorandom code preferably has good autocorrelation sidelobe properties at least up to a shift corresponding to the round-trip delay to a target at maximum range. The pseudorandom codes used by different transmitters of a MIMO radar should also be preferably mutually orthogonal or have low cross-correlation. In a first implementation of a radar embodying the invention, the codes are merely random and a long correlation length relied upon to reduce cross correlation and autocorrelation to the point where subtractive interference cancellation can take over and further suppress strong targets to reveal weaker targets. Optionally, the sequences of random binary values (codes or chips) may be provided by a truly random number generator or a pseudorandom number generator. Such number generators are explained in more detail in U.S. Pat. No. 9,575,160, which is hereby incorporated by reference herein in its entirety.

The digital chip code from generator **1010** is fed to I,Q waveform selection logic module **1020**, the purpose of which is to select the I,Q waveform to be modulated for the current chip period in dependence on the current chip and the chip history, in order to produce a signal having a signal frequency varying according to a predetermined shaping function. In one implementation, the number of possible waveforms is limited to eight, and thus requires three address bits (a**0**, a**1**, and a**2**) from selection logic **1020** to address waveform memory **1030**. In another implementation, the waveform depends on fewer than three successive chips. Each waveform may be described by a number of complex I,Q sample values, such as 4, 8, or 16 samples per chip. Counter **1040** is driven by a sample rate clock which is correspondingly 4, 8, or 16 times the chip rate clock that is used to select each I,Q sample pair in turn from the memory. Counter **1040** may be a "divide by 4" using two flip-flops for the case of 4 samples per chip, a 3-stage divider for 8 samples per chip, or a 4-stage divider for 16 samples/chip. The divided, down-sample rate clock is the desired chip rate clock and may be used to clock the digital code generator **1010**. Each stage of counter **1040** produces a digital output as a further address bit to memory **1030**. In the case of 8 samples/chip, three counter bits (t**0**, t**1**, and t**2**) are provided to memory **1030** to select one of the 8 samples. The selected sample (0 to 7) of waveform (0 to 7) comprises a digital I and Q value with a word length in the range of 8 to 16 bits. The digital I and Q values are fed into respective I and Q digital to analog converters (DAC) (**1050**A, **1050**B) where they are converted to analog voltages or currents. At very high speeds, it is desirable that high speed analog signals be balanced, as the quality of an on-chip ground cannot be relied upon for single-ended signals at very high frequencies. The balanced analog I and Q voltages from respective DACs (**1050**A, **1050**B) are then smoothed using respective low-pass filters (**1060**A, **1060**B) which may be deliberately engineered, or may be a collection of incidental bandwidth restrictions produced due to component frequency response limitations. Either way, the filtering needs to be sufficient to contain the transmitted spectrum to meet the out-of-band limits specified by the frequency management authority. The filtered balanced I,Q signals then modulate quadrature carrier signals produced by quadrature local oscillator (QLO) **1070** (may also be referred to as a frequency generator) using a pair of balanced modulators (**1080**A, **1080**B) (may also be referred as I,Q modulators). The quadrature local oscillator may also be referred to as a carrier frequency generator operable to generate a carrier signal that is frequency modulated by the pair of balanced modulators (**1080**A, **1080**B). Furthermore, the I, Q waveform selection logic **1020**, the waveform memory **1030**, the digital-to-analog converters **1050**A, **1050**B, the low pass filters **1060**A, **1060**B, and the balanced modulators **1080**A, **1080**B may be collectively referred to as the modulator. Gilbert-cell mixers using 28 nm MOSFET transistors have proven capable of modulating an 80 GHz carrier signal with 2 GB digital code rates. Gilbert cell mixers driven by similar QLOs may be used in the radar receiver in order to produce zero-IF, homodyne receivers.

In a MIMO system, all transmitters and receivers preferably have a known phase relationship in order to allow the receiver outputs to be coherently combined by beamforming matrices. In one implementation, the desired phase relationship is guaranteed by injection-locking each transmitter and receiver's QLO (frequency generator) to a common standard. For a millimeter wave radar operating around 80 GHz, the common standard may be a sub-harmonic of the desired millimeter wave frequency, such as ⅕th or 16 GHz, at which frequency it is easier to fabricate an accurate digital frequency synthesizer or generator to give programmable center or mean frequencies.

The modulated signal at the radar carrier frequency is amplified to a transmit power level in constant envelope power amplifier (PA) **1090** which also operates push-pull (i.e., balanced). The push-pull PA **1090** is cross neutralized to reduce Miller feedback, improve the high frequency gain and reduce the S12 parameter. On-chip Balun transformer **1095** may be used to convert the push-pull signal to single ended to bring the signal off-chip through a ball-bond surrounded by grounded ball-bonds.

FIG. **6** is a graph illustrating the typical eye diagram of the I and Q parts of the transmitted carrier using Gaussian minimum shift keying (GMSK) when no limit is placed on the number of stored waveforms; that is, each transition can depend on as much past history as the impulse response length of the selected Gaussian filter exhibits. For FIG. **6**, a Gaussian filter with BT=0.3 was used. A filter with BT=1 means the −3 dB bandwidth is equal to the chiprate, and BT=0.3 means the 3 dB bandwidth is 0.3 of the chiprate. Moreover, in common with the definition of GMSK used in the GSM system, the Gaussian premodulation filter is not fed with square waves (with a polarity equal to the bit values), but by impulses of unit area (with polarities given by the bit values). A square wave bit stream already has an implied sin(x)/x frequency-response shaped filter that shapes the waveform from impulses to square waves, and it is desired to investigate the performance of filters that are not constrained to include this inherent sin(x)/x factor.

FIG. **34** illustrates a flow chart that was used to compute the waveforms of FIG. **6** and subsequent graphs. An 8-bit linear feedback shift register was used to generate a maximum length sequence of 255 bits at step **1**, and the sequence extended to 256 bits by adding one more bit to obtain a power of 2 bits. If the added bit is a zero, the extended 256 bit sequence will have an equal number of 1's and 0's.

At step **2**, each bit is placed in the center of a group of NSPB samples with the other samples zero, to represent an impulse having the desired bit polarity. The bit values are multiplied by NSPB to give the impulse unit area. The number of samples per bit is also chosen to be a power of 2, that is 4, 8, 16, 32, 64, 128 or 256, so that the total number of samples is a power of 2 equal to 1024, 2048, 4096, 8192, 16384, 32768 or 65536. The purpose is to allow the use of a fast, base-2 FFT at step **3** to produce the spectrum of the unfiltered impulse waveform. At step **4**, the spectrum is weighted by the frequency response of the shaping filter, e.g., a Gaussian filter. The filtered frequency modulating waveform must be integrated to obtain the phase waveform. This is conveniently done in step **5** while the signal is still in the frequency domain by dividing each spectral line by j times its own frequency. When the whole sequence is 256 bits long, the line spacing is 1/256 of the bitrate, so the frequency of each spectral line is simply determined. At step **6**, an inverse FFT produces the time waveform from the filtered and integrated spectrum.

At any point before step **7**, a suitable scaling is applied so that the desired frequency deviation or modulation index is obtained. At step **7**, the I,Q waveform is computed by taking the cosine and sine of the phase modulation samples, which also has the effect of reducing the phases modulo-2π. At this point, if the I,Q waveform does not join up end-to-end, a phase slope may be applied across the I,Q waveform to force it to join up end to end. This is equivalent to a very small frequency shift which can be used later if necessary to ensure that any filtering is correctly centered. The purpose of ensuring end-to-end continuity is that the FFT at step **10** assumes a cyclic waveform, without which artifacts may appear on the spectral sidelobes so calculated.

At step **8**, the eye diagram is plotted, and manually a phase adjustment is determined that brings the eye diagram into focus such that maximum eye-openings of the I and Q bits are obtained and so that all trajectories converge to the minimum number of different I and Q waveforms.

At step **9** the correlation function and autocorrelation functions may be calculated and displayed, and then the spectrum calculated at step **10** is displayed at step **11**.

The flow chart may be extended to add other filtering such as the low pass filters **1060**A and **1060**B of FIG. **5**, and receive filtering, and the effect on eye diagram, correlation function, and spectrum may be calculated and displayed as at earlier steps.

Note that in order to display an eye diagram having the best eye openings that best indicate the values of the modulating symbols, it may be necessary to determine a common phase rotation to be applied to all I,Q values to remove any phase shift that may be an artifact of the program simulating the modulation. In the simulation program used to produce the results herein, this common phase artifact was determined to be equal to ⅝ths radians, and so the waveform was rotated by −⅝ths radians at step **8** to display the best eye openings.

After applying the above phase shift, by inspection there appear to be eight possible I,Q waveforms except at the position marked X on the rising flank and its corresponding position on the falling flank. The number of waveforms is simply determined by drawing a vertical line at any time point and counting the number of distinct trajectories that cross it. The number is four each for I and Q near the center of the I-eye or Q-eye for a total of eight, but they diverge slightly to 16 in the vicinity of point X. That means that the waveform at point X depends on four bits, while the waveform at other times depends only on three bits. The best phase shift mentioned above will be found to reduce the number of trajectories to a minimum by converging trajectories that were otherwise apparently divergent due to the phase shift produced by the modulating program. Manually adjusting the phase shift while observing the eye diagram will be seen to bring the picture into focus.

The number of bits on which the waveform depends can also be seen by computing a correlation between the output waveform and the modulating chip code. At this point it is necessary to explain the relationship between the digital code chip polarities and the polarity of the I value at the maximum I-eye opening and likewise the polarity of the Q-value in the center of its eye. When digital frequency modulation using MSK or GMSK is employed, each modulating bit polarity determines whether the I,Q vector rotates clockwise or anticlockwise by 90 degrees over the bit period. Thus, after two bit periods, the I,Q vector will have rotated by either 0 or 180 degrees. In between, the vector lies at either 90 or 270 degrees. Thus, the polarity of even bits determines whether the vector will end up at 0 or 180 degrees and the polarity of odd bits determines whether the vector will end up at 90 or 270 degrees. However, the effect is cumulative, as shown in the table below:

1	0	0	1	1	1	0	0
90	0	−90	0	90	180	90	0

In the above table, bit number **1** is a 1, sending the phase clockwise from an assumed zero starting value to +90 degrees. The second bit is a zero, sending the phase counterclockwise 90 degrees back to 0. Bit **3** is a 0, sending the phase 90 degrees counterclockwise to −90, and so forth. Thus, the relationship between phase and frequency-modulating bit sequence is:

$$\phi n = \mathrm{mod}\ 2\pi[\Sigma\pi Bi/2],\ i=0 \text{ to } n \tag{1}$$

This may also be written as:

$$\phi n = \mathrm{mod}\ 2\pi[\phi n-1+\pi Bn/2] \tag{2}$$

Thus, if a 2-bit state variable is used to keep track of where the phase ended up last time (that is, the value of φn−1), then the phase at the end of the current period can be determined from equation (2).

In the GSM digital cellphone communications system, a simpler relationship between I,Q polarities and modulating bits was arranged by the use of precoding. If the desired modulating chip code is designated Ci, then modulating bits Bi are derived from the desired modulating chip code Ci, according to the precoding equation (3) below:

$$Bi = C_i.\mathrm{xor}.C_{i-1} \tag{3}$$

The relationship between Bi, Ci, phase, and I,Q peak value polarities may be seen in the following table:

C	1	0	1	1	0	1	1	1	0
B	1	1	1	0	1	1	0	0	1
Phase	90	180	270	180	270	0	−90	−180	−90
I + jQ	j	−1	−j	−1	−j	1	−j	−1	−j
$-j^n$ (I + jQ)	1	−1	1	1	−1	1	1	1	−1

The final row is derived by multiplying the penultimate row of I+jQ values by $-(j)^n$. The result of this systematic progressive phase twist, which increases at 90 degrees per bit, is to throw the Q values up into the real plane, making all values real and in agreement with the original C-values. In GSM, this progressive twist is applied at the receiver so as to reproduce the code C generated at the transmitter. Without the progressive twist, it may be seen from the I+jQ values that the sign progression of I bits is

−1 −1 1 −1 compared to the corresponding bits of C −1 1 1 1

showing that there is a sign alternation. The same is true for Q bits

j, −j, −j, −j, −j compared to 1, 1, −1, 1 −1

Therefore, an alternative method of ensuring that the signs of I alternating with Q at the receiver correctly reproduce the intended code C would be to flip the signs of the C bits at the transmitter according to the pattern:

+ + − − + + − − + + − − + + − − . . .

Consequently, there are optional methods for ensuring that the chip sequence C produced by the code generator **1010** at the transmitter is reproduced at a point in the receiver chain where it can be correlated with a locally generated replica of C. If this is not done, then correlation at the receiver must use the expected signs of I and Q. The autocorrelation sidelobe characteristics when using the latter method will not be the same as the autocorrelation characteristics of code C, but of code C with bits flipped according to the above alternating sign pattern. To obtain autocorrelation characteristics intended by design, it is necessary to ensure that the receiver correlates with a code having the desired characteristics, and this is ensured by the use of appropriate transmitter precoding in the I,Q waveform selection logic unit **1020** paired with the correct signal treatment at the receiver. The method chosen for the transmitter, i.e., any desired precoding, is built into I,Q waveform selection logic **1020**.

Using GMSK, the frequency pulse shaping produced by the Gaussian filter may have an effect beyond the current chip. The phase change produced over one chip period by GMSK frequency pulses may fail to reach 90 degrees over one chip period, but when integrated over all chip periods affected by a given chip, the cumulative phase change to the signal produced is exactly +90 degrees so that the four principal terminal positions of the signal vector remain fixed and do not slowly rotate. This characteristic is maintained in this invention for all frequency pulse shapes considered by constraining the area integral of a frequency pulse shape over its entire impulse response length to be a fixed value.

When the receiver is on the same silicon chip as the transmitter, the local replica for correlation is simply derived from the code generator **1010** by delaying it if necessary.

When the precoding of equation (3) is applied at the transmitter, and the receiver applies a systematic progressive 90 degree per chip twist to received signal samples, the twisted samples may be correlated with the shifts of the code C produced by the code generator **1010**. If the receiver samples the received signal at N samples per chip, then selecting samples (e.g., 0, N, 2N, 3N), progressively twisting the samples and correlating with shifts of the code C, produces points on the correlation function (e.g., 0, N, 2N, 3N). Then, selecting points 1, N+1, 2N+1, 3N+1 etc., progressively twisting them and correlating with C, produces points 1, N+1, 2N+1, 3N+1 etc. of the correlation function. Continuing in this way produces the correlation function for all relative time shifts in steps of 1/N of the chip period.

The above described correlation function is illustrated in FIG. **7**. The magnitude is plotted in dBs, and the horizontal divisions are one chip periods. This function is the correlation of the transmitted signal with the corresponding digital code, or equivalently it is the correlation of the received signal with the transmitted code when the receiver does not add additional filtering. Such a wideband receiver is undesirable however, as a bandpass filter is required to limit noise.

The correlation function of FIG. **7** illustrates that, for sampling in the center of the eye, the peak correlation is unity as it just reproduces the mean power of the signal which has been set to unity, and the correlation at +/−1 chip period is about −14 dB. The correlation at +/−2 chip periods is −80 dB, so the transmitted signal depends substantially only on 3 consecutive bits when sampled at the center of the eye. This is exactly in correspondence with what can be seen in in FIG. **6**. If however, the signal is mis-sampled by half a chip period, the correlation magnitudes are shown in the table below:

−1.5 chips	−0.5 chips	+0.5 chips	+1.5 chips
−39 dB	−4 dB	−4 dB	−39 dB

The above table shows that a 0.5 (one half) chip mis-sampling results in a signal that depends on 4 chips. The correlation +/−2.5 chips away is however zero. This also corresponds with what may be seen in FIG. 7 at point X, where the signal has 16 different trajectories corresponding to a dependence on 4 chips.

The receiver however cannot remain wideband. The noise bandwidth must be limited. One way of limiting the bandwidth is to use a matched filter, which is known to achieve maximum signal-to-noise ratio. A matched filter corresponds to correlating the signal with the complex conjugate of itself. This produces the autocorrelation function (ACF). The ACF for the same signal is shown in FIG. 8.

FIG. 8 shows that with optimum sampling, the ACF at +/−1 chip period is about −7 dB and is +/−31 dB at +/−2 chip periods. The signal now therefore depends somewhat on five consecutive chips due to the additional ISI introduced by matched filtering. With half a chip mis-sampling, the ACF has the values shown in the table below.

−2.5 chips	−1.5 chips	−0.5 chips	+0.5 chips	+1.5 chips	+2.5 chips
−53 dB	−17 dB	−2 dB	−2 dB	−17 dB	−53 dB

With half a chip mis-sampling, the signal is showing a dependence on either 4 chips or 6 chips, depending on whether a correlation level of −53 dB is significant in the application.

In a communications system, correlation values on the order of −30 dB are not of significance because they do not significantly affect information error rates. In a radar system however, a strong target echo can easily be 30 dB above a weak target echo two chips away. Therefore, achieving low autocorrelation sidelobes is of greater importance in radar applications. If autocorrelation sidelobes remain high several chips away, strong target subtraction may then be necessary to reveal weaker target echoes with neighboring ranges. The complexity of strong target subtraction may therefore be reduced or eliminated entirely if correlation sidelobes can be adequately suppressed.

A number of ways of reducing autocorrelation sidelobes will now be discussed. Firstly, it may be acceptable to use a slightly wider filter than the matched filter in the receiver. To get an idea of suitable receiver bandpass filter bandwidths, the spectrum of the signal shown in FIG. 9 is used. The horizontal divisions are 0.5 times the chiprate. The −3 dB bandwidth is approximately +/−0.25 times the chiprate, about the same as the Gaussian premodulation filter. Therefore, a Gaussian filter of the same BT factor can be contemplated for the receiver filter.

FIG. 10 illustrates correlation sidelobes using a Gaussian receive filter with BT=0.3. There is a 1.05 dB loss of power though such a filter and a 2 dB loss in peak correlation. However, the noise bandwidth of the filter is only 0.63 bitrates, which is a reduction of 1.95 dB, substantially compensating for any loss of signal power and correlation magnitude. The signal-to-noise ratio is therefore about the same as with a matched filter correlator. The sidelobes however are now reduced from −31 dB at +/−2 chips, using the matched filter, to −37 dB relative to the peak of correlation. The signal-to-noise ratio effects and the correlation sidelobes can now be explored as a function of the receiver's BT factor. FIG. 11 illustrates how the sidelobe levels at +/−0.5 chip, +/−1 chip, +/−1.5 chips, +/−2 chips and +/−2.5 chips depend on receiver filter BT. Also, the noise bandwidth and peak correlation loss are shown, and combined to show the SNR loss involved in choosing higher receiver BT factors to reduce correlation sidelobes. The correlation at +/−0.5 chip has the practical significance that it represents the loss of peak correlation that occurs due to a target echo arriving with a delay that is a non-integral number of chip periods. FIG. 12 shows the latter as well as noise bandwidth, peak correlation loss, and net SNR loss on a finer dB scale.

Many other filter responses could also be explored, such as boxcar filters, Bessel filters and the like, and the number of cases that can be explored are too numerous to address in this application, the purpose of which is directed more towards choice of modulation, which is a transmitter question rather than a receiver question. Attention is therefore turned to what can be done on the transmitter side to reduce correlation sidelobes.

FIG. 7 shows that the correlation function for GMSK with BT factor=0.3 essentially has a 5-chip spread. A 4-chip spread is evident from the 16 trajectories visible in FIG. 6, but the 5th chip dependence is there, only too small to be visible by the naked eye on the eye diagram. Were it not for the divergence of the trajectories at location X in FIG. 6, there would be no more than 8 trajectories and therefore only 3 chips of correlation spread. The waveform may therefore be handcrafted to converge these trajectories to a total of 8.

The first step in handcrafting the waveform is to compute, for a given group of three chips within +/−1 chip of a waveform point, the average of all waveform values over the four other combinations of the two chips at +/−2 chips away. The average waveform points are intended to be stored at a given number of samples per chip in waveform memory (**1030**) of FIG. 5 for all 8 combinations of the group of three chips, and selected from memory when those 3 chip values are presented as address a**2**,a**1**,a**0** from waveform selection logic (**1020**). Now the waveforms exhibit many symmetries, such as I/O symmetry, time-reversal symmetry, and +/−symmetry, but for very high chiprates such as 2 GB/s it can be more burdensome to try to exploit those symmetries to reduce the memory size than to merely accept the full memory size. At lower chiprates, exploiting the symmetries might result in a net reduction of silicon area.

FIG. 12 illustrates the eye diagram of GMSK with BT=0.3 when the above waveform averaging has been done to constrain dependence to 3 successive chips. It may appear that the 4-chip dependence at point X of FIG. 13 has not been entirely eliminated. However, the correlation function of this waveform is shown in FIG. 14, and indicates that indeed there is a precipitous drop on the chip dependence beyond +/−1 chip. Substantially, 3 chip-only dependence is maintained for target echoes with up to +/−0.5 chip mis-sampling.

The apparent failure to get rid of the anomalies at location X in FIG. 6 is an artifact of the graph plotting program. There are in fact only 2 possible waveform points on each side on each anomaly, but the graph plotting program draws lines joining either one of the leftmost points to either one of the rightmost points by linear extrapolation. Nevertheless, a receive filter would do precisely that, and so it is desirable to remove this discontinuity. This arises because the three chips on which the leftmost waveform values depend are for example b**2**,b**3**,b**4** and then this changes suddenly to a dependence on b**3**,b**4** and b**5**, as they are now the nearest chips to the rightmost point. In order to avoid this discontinuity, those specific points at location X of the anomaly may depend only on the overlapping symbols b**3** and b**4** and may not depend on either the oldest bit b**2** of the previous symbol shift nor the newest bit b**5** of the subsequent symbol shift, but must be converged to a total of four points depending only on b**3** and b**4**.

The effect of such a waveform discontinuity is clearly seen in the spectrum of FIG. 15. While the correlation function has been improved, the far-out spectral sidelobes have risen from a −150 dB level to a −70 dB level. This is to some extent inevitable, as the power spectrum is the Fourier transform of the autocorrelation function; however, eliminating the discontinuity should not degrade the correlation function but should improve the spectrum.

While producing the waveform of FIG. **13** was readily automated, eliminating the discontinuity in FIG. **13** is truly more akin to handcrafting. The reason is, if the points at location X of the anomaly are replaced with their average, this will cause a discontinuity with the preceding and following points. Therefore, a smooth modification of the curves along their whole length is required to force convergence at the four points X. This may be achieved by the following procedure.

In step **1**, two values at the left-hand side of the anomaly are designated as a**1** and b**1** and those on the right are designated as a**2** and b**2**. The values of notional points midway between the left and right points on their respective waveforms are computed as $a_{1.5}=(a1+a2)/2$; and $b_{1.5}=(b1+b2)/2$.

In step **2**, if the value of $a_{1.5}$ is the greater and the value of $b_{1.5}$ is the smaller, the factor $1+\alpha$ is computed, by which waveform a must be reduced and waveform b increased at that notional point to force convergence, as:

$$(1+\alpha)b_{1.5}=a_{1.5}/(1+\alpha) \tag{4}$$

$$\alpha=\sqrt{(a_{1.5}/b_{1.5})}-1$$

Now, it is desired that the above factor should modify the waveform at the desired point of convergence, but that the factor should gradually diminish to unity at the center of the eye and at the ends where the waveforms are already acceptable.

This is done by applying a factor $1+0.5\alpha(1-\cos(\theta))$ to modify the waveform points, where θ varies from 0 to 180 degrees along the waveform from each end to the middle. This factor is unity at the ends and in the middle, but is the desired factor $1+\alpha$ at the anomaly.

FIG. **16** illustrates an exemplary correlation function of the waveform when handcrafted as explained above. The chip-dependence outside of +/−1 bit descends even more precipitously than before. FIG. **17** confirms that the discontinuity has been removed by handcrafting, and FIG. **18** shows that the far-out spectrum has been reduced about 10 dB. Of course, the far-out spectrum may be further reduced by the low-pass roofing filters (**1060**A,B) with the reintroduction of some sidelobes of the correlation function. To avoid such sidelobes becoming troublesome, the filter cutoff frequencies should be, for example, Gaussian filters with a BT in the 1.5 to 3 range. A sharp filter will produce more ringing and simulation has shown that a sharp cutoff of about 3 times the bitrate keeps the ringing on the ACF down to about the −70 dB level.

If it is desired to further reduce the correlation sidelobes, one method of achieving this is to increase the BT of the GSMK modulation. However, this is a straight choice between spectral sidelobes and correlation sidelobes. The resulting waveforms must be handcrafted anew for each choice, and sufficient information has been disclosed above for a person skilled in the art to analyze such a choice for a particular application. Attention is thus now turned to alternative waveforms that can be useful in an exemplary automotive MIMO radar system, and which may reduce correlation sidelobes further while achieving a better compromise with spectral sidelobes than GMSK.

GMSK waveforms have a 3-symbol dependence because of the 8 trajectory waveforms that may be seen in FIGS. **6**, **12**, and **17**, even at the optimum sampling point. GSMK has that characteristic because an I-bit lying between two Q bits of equal polarity cannot achieve full amplitude as there is no Q zero crossing between the two equal Q-bits. If Q is non-zero, I cannot be unity due the constant envelope constraint where $I^2+Q^2=1$. The peak value in the center of the I-bit may in fact be predicted to be:

$$I\text{peak}=+1,\ \text{if}\ (Q1.\text{xor}.Q2)=1 \tag{5a}$$

$$I\text{peak}=+\sqrt{(1-|Q\text{min}|^2)},\ \text{if}\ (Q1.\text{xor}.Q2)=0 \tag{5b}$$

In order to have single-chip dependence in the middle of the eye, Qmin must therefore be zero, that is, the Q waveform should go to zero between two Q bits, even when they are the same.

FIG. **19** introduces some new diagrams that assist in understanding constant-envelope, digital modulation.

The trellis diagram in FIG. **19** indicates how the phase changes when the frequency is modulated according to the frequency modulation waveform illustrated below the trellis diagram. Assuming that the phase at point Q−1 is −90 degrees, the first frequency step up to +dF causes the phase to change at the rate of $2\pi\cdot dF$ radians per second. If dF=0.25B=0.25/T, where B is the bit rate or chip rate and T is the reciprocal of B, namely the chip period, then the phase change over one chip period from Q−1 to Io is exactly 90 degrees, so that the phase moves from −90 to 0 from point Q−1 to Io. If Q1 is also encoded into a +dF frequency shift, the frequency remains at dF for a further time T and the phase changes by a further 90 degrees to the value +90 degrees at point Q1. The constellation diagram shows by asterisks where the phase ends up at points I0,Q1,I2,Q3, etc. Points denoted by In have terminal phases that are either 0 or 180, where the real part of the complex vector is +/−1 corresponding to the maximum eye-opening of the real part I, while the imaginary part goes to zero corresponding to a zero crossing of the imaginary part, Q. Correspondingly, constellation points denoted by Qn have terminal phases that are either +90 or −90, and the I-values go to zero at those points.

In FIG. **19**, the frequency deviation is either +dF or −dF and changes abruptly from one value to the other, while the phase changes at a constant rate from one constellation point to the next. This modulation is known as "minimum shift keying" (MSK), and has the eye diagram illustrated in FIG. **20** and has the spectrum of FIG. **21**. The spectral sidelobes are seen to be of the order of 15-20 dB higher than those of the handcrafted GMSK modulation illustrated in FIG. **18**, due to the absence of filtering to round the waveform transitions. The eye diagram illustrates a small anomaly at zero crossings which is partly an artifact of the graph-plotting program interpolating between the finite number of samples (16 in FIG. **20**) used per bit period. Nevertheless, this is exactly what will occur in a receiver bandpass filter and affects the resulting correlation function. The correlation function is therefore plotted in FIG. **22** with the number of samples per chip varying from 8 to 256, in factors of 2. It can be seen that the limit, for a large number of samples per bit, corresponding more closely to a continuous waveform, is a correlation function that falls precipitously to zero at +/−1 chip offset. With precise mid-eye sampling, the waveform therefore depends on only one chip, but with mis-sampling it depends on two adjacent chips, one I-chip and one Q-chip, as may be seen in the eye diagram of FIG. **20**. This is a reduction of GMSK's 3-chip dependence with mid-eye sampling and 4-chip dependence (or 2-chip, with handcrafting) with mis-sampling, although this only seems to be achieved with a large number of samples per bit. Using 8 samples per chip, and with ½-chip mis-sampling, the waveform may be seen from the correlation function value at +/−1.5 chips to depend on two additional bits that have an influence at the −60 dB level. This drops to −70 dB using 16 samples per chip and continues to reduce with greater numbers of samples per chip. However, further research shows that the skirts of the correlation function with small numbers of samples per bit were due to slight numerical inaccuracies that made the waveforms slightly different in dependence on past history. Handcrafting by averaging the corresponding points in the eye diagram, storing the averaged values in a waveform lookup table (e.g., memory **1030** of FIG. **5**), and then using the average points, results in the sidelobe skirts being eradicated, which is illustrated in FIG. **27** for 8 samples per chip and in FIG. **28** for as few as 4 samples/chip.

It is desirable to reduce the spectral sidelobes far away from the main lobe to a level lower than what unfiltered MSK achieves. This should be accomplished by not changing the frequency abruptly between +dF and −dF but rather by using a smoother transition. If smoother transitions are produced by low-pass filtering the frequency modulating waveform, this is tantamount to using GMSK and will re-introduce additional intersymbol interference (ISI or correlation sidelobes). To obtain a different result, shaping is used rather than filtering. The shaped waveform can be made the same for each chip and independent of the value of a preceding or following chip, thereby achieving spectral improvement without the addition of correlation sidelobes (aka ISI). Moreover, to ensure that the phase ends up at the same constellation points of +/−90 or 0/180 after each chip, and not a value depending on chip history, the area under the shaped frequency waveform must remain the same value of dF×T=0.25. FIG. **23** illustrates that a raised cosine frequency pulse that peaks at 2dF has this property. FIG. **24** illustrates the eye diagram for this modulation and FIG. **25** illustrates the spectrum, demonstrating the more rapid fall of the spectral sidelobes as a result of the raised cosine shaping. The correlation function before handcrafting the waveform is illustrated for 16 samples per chip in FIG. **26**. After handcrafting the waveform by averaging all corresponding points to form a waveform memory and using the waveforms from memory, the correlation function remains substantially ideal down to as few as 4 samples per chip, as illustrated in FIG. **29**.

The effect of receiver filtering when the transmitter uses handcrafted raised cosine digital FM is now illustrated in FIGS. **30** and **31** to compare with using GMSK, which was illustrated in FIGS. **11** and **12**. The practical significance of these parameters is as follows: If the radar system needs to implement strong target subtraction in order to unmask weaker target reflections that are close in both range and Doppler, then the complexity of the strong target cancellation procedure is proportional to the number of correlation sidelobes after the receive filter that are significantly strong. For example, if it is desired to cancel a strong target echo to a level of −60 dB relative its uncanceled value, then FIGS. **30** and **31** illustrate that, for a receiver filter BT factor of 0.53 that gives a 1 dB loss of signal-to-noise ratio compared to a matched filter, the correlation sidelobes at +/−1.5 chips are at a level of approximately −62 dB. Thus, canceling the principal lobe and sidelobes at +/−1 chip will result in a 62 dB suppression even with the maximum +/−0.5 chip mis-sampling. Compared with FIGS. **11** and **12**, the amount of suppression using GMSK would be approximately 48 dB. Thus, the raised cosine modulation provides a significant improvement over GMSK as regards to strong target suppression with a 3-tap interference canceler.

Other receiver filters can be considered, such as Boxcar filters, Bessel filters and the like, however, the present invention is more concerned with determining an optimum transmitter modulation. The transmitter modulation performances have therefore been compared using the same range of receiver filter characteristics, typified by a Gaussian filter with a range of −3 dB points relative to the chiprate determined by using various BT factors.

The choice of a raised cosine, as mentioned above, was arbitrarily based on it being a known smooth function. A consideration may also be made as to what other properties such a function should have for a radar application, with a view to producing optimized properties. FIG. **32** illustrates the shape of the exemplary class of functions to be investigated. The function is zero for a bit interval of 0.5<x<−0.5, will have unity area, so as to equate to a unit area impulse in terms of the phase change it will cause when used as a frequency modulating waveform, and will have as many zero derivatives as possible at +/−0.5. As the function will be multiplied by the bit polarities, when the bit polarity changes at x=+0.5, any non-zero derivative at that point flips in sign, exhibiting a step, and the next highest order derivative will therefore exhibit impulses. The ultimate rate of fall off of spectral sidelobes is 6N dB/octave when N is the order of the derivative of the waveform at which impulses first appear. Impulses have a flat spectrum, so working backwards, integrating N times will produce an increase in spectral roll-off slope by an extra 6 dB/octave for each integration. Therefore it is desired that the function should have as many zero derivatives as possible at x==+0.5 in order to avoid discontinuities when the function is flipped by the random sign of a code chip.

Therefore, given the criteria a function f(x) should satisfy, namely:

a. (i) Unit area when integrated from x=−0.5 to x=+0.5.
b. (ii) As many zero derivatives as possible at x=+0.5, and optionally
c. (iii) a prescribed not-to-be-exceeded value at x=0,

a set of simultaneous equations can be solved for the coefficients of a polynomial in $(x/2)^2$ that meet the above criteria, of which a few are plotted in FIG. **33**.

The polynomials found by the above method were of the form

$$ao+a1x^2+a2x^4+a3x^6 \tag{6}$$

with the following coefficients:

	a0	a1	a2	a3	a4
zero order	1				
first order	1.5	−1.5			
second order	1.875	−3.75	1.875		
third order	2.1875	−6.5625	6.5625	−2.1875	
fourth order	2.46094	−9.4375	14.76563	−9.4375	2.46094

FIG. **33** illustrates the shaping functions of second, third and fourth order that are computed without constraint (iii) above. However, if constraint (iii) is applied, curves with a peak frequency deviation limited to different values can be obtained for each order by giving up one of the zero derivative constraints (ii).

The effect on eye pattern, correlation sidelobes, and spectral sidelobes may also be explored to determine shaping functions that may be better in a given application (such as exemplified by the raised cosine shape discussed herein).

However, the over-exploration of different functions has limited merit because such a function will only be used for a limited number of samples per bit (e.g., 4, 8 or 16, and those 4, 8 or 16 values are going to be quantized to a limited number of bits of accuracy). When using N samples per bit, the spectrum is only defined out to +/−N/2 chiprates, and thus, small differences in the functions that cause higher or lower far-out spectral sidelobes may be masked by the time and value quantizations. Attention is thus turned to the effect of value quantization of the I,Q waveforms and methods to determine the best quantized values and how to digital-to-analog convert them.

When I,Q values of digital FM signals are computed to a high degree of accuracy, a constant envelope will be maintained, namely $I^2+Q^2=1$. When however, the I and Q values are quantized to integer values less than some maximum value, such as +/−31 for 6-bit quantizing, +/−63 for 7-bit quantizing, or +/−127 for 8-bit quantizing, it is not possible to guarantee that the squares of all pairs of integers sum to the same integer value, and thus, a constant envelope cannot be maintained exactly, and the quantized I,Q values will have both amplitude and phase errors. However, since the transmit power amplifier is hard limiting, the amplitude errors will be substantially shaved off, leaving only the phase errors. Therefore, in one exemplary embodiment, a higher priority when selecting quantized I,Q values is given to pairs of values that are closest in phase to the unquantized vector without regard to amplitude error. Too much amplitude error may not be acceptable, but seeking pairs of quantized I,Q values (Kx,Ky) that are closest in phase angle, where Kx is within +/−1 quantizing step of the closest quantizing to I and Ky is within +/−1 quantizing step of the closest quantizing to Q, should give lower spectral sidelobes after hard limiting. This was confirmed to be so. However, there are low-pass filters (**1060**A,B) after the digital-to-analog converters (**1050**A,B) of FIG. **5** that alter the modified I,Q values, so it is necessary to compute the merit of this alternative quantization after these filters are included. This was done using Gaussian filters with a −3 dB cutoff point of 2 bitrates, and it was found that it was still beneficial to search for quantized values within +/−1 LSB that best matched the phase of I,Q.

Mathematically, integer values (Kx',Ky') within +/−1 of (Kx,Ky) are sought for which:

$$(Kx'/Rk-I/R)^2+(Ky'/Rk-Q/R)^2 \text{ is a minimum}$$

where $Rk=\sqrt{(Kx'^2+Kx'^2)}$ and $R=\sqrt{(I^2+Q^2)}$.

The modified values (Kx',Ky') were found to give lower spectral sidelobes after filters (**1060**A,B) and hard limiting in the transmit power amplifier.

Another practical imperfection that can give rise to elevated spectral sidelobes is digital-to-analog converter (DAC) accuracy. If the DAC does not give equal steps, this can result in additional quantizing noise. In particular, if a strong signal cancellation unit attempts to mimic the quantizing in the transmitter in order to maximize cancellation, the differences between the transmit DAC and the model used for cancellation will result in less effective cancellation. To mitigate this, a special form of DAC may be used that effectively guarantees equal quantizing steps in the mean, and this is briefly described below.

An exemplary 8-bit DAC (**1050**A,B) comprises 256 nominally equal current sources, each of which can be turned on and off by logic fed via an 8-bit value. When the 8-bit value is zero, no current sources are turned on, and when the 8-bit value is 255, 255 current sources are turned on (with one current source remaining turned off). In one exemplary embodiment, the 256 current sources are arranged in a ring, with those that are turned on occupying a first segment of the circle and those that are turned off occupying the other part of the circle. Whenever a new 8-bit value is received, it is first determined whether more current sources will be turned on, or whether current sources will be turned off. If more current sources are to be turned on, the additional one(s) of the currently OFF current sources clockwise of the ON segment are turned ON, while if fewer current sources are to be ON, then current sources counter-clockwise of the currently ON segment are turned OFF. In this way, the ON segment of current sources and the OFF segment of current sources continuously rotate giving all current sources equal use in the mean for contributing to every desired analog value. Moreover, the time between a current turning on and off is maximized, thus reducing the effect of any speed limitations. In this way, the error spectrum in the mean is zero and is reduced for lower frequencies so that the error power spectrum is quadratic rather than flat with reduced total net error power. In one exemplary embodiment, the digital-to-analog converter (DAC) is also balanced, like much of the rest of the high-frequency circuitry for the reasons mentioned above. A balanced DAC would transfer a current from a "+ output" to a "− output" in dependence on the digital value, thus providing a bipolar conversion with the digital value represented in the difference of the currents at the + and − outputs.

Other methods for optimizing the spectrum can be attempted when the number of samples per bit used to represent shaped digital FM signals is small. For example, at 4 samples per bit, if the vector is starting out at the 90 degree position [(I,Q)=(0,1)] and heading for the 0 degree position [(I,Q)=(1,0)] in four steps, the first sample is (0.1), the middle sample, no. 3, is at 45 degrees (0.7071,0.7071), and the 5th sample is (1,0). Only samples 2 and 4 remain to be defined and symmetry dictates that sample 2 is the same angular displacement from 90 degrees as sample 4 is from 0 degrees. Therefore, there is only one variable that can be explored to reduce spectral sidelobes.

Alternatively, the sample instants can be displaced by half a sample either side of the +/−90 and 0/180 points. The displacement is then a first variable and the angular position of the samples on either side of the 45 degree points is then a second variable. The spectrum can now be explored and optimized as a function of those two variables. The correlation function may be broader for this alternative, however, as the constellation points all depend on two bits and never only one.

Yet again, it can be beneficial if the vector dwells for two samples around each of the +/−90 and 0/180 degree points. The latter case was investigated and the values optimized for best spectrum, giving the following I,Q values quantized to 8 bits accuracy are listed below:

I	Q
0	127
52	117
117	52
127	0

The above values are used either with a + or − sign depending on the I and Q bit polarities required. It will be seen that the values (0,127) or (127,0) are repeated twice at the junction of two successive bits.

When sampling as coarse as 4 samples per bit, it is necessary to have a sharper cutoff in the post DAC filters to suppress sidelobes beyond +/−2 bitrates; for example, a Gaussian −3 dB cutoff in the region of 0.8 bitrates. Moreover, after hard limiting in the power amplifier, the correlation sidelobes were improved compared to using higher cutoff frequencies. The eye diagram, when using the above I,Q values, is illustrated in FIG. **35**. The spectrum with a Gaussian post DAC filter BT factor of 0.8 is illustrated in FIG. **36**, while the correlation sidelobes are illustrated in FIG. **37**.

With 8 samples per bit, if the starting and ending sample values are as above at 90 degrees and 0 degrees respectively, then the middle sample 5 will be 45 degrees and samples 2, 3, and 4 will be at the same angles from 90 degrees, as samples 8, 6, and 7 will be from 0 degrees, so there are three variables to explore. Defining the quantity to be optimized, for example, as the total spectral energy beyond an exemplary +/−1.5 bitrates, it is within the computational capabilities of a PC to explore this as a function of three variables within a reasonable time if so desired.

Several methods have been discussed for optimizing a constant envelope modulation for use in a millimeter wave digital FMCW automotive radar with regard to the parameters that are important in such a system. The modulation is defined by a limited number of I,Q samples per bit, such as 4, 8, or 16, that are quantized in an optimum manner to a limited word length of, for example, 6, 7, or 8 bits. The I,Q samples are stored in memory (**1030**) from where they are recalled in dependence on the polarity of the modulation bits from a code generator, which may be precoded, and with regard to the current angular quadrant. Precoding and keeping track of the quadrant is performed by the state machine of I,Q selection logic (**1020**). The selected quantized I,Q samples are digital-to-analog converted using the above described analog-to-digital conversion techniques that shape the digital to analog quantization error noise to facilitate accurate subtraction of strong target echoes in the receiver by using a replica of the transmit modulator to generate a delayed, phase changed, and amplitude-weighted version that best matches the signal to be subtracted. The digital-to-analog converted analog signals are low-pass filtered by post digital-to-analog filters (**1060**A,B) and then a radar carrier signal is quadrature modulated at a desired center or mean frequency.

The exemplary embodiments disclosed herein cover many variations of constant envelope signals including GMSK, Raised Cosine shaped pulse-FM, and polynomial shaped pulse FM, and a person of normal skill in the art can derive many other variations using the principles exposed herein without departing from the spirit and scope of the invention as described by the attached claims.

Near-Field Interference Cancellation:

FIG. **38** illustrates an exemplary physical arrangement of an automotive radar installation that may use the modulation methods described above. Typically, a forward-looking radar may be mounted behind the front bumper (**1400**) of the automobile. The radar comprises a multi-layer microstrip printed wiring board **1200** on which a number of transmit and receive antenna elements **1300** are printed to form a multiple-input, multiple-output (MIMO) array. It may be shown that the NM signals received at N receivers from each of M transmitters can be treated as having been received from an array of NM virtual antenna elements, the virtual location of virtual antenna (i,j) being approximately midway between the location of transmit antenna j and receive antenna i. Thus, for example, a horizontal array of 8 receive antennas and a vertical array of 8 transmit antennas forms an 8×8 rectangular array of 64 virtual antennas, providing angular resolution in both azimuth and elevation. Moreover, it may be shown that a horizontal array of 8 receive antennas spaced 1.5 Lambda (wavelength) apart, combined with a horizontal array of 8 transmit antennas spaced 2 Lambda apart, form a virtual array of 43 elements spaced Lambda/4 apart. There are actually 64 elements, but some are co-located. There would be 43 distinct element locations. This is equivalent in directivity to a receiver array of 43 elements spaced Lambda/2 apart, because the phase slope across the array in a radar application is doubled due to the go and return paths undergoing the same phase shift. The virtual antenna signals may thus be combined according to a set of coefficients that would give a desired pattern for a 43-elements receive array with a Lambda/2 spacing, thus providing highly enhanced spatial resolution for the given total aperture and physical element count.

The printed microstrip board **1200** having the printed antenna elements also carries a semiconductor chip package **1100** that comprises all of the active transmitter, receiver, and digital signal processing circuitry. A large number of RF and digital I/Os are accommodated using a ball-grid array. A solder ball connection is moreover the only form of connection that provides a good chip-to-board signal connection for millimeter wave signals at 80 GHz. Each signal ball **1102** is surrounded by ground balls **1101** which are all connected together and to ground to provide the nearest thing to coaxial connections and to provide screening of one signal ball from another. Nevertheless, due to the small size of the package, the distance between transmitter signal balls and receiver signal balls (d**3**) does not provide perfect transmit-receive isolation, which is limited to perhaps −40 dB of unwanted on-chip spillover. This will be different for each transmitter/receiver combination as the distance d**3** is different for each. The small size of the printed microstrip board **1200** also limits antenna-to-antenna isolation, due to finite transmitter-receiver antenna separations (d**2**). This source of local near-field spillover may also be in the −35 dB region and will be different for each transmitter and receiver combination. In addition, the printed circuit board **1200** is mounted a distance (d**1**) behind the automobile bumper **1400**, and that distance d**1** varies due to curvature of the automobile bumper **1400**. Although the bumper **1400** is made of a nominally radar-transparent plastic, the discontinuity between its dielectric constant and that of air results in a finite reflection coefficient which will couple each transmitter signal to each receiver in varying amounts and with varying delays. The bumper reflection is likely to be the largest of the local interfering spillover signals at perhaps −30 dB worst case and is also likely to be of the greatest round-trip delay. It is also possible that there could be multiple reflections from a signal bouncing to and fro between the bumper **1400** and the printed circuit board **1200** or other car structure, although the level will reduce with each successive reflection. It may be necessary to remove multiple reflections later for optimum radar performance but this disclosure is concerned mainly with removing enough spillover in a first stage of spillover cancellation to avoid saturation or other non-linear effects in the analog and digital signal processing chain.

An exemplary signal processing chain of a receiver is illustrated in FIG. **39**. A dual input RF preamplifier **1110** has duplicated first stages of low noise amplification **1111** either of which may be enabled to accept an input from a first antenna element or from a second antenna element. The gain of the first stages **1111** is about 5 dB and the noise figure is about 5 dB. All inputs and outputs are differential and the amplifier stages are also all differential so as not to rely on the quality of a ground plane at 80 GHz. Where conversion from single-ended (unbalanced) to differential (balanced) is required, on-chip 80 GHz baluns are fabricated as single or 2-turn transformers using one or more layers of 10-layer metallization. Such transformers are also useful for applying a power voltage of 1 volt DC to the drains of 28 nm MOSFET transistors.

At such high frequencies, achieving gain is facilitated by cross-neutralization, so as to reduce the feedback scattering parameter (S12). Cross-neutralization of differential (push-pull) amplifiers is for the purposes of reducing the feedback term, also known as S12.

The first preamplifier stage selected to be active is followed by a second amplification stage **1112** of about 10 dB gain. The combined gain of the first **1111** and second **1112** gain stages of the preamplifier **1110** results in a total preamplifier gain of 15 dB, which is required to swamp the noise figure of quadrature downconverter (**1118**-A and **1118**-B) and the following stages.

The largest unwanted spillover signal is the reflection from the automobile bumper at about −30 dB maximum. With transmitters of +7 dBm, the spillover signal from each is thus −23 dBm. Since the transmitters transmit uncorrelated codes, the eight transmitters could occasionally combine to produce a peak voltage of 8 times that of a single transmitter, that is, 18 dB stronger, resulting in a peak interference level of potentially −5 dBm at the preamplifier input, although the mean power is only 9 dB stronger than that of a single transmitter. With 15 dB of gain, the output would have to be +10 dBm, which is beyond the maximum output level capability of 0 dBm of 28 nm transistors having a DC supply voltage of only 1 volt. Therefore, it is necessary to reduce the interference level by at least 10 dB to avoid saturation. Moreover, this reduction must be achieved early enough in the chain so as to catch it before it is amplified to an intolerable level. The latest point in the chain at which this can be done is after the first stage of preamplification **1111** where the peak interfering level does not exceed 0 dBm. Thus, the function of spillover cancellation unit **2000** is to produce an equal and opposite interfering signal which may be added to the output of the first preamplifier stage **1111** in order to cancel the interference before it hits a second preamplifier stage **1112**. Since saturation more often comprises running out of voltage swing rather than running out of current swing, it is useful if the interference cancellation signal **2001** is a current which is added to the output current of the first amplifier (**1111**) by means of a parallel connection, thus cancelling the current swing, and thus reducing the signal voltage swing.

Another factor to be taken into account is the limited dynamic range of analog-to-digital converters (ADCs) **1115**-A, **1115**-B from the quantizing noise floor to full scale. The cancelled level of interference must be kept below the ADC full scale code while the quantizing noise floor should be below thermal noise so as not to degrade the overall radar noise figure. The ADCs **1115**-A, **1115**-B are of 8-bit resolution which may be thought of as a sign bit plus 7 bits of magnitude, and operate at 2 gigasamples/second. A practical realization is nine ADCs operating with staggered sampling clocks, with a sampling rate of 2/9 GHz. The peak quantizing noise of a 7-bit ADC is ±+½ LSB, which is approximately 1/256 of full scale, or −48 dB, which may be considered to be distributed in frequency from 0 to half a sampling rate, that is from 0 to 1 GHz.

However, the distribution is triangular from 0 to ½ an LSB, which power-averages to another 5 dB lower. Thus, the noise floor is −53 dB below full scale for both the I converter and the Q converter, making −50 dB net referred to the RF domain. For this to be, for example, 6 dB below thermal noise, the greatest signal level, which is likely to be the unwanted interference level, must be no more than 44 dB above the thermal noise, so that, when the gain is adjusted to just result in the ADCs not reaching full scale, then the quantizing noise will be 6 dB below thermal noise.

To compare quantizing noise with thermal noise, the thermal noise level is evaluated in the same bandwidth as quantizing noise, of half the sampling rate, or 1 GHz, so their spectral densities may be compared. The noise level in a 1 GHz bandwidth at the input of first preamplifier stage **1111** is:

$$5\ \mathrm{dB}(NF)+10\ \mathrm{Log}^{10}(1\ \mathrm{GHz})\ \text{above}\ KT,\ \text{or}\ +5-173+90=-78\ \mathrm{dBm}$$

Thus, the quantizing noise referred to the input should be no more than −84 dBm. The full scale ADC level referred to the input is 53 dB higher than that, or −31 dBm. The peak interference level of +7 dBm+18 dB−30 dB=−5 dBm should therefore be suppressed by 26 dB so as not to exceed −31 dBm referred to the input. This is more stringent than the suppression required to merely avoid saturation. Moreover, there are other signals, which may be noise like to consider, thus suggesting that further headroom is needed and spillover suppression in the 30 dB range or more should be the target.

Note that the system performance may require much greater suppression of spillover than that required to avoid non-linear saturation or overload of the ADCs. However, if such effects are avoided before the ADCs convert the signal to the digital domain, a more intense signal processing algorithm can be devised in the digital signal processing domain in order to achieve a desired level of performance. For example, involving multi-pass signal processing with successive cancellation of signals in order from strongest to weakest.

The quadrature downconverters **1118**-A, **1118**-B of FIG. **39** are followed by analog filters **1116**-A, **1116**-B to restrict the bandwidth prior to the ADCs **1115**-A, **1115**-B, the effects of which, and suitable bandwidths for which were more fully discussed above, and by variable gain amplifiers (VGAs) that can have their gains set so as to match the signal level to the dynamic range of the ADCs **1115**-A, **1115**-B.

FIG. **41** illustrates an exemplary spillover cancellation unit **2000** with a more detailed internal configuration. FIG. **40** provides an additional illustration, by depicting an 80 GHz modulator using 28 nM MOSFETs in a Gilbert cell configuration. An I-modulator **2008**-A comprises a first Gilbert cell driven by anti-phase 80 GHz local oscillator signals from Quadrature local oscillator QLO **2007** which may be thought of as COS and −COS signals. However, the signals might be nearer squarewaves than sinewaves. The QLO also provides SIN and −SIN signals to a second Gilbert cell, Q-modulator **2008**-B. Differential I modulation signals are applied to an input of modulator **2008**-A and differential Q signals are applied to an input of modulator **2008**-B from respective differential DACs **2050**-A, **2050**-B, and the 80 GHz current outputs of the two Gilbert cells are paralleled to produce a differential interference cancellation output current signal that will be parallel-connected to the differential outputs of first stage preamplifiers **1111**. Gilbert cells **2008**-A, **2008**-B may operate with a constant tail current **I0** or be of the "class-B Gilbert cell." The differential I and Q

DACs **2050**-A, **2050**-B may have current or voltage outputs accordingly, as required by the type of Gilbert cell selected. It was described above in connection to FIG. **5** how DACs can be designed to shape their quantizing noise spectrum away from zero, so as to push quantizing noise outside the wanted signal spectrum.

FIG. **41** illustrates the configuration of the Spillover cancellation unit using a plurality of modulators **2200-1** to **2200**-*n*, such as those illustrated in FIG. **40**. Since each transmitter causes spillover by three separate paths, namely bumper reflection, on-chip coupling, and antenna-to-antenna coupling, which have different phase shifts and amplitudes, but may also have different delays, there may be the need to estimate three differently delayed and weighted versions or replicas of each of the eight transmitter signals and modulate each. Hence, in one configuration, there can be 24 modulators (**2200-1** to **2200-24**) in each spillover cancellation unit **2000**. The signal processing unit **2300** receives the known bit streams from each of the eight transmitters and numerically reconstructs an up-sampled, delayed, and weighted version of the (I,Q) values that are fed to the modulators. The numerical construction of the delayed and weighted versions or replicas of the transmitter signals can be considered as following a "recipe" for each version or replica, such that these versions or replicas serve as cancellation signals of the spillover caused by respective transmitters. Referring to FIG. **5**, the bit streams are the chip sequences c**1**,c**2**,c**3** from the transmitters' code generators **1010**. The DSP unit **2300** of FIG. **41** may comprise its own waveform memory **1030** and sample clock counter **1040**, the purpose of the latter being to provide the facility to finely adjust the delay in steps of one sample relative to the transmit timing. An advantageous method of applying the amplitude weighting and phase adjustment "recipe" is to pre-compute modified contents of the memory **1030** that is used in the spillover cancellation unit **2300** by multiplying the corresponding contents of the transmitter memory **1030** by a desired complex weighting constant. Because the weighting is expected to be constant for relatively long periods of time, this pre-computation of weighted memory contents can be done infrequently, such as during a power-up calibration phase and at suitable intervals thereafter. One of the spillover signals however, namely the bumper reflection, suffers from microphony (the transformation of mechanical vibrations into electrical noise) due to mechanical vibration in the 300 Hz region, which may require the weighting to be updated in phase at about 250 μs intervals in order to track the microphony-induced phase-modulation. Thus, the mathematical components and/or parameters of the waveform(s) (following the recipe(s)) for the cancellation of the transmitter spillover is stored in memory.

To reduce analog circuit complexity, another exemplary implementation reduces the number of FIG. **40** modulators to one, and sums the weighted cancellation signals for all three delays of all eight transmitters digitally first. In principle, the summed signal waveform could be stored in a single memory, such as waveform memory **1030** (illustrated in FIG. **5**), except that, if it depends on three bits from each transmitter, the total number of address bits for 8 transmitter codes of 24 would result in a very large memory. Thus, the scope for pre-combining spillover cancellation signals for more than one transmitter is a trade-off between memory size and the silicon area and power consumption of arithmetic logic circuitry. It is more practical however, to consider combining the spillover cancellation signals for one transmitter and its three paths, as the total delay spread (or ISI) of the modulation and the three paths may be only four bits, requiring 16 waveforms to be stored. FIG. **42** illustrates an exemplary spillover cancellation waveform generator **2000**, in which the I,Q spillover cancellation signals for each transmitter and spillover path are summed digitally within digital signal processing unit **2300** and the numerical sum of the I's and sum of the Q's (also known herein as the recipe) is output to a single modulator **2200**.

In FIG. **42**, the digital signal processing **2300** can use one waveform memory per transmitter per spillover path, which is a total of 24 waveform memories, the contents of each of which have been pre-multiplied by a respective phase and amplitude weighting factor. In this case, each waveform memory may store, for example, eight waveforms at a sample rate of 4 or 8 samples per chip of I and Q, optimally quantized to 8-bit values, for example. Alternatively, digital signal processing **2300** may comprise one waveform memory per transmitter to store the recipe for the composite waveform resulting from all three spillover paths for that transmitter, with the waveform memory now storing 16 waveforms addressed by four consecutive modulating bits, at a sample rate of 4 or 8 samples per chip, and quantized likewise. Delay adjustments can occur by a combination of selecting the optimum shift of the 3 or 4 transmitter bits to address the memory, delaying the output samples by one or more samples at the output sample rate, and computing the contents of the waveform memory to be a sample sequence shifted by up to +/−half a sample, by for example, interpolation. Thus, a continuous range of delay adjustment is available in steps of one chip, one sample, and a fraction of a sample.

FIG. **43** illustrates the arrangement when there is one waveform memory **2330**, per transmitter, per path. While only one waveform memory **2330** is shown, all 24 being substantially identical, their outputs are digitally added and truncated to the word length of DACs **2050**-A, **2050**-B before outputting. The chip stream that will modulate the associated transmitter enters shift register **2301**, which provides delays of a few chips. Whole chip delay selector **2302** selects the best shift of three consecutive bits to use for each spillover path for the transmitter. A common shift register can in principle be used for all spillover paths, each having its own whole-chip shift selector **2302**, if necessary. It is possible that only one spillover path, the bumper reflection, requires a shift of one whole bit, so it may only be necessary to have a whole-chip shift selector for that one path. Whole-chip shift selectors **2302** receive data selecting the shift to be used from a control processor that establishes the best shift during system calibration.

The 3-bit shift selected by each selector **2302** addresses waveform memory **2330**, which has its contents optimized and loaded during system calibration. The contents waveform memory **2330** are pre-weighted by multiplication with a complex weighting factor. It was previously mentioned above that in order to obtain a sample readout rate of 4 or 8 times a 2 GHz chip rate, it may be necessary to multiplex slower memories. Thus, the memory may consist of 4 or 8 memories, each outputting one of the 4 or 8 samples per chip of I or Q. The I value and companion Q value may be stored in parallel memories. An I multiplexer **2304** rotating at the sample rate selects the sample from the appropriate memory, and likewise, a ganged Q-multiplexer rotating in synchronism selects the companion Q-sample. A finer time delay than one chip can be obtained by advancing or retarding the rotation of the multiplexer **2304** by a number of whole samples by adding or subtracting a whole sample delay number in unit **2303** from the sample select index provided by the sample counter **2340**. Sample counter **2340** is a 3-bit counter when using 8 samples per chip, a 2-bit counter when using 4 samples per chip, or a 4-bit counter if using 16 samples per chip, and multiplexers **2304** are correspondingly 8, 4 or 16-way multiplexers.

Other design details relevant to FIG. **43** are omitted for brevity, but it is pointed out that, if it is desired to provide fine timing adjustment by sample selection over the whole range of +/−0.5 chips, then steps must be taken to synchronize the address change into memory **2330** according to the number of samples shifted; for example, the address for the memory storing sample number 8, the latest in a sequence, may change 8 samples later than the address change into the memory storing samples number 1. This issue may be avoided in the alternative solution illustrated in FIG. **44**, which shows one waveform memory **2330** being used to store the composite spillover cancellation waveform for all three paths of a transmitter.

In FIG. **44**, a whole-chip delay selector is now programmed to select the best shift of four consecutive transmit chips, based on the assumption that the total delay spread of all spillover paths, plus the ISI of the modulation, is within four chips total. The selected 4-bit shift now addresses waveform memory **2330** which is loaded with 16 different waveforms. Each waveform is the sum of the separately delayed, amplitude and phase-weighted spillover signals for any number of spillover paths, providing that the delay spread of all paths, plus the delay spread or ISI of the modulation, is within 4 chips total. It is no longer necessary to provide the selection of a number delays, as the stored waveforms can be pre-shifted by any amount within +/−half a chip. For example, the waveform of a given spillover path can be computed to depend on only the first three of the four selected bits or only on the last three, which represents delay extremes of +/−half a chip about a center value. Waveforms for a delay value in between: simply use the first m samples of the waveform corresponding to the first 3 of the 4 selected bits and the last N-m samples of the waveform corresponding to the last 3 of the 4 selected bits. The two waveform segments are guaranteed to dovetail together with no discontinuity when the handcrafting of the modulation waveshape over a chip period is carried out according to the methods described herein. Thus, the system calibration phase simply comprises determining the optimum contents of memory **2330** of FIG. **44** that best annul the spillover.

Several methods of generating the spillover cancellation waveforms have thus been described above and attention is now turned to how the spillover cancellation waveform memory contents are determined during the system calibration phase.

Upon power up initialization or system recalibration, a short time period is set aside during which the system is operated in such a way as to determine the spillover cancellation unit settings, such as memory contents, to be used until the next system calibration phase. In the calibration mode, the freedom exists to determine how many transmitters are operating, for example zero, one at a time or more, and what code or modulation they are transmitting with. For example, if the transmit waveform memories are loaded with an MSK waveform, a chip sequence can be transmitted that results in a CW signal being generated at +/−1/4 the chiprate from the carrier. By measuring the phase of the signal that emerges from the receiver ADC for a CW transmitted signal of +1/4 the chiprate above the carrier, and then 1/4 the chiprate below the carrier, the delay may be deduced from:

$$dT=d\phi/d\omega$$

By operating the transmitter at lower chiprates, thereby reducing successively by factors of two, the complete frequency response of the channel from a transmitter to a receiver output can be determined in frequency steps of one octave of frequency displacement from the carrier. The same method may be used to determine the frequency response from the input of the spillover cancellation DACs to the receiver output.

The modulation may also be chosen to be, for example, a short M-sequence, such as 1110010 repeated. This exhibits substantially all possible combinations of three and four consecutive bits, when +/−symmetry is also exploited. By observing the samples that come out of the receiver I and Q ADCs, it is now desired to choose the contents of the waveform memories **2330** in FIG. **44** or in FIG. **43** in order to reduce the loading of the ADC dynamic range as far as possible, that is, to reduce the maximum modulus of all I and Q values emerging from the receiver. Alternatively, the RMS value of the I,Q signals emerging from the receiver ADCs might be minimized. Thus, there is a process operating on the receiver ADC outputs that determines a figure of merit to be optimized and which will then indicate that best possible spillover cancellation has been achieved by spillover cancellation unit **2000**. Hereinafter, reference to “optimizing spillover cancellation” or achieving maximum spillover cancellation” shall mean choosing parameters of the recipe for the waveform(s) that achieve the best value of such a figure of merit.

An exemplary radar may be operated at a variety of chiprates from 2 GB/s downwards in steps of 2:1. For all chiprates, transmitter oversampling in one implementation is always 8 samples per I chip period and 8 samples per Q chip period, making the DAC sample rate 8 GB/s for 2 GB/s chip rate (1 GB/s on I and 1 GB/S on Q), and thus, the spillover cancellation memories and DACs logically operate at the same speed and with the same oversampling as the waveform generator of the transmitter signal desired to be cancelled. On the other hand, in this same implementation, the receiver I and Q ADCs always operate at 2 GB/s, giving only 2 samples per I chip and per Q chip at 2 GB/s chip rate, but more samples per chip at lower chip rates.

At 500 MB/s transmitter chip rate, the receive I,Q sample rate and the transmit I,Q sample rates become equal. At lower chiprates, the receiver sample rate may be downsampled by using a downsampling low-pass filter so that once again it is possible to conform the receiver I,Q sample rates to the transmitter I,Q sample rates. However, at higher than 500 MBs, there are fewer received samples available in the digital domain than transmit samples. Different optimization strategies for the spillover cancellation may be appropriate for different ratios of receiver sample rate to transmit sample rate. In one sub-implementation, it can be attempted to cancel all of these multiple samples per chip. There is only enough information to potentially do this when the receiver sample rate is commensurate with the transmitter sample rate. In a simpler sub-implementation, the multiple received samples per bit are reduced to one sample per bit by a downsampling filter. In this sub-implementation, it is only attempted to cancel the spillover interference effects on this final one sample, per bit.

The “recipe” for the spillover cancellation signal which annuls the spillover at the output of preamp stage **1111** may be determined partly by systematic means and partly by a brute force search during the initial power-up calibration phase.

It was explained above how the frequency response of the channel from the input to the spillover cancellation DACs to the receiver output can be determined. When, during the calibration phase, it is attempted to cancel the spillover from a single transmitter, a state of partial success may be reached in which there is a reduced, but still significant residual amounts of uncancelled spillover present at the output of the receiver. This can be distinguished from noise if necessary by correlating it with the transmitter signal. It is then desired to determine how to adjust the spillover cancellation signal to reduce the uncancelled spillover. This may be done by modifying the measured amount of uncancelled spillover using the inverse of the determined channel in order to determine the change needed to the spillover cancellation injection amount. For example, if the amount of uncancelled spillover has a complex correlation with the transmitted signal of Z, and the channel mid-band transmission factor from the spillover cancellation DAC input to the receiver output is the complex number H, then the cancellation signal stored in the waveform memory **2330** will be increased by a complex amount Z/H times the transmitted signal waveform. It can also be determined if the delay should be adjusted. If the residual uncancelled spillover signal is correlated with different time shifts of the transmitted signal, it can be determined whether the time delay of the cancellation injection signal should be advanced or delayed a little, or whether the residual belongs to one of the other spillover paths having different delays After the above method no longer achieves any further improvement, a brute force search can be made over the delay of the spillover cancellation signal for each path and its complex weighting coefficient. Finally, the optimum set of cancellation parameters (I.e., the recipe) is used to compute the contents of waveform memories **2330** of FIGS. **43** and **44**. In FIG. **43**, there is one memory, per path, for each transmitter, while in FIG. **44**, the waveforms for all three paths of one transmitter are combined into one memory **2330**.

It can also be decided to combine only two paths into one memory **2330** and to leave the third path separate. The latter is appropriate when two paths are very stable, namely the antenna-to-antenna coupling, and the on-chip coupling, while the third is mechanically less rigid, i.e., the bumper reflection. In the latter case, the complex coefficient for that path may be applied by a specific multiplier and updated more frequently, typically every 200-300 us while the radar is in normal operation, in order to dynamically track and reduce the spillover from that path.

The above method may be used after down-sampling the received signal to one sample per bit. The one sample per bit out of the receiver may be correlated with one sample per bit of the transmitted waveform over a long sequence. With a transmitter oversampling of 4 samples per bit, this gives four correlations, one for each sample phase. The highest correlation value indicates the delay in ¼ bit steps from transmitter to receiver.

On the other hand, as mentioned above, an attempt can be made to cancel the spillover at multiple received samples per bit when the number of received samples per bit from which spillover is to be cancelled is commensurate with the transmit oversampling factor. In this case, the received signal can be recorded at the exemplary transmit over sampling rate of 4 samples per bit during a calibration phase in which a short repetitive code is transmitted. Received samples corresponding to like patterns may be averaged over as many repeats as desired to average out noise and the average pattern of values analyzed to determine what the interfering waveform is at each receiver for each possible pattern of successive transmit chips. This waveform is a combination of all paths and may depend on four successive chips depending on the modulation used and the bumper reflection delay. Longer test codes can be used if necessary to cope with a wider spread of intersymbol interference (ISI). This process is known, in the communications field, as "channel estimation." Once the channel has been accurately estimated, it can be predicted what will be received, given what is to be transmitted. By operating each transmitter in turn, the waveforms for each transmitter as received at each receiver can be obtained in a very short period of time due to the elevated chip rate used. Determining what will be received for each possible pattern of bits transmitted accurately characterizes both linear and non-linear channels, and thus works for non-linear modulation.

In order to develop the spillover signal, it must be taken into account that the spillover has been observed after passing through blocks **1112** of FIG. **39** (which might include a bandwidth limitation), through down-convertors **1118**-A, **1118**-B, and through QLO **1117**, which will change the phase, and through filters **1116**-A and **1116**-B and variable gain amplifiers (VGAs) **1119**-A and **1119**-B, all of which may change the amplitude and phase of the spillover signal due to their respective gains and phase shifts. Thus, it is necessary to take account of the characteristics of the path from the point of injection of the spillover cancellation signal to the point after the ADCs **1115**-A, **1115**-B, where it is observed, and to pre-compensate the spillover cancellation signal for this signal path.

Characterizing the path from the spillover cancellation signal injection point between blocks **1111** and **1112** and the point of observation of the success or otherwise of the cancellation process after the ADCs **1115**-A, **1115**-B may be done during normal radar operation by use of the additional signal called "Channel Probe Signal" that enters the digital signal processing unit **2300** of FIG. **41**. This signal can be any known perturbation of the cancellation signal that can be distinguished from the transmitter signals, or indeed it can comprise a signal, the effect of which alone may be observed by turning ALL transmitters off. However, the channel can be more readily determined during the calibration phase by the other methods outlined above, such as by measuring the frequency response of the channel. The observed average residual spillover signal waveform at multiple samples per bit is now subjected to the inverse frequency response of the channel to determine how the spillover cancellation injection signal should be constructed.

In practice, the inverse frequency response of a bandpass channel may not be mathematically well-conditioned, so instead the combination of the three paths may be determined, which, when concatenated with the measured channel frequency response from the cancellation injection point to the receiver output, would match the received average spillover signal in a least-squares error sense.

The cancellation of spillover already in the analog domain before receiver digitization, as discussed herein, has purposely avoided receiver chain saturation or other non-linear effects. The amount of cancellation required for this is limited to the 20-30 dB level. However, to avoid reduction of radar sensitivity to small distant radar target echoes, a much larger degree of spillover cancellation is desired, on the order of 60-70 dB. The latter amount is to be achieved by more advanced digital signal processing. To avoid prejudicing the later achievement of the higher spillover cancellation figure, however, the approximate spillover cancellation signal developed herein will be added back in to the signal in the digital domain. The amount that will be added back in will be substantially exactly what was subtracted. Since it will be added back in after the receiver ADCs, it is also for this purpose necessary to know the channel between where the digital cancellation signal waveform was defined (i.e., at the output of memories **2330**) and where it will be added back in. In this case, the channel does not need to be inverted as it will applied in the forward direction.

FIG. **45** illustrates the elements of the radar involved in determining this forward channel. Each transmit bit stream addresses a respective waveform memory **2330** to produce digital I,Q signals. These are analog-to-digital converted to obtain analog signals, low-pass filtered, up-converted using a Gilbert cell modulator to obtain a cancellation current, and subtracted from the output current of LNA**1** **1111** to annul the spillover current and thus the voltage at that point. After further pre-amplification in LNA**2** **1112**, bandpass filtering in analog bandpass filter **1113**, down-converted in the I, Q downconverters **1118**, analog low pass filtering (**1116**) which is integrated with variable gain amplifiers **1119** and analog-to-digital converted in ADCs **1115**, the signal emerges once more in the digital domain. It may then be subjected to bit-rate matched filtering to down-sample the sample stream to one sample per bit using digital down-sampling filter **2101**, which can for example be a simple "boxcar" filter having a sin(x)/x frequency response. Within the spillover cancellation unit **2100**, a compare unit **2102** compares the digital I,Q samples out of the waveform memory **2330** with the one sample per bit digital samples out of down-sampling filter **2101** in the exemplary process, discussed below.

One sample per bit out of the multiple samples per bit from the memory **2330** is correlated with the one sample per bit out of the filter **2101** to determine a channel for that sample phase to the output. This is repeated for each transmitter sample phase. When the sub-streams represented by selecting one sample per bit of a particular transmitter sample phase are correlated, the determination of these channels is not independent. In this case, an auxiliary piece of hardware can be used to correlate the different shifts of the transmitter sample streams to obtain the autocorrelation matrix, the inverse of which is used to de-correlate the measured channel matrix. Alternatively, a simpler method is to load memory **2330** in the calibration phase with only one non-zero sample, e.g., unity, in one sample phase position only. The channel impulse response is then determined for that sample phase, then the non-zero sample is moved to a different sample phase and the channel impulse response determination repeated. In this way, a channel impulse response may be determined from each of the sample phases of the transmit spillover cancellation stream to the receiver output. This is then used as explained below.

In order to add back in exactly what was subtracted, the digital I,Q output values are subjected to the channel impulse responses determined above. Namely, sample no. 1 from each bit period is passed through the channel determined for the path sample 1 to receiver output in order to determine what effect it has had on the output to have subtracted that sample from the signal earlier in the chain. That amount is then to be added back in. This is repeated for sample 2 of each bit period, and so forth. A hardware structure that implements this is the bank of N (exemplary 4) FIR filters illustrated in FIG. **46**, one for each sample per bit period that is stored in memories **2330**.

In FIG. **46**, a first FIR filter **4000-1** processes a first I,Q sample selected from each bit period of the I,Q values fed to spillover cancellation DACs **2050**, of which, in an exemplary implementation corresponding to FIG. **42**, there is one pair per receiver. The first sample for a given bit period enters the first one of the delay memories **4003** on the left. Corresponding samples for previous bit periods are stored in the other memories **4003** from left to right. The value in each memory is multiplied by an associated one of the complex multipliers **4001** with a preloaded complex channel coefficient from the compare unit **2102** of FIG. **45**. The complex-weighted samples are then combined in the complex adder **4002** to provide the FIR output for that sample phase. This is repeated for each of the N sample phases per bit period at which the spillover cancellation signal is generated using FIR filters **4000-1** to **4000**-N. The N resulting outputs are then combined in the final adder **4900** to determine the one complex sample per bit value that will be added back in to the receive signal path. Thus, the 8-bit I samples and the 8-bit Q samples that are fed to spillover cancellation DACs **2050** at a rate of an exemplary 4 samples per bit are determined by the FIR filters of FIG. **46** to have resulted in a subtraction of a certain value from each of the 1-sample per bit receiver output values from filter **2101**, which value is promptly added back in digitally to cancel any imperfections of the analog spillover cancellation. The total, uncancelled spillover signal is thus restored in the digital domain after analog blocks that the uncancelled spillover signal may have saturated have been bypassed. Now the full spillover signal can be subjected to a more accurate cancellation algorithm in the digital domain.

Thus, it has been disclosed above how a digital FMCW radar may be built that transmits and receives at the same time using multiple transmitters and receivers. The outputs of n receivers of radio signals from each of m transmitters may be combined to yield the spatial resolution of an m×n antenna array. The key issue of CW radar, that of transmitting and receiving at the same time, is especially challenging when each receiver is interfered with by the sum of all transmitter signals spilling over due to local coupling and reflections. This is mitigated by the invention disclosed herein, which determines and subtracts at an early point in each receiver path the interfering signals from own transmitters to reduce the interference to the point where it does not overload any part of the receiver chain, in particular, analog-to-digital converters. Moreover, since analog interference subtraction is not as accurate as digital interference subtraction, substantially the exact same amount of spillover signal subtracted from each receiver in the analog domain is added back in to each receiver path after digitization where the word length can be increased to allow whatever headroom is necessary to encompass the interfering spillover signals. Other refinements include methods and circuits for the realization of very high sample rate ADCs and DACs and their calibration, DC offset subtraction, gain matching between I and Q channels and correction of quadrature phase errors. Any prior art method may be employed to construct suitable circuit blocks such as DACs, ADCs, memories, complex multipliers, and correlators, etc.

Changes and modifications in the specifically described embodiments can be carried out without departing from the principles of the invention, which is intended to be limited only by the scope of the appended claims, as interpreted according to the principles of patent law including the doctrine of equivalents.

The invention claimed is:

1. A radar system for a vehicle, the radar system comprising:

a plurality of transmitters configured for installation and use on a vehicle, wherein the transmitters are configured to transmit digitally modulated radio signals;

a plurality of receivers configured for installation and use on the vehicle;

wherein the transmitters and the receivers are configured to operate simultaneously in a same frequency spectrum during an operational period;

wherein a first receiver of the plurality of receivers receives at least one interfering signal due to local signal coupling from at least one transmitter of the plurality of transmitters, and wherein the local signal coupling comprises at least one interfering path or mechanism;

a spillover cancellation unit comprising a digital modulator configured to output a delayed, amplitude weighted, and phase changed replica of each of the at least one interfering signal transmitted by respective ones of the at least one transmitter of the plurality of transmitters as received through respective ones of the at least one interfering path or mechanism;

a combiner configured to combine into a signal path of the first receiver the delayed, amplitude weighted, and phase changed replica of each of the at least one interfering signal transmitted by respective ones of the at least one transmitter of the plurality of transmitters from which interference is to be suppressed to subtract the at least one interfering signal from the first receiver's signal path; and

wherein the first receiver receives the transmitted digitally modulated radio signal reflected from objects in the environment without saturating the signal path of the first receiver due to the subtraction of the at least one interfering signal from the first receiver's signal path.

2. The radar system of claim **1** further comprising a re-addition combiner configured to re-add into a later point of the first receiver's signal path a signal constructed that substantially adds back the interference which was subtracted earlier in the first receiver's signal path.

3. The radar system of claim **2**, wherein the re-addition combiner is configured to add the interference into the signal path in the digital domain so that spillover cancellation in the digital signal processing domain will remove the spillover components.

4. The radar system of claim **1**, wherein the digitally modulated radio signal is digitally frequency modulated with digital code sequences.

5. The radar system of claim **1** comprising one or more semiconductor chips attached to a printed circuit board comprising printed antennas and installed in the vehicle, the plurality of interfering paths comprising (i) an on-chip or chip-to-chip transmitter to receiver coupling path, (ii) a transmitter antenna to receiver antenna coupling path, and (iii) a reflective path that reflects a signal transmitted by a transmitter antenna from a nearby part of the vehicle to a receiver antenna.

6. The radar system of claim **1**, wherein the transmitters are configured to be digitally modulated by a bit stream by means of a first waveform memory addressed by bits of the bit stream, and wherein the modulator comprises a second waveform memory addressed with the same bits of the same bit stream, wherein the second waveform memory is configured to create the delayed, amplitude weighted, and phase changed replica of the transmitter signal corresponding to the interfering signal as received through the one of the plurality of interfering paths or mechanisms.

7. The radar system of claim **1**, wherein the combiner is located at a point in the receive signal path prior to a down-converter configured to down-convert the radar frequency to an intermediate frequency or to a complex (I,Q) baseband.

8. The radar system of claim **1**, wherein the digital modulator is a replica of a digital modulator of a particular transmitter from which interference is to be suppressed.

9. A continuous wave, multiple-input, multiple-output (MIMO) radar system for use on vehicle, the MIMO radar system comprising:

a plurality of receivers coupled to associated receive antennas;

a plurality of co-located transmitters coupled to associated transmit antennas, and configured to transmit radio signals on a programmable radio carrier frequency modulated with digital symbol sequences;

a spillover cancellation unit and associated first combiners configured to cancel interference from a signal path of each of the plurality of receivers due to local spillover from the plurality of transmitters;

wherein for each of the plurality of receivers, the spillover cancellation unit comprises a signal generator configured to produce a cancellation signal for each respective receiver of the plurality of receivers as defined in part by the digital symbol sequences; and

wherein the first combiners are configured to combine each spillover cancellation signal into the received signal path of each intended receiver, wherein the interference from the plurality of transmitters due to the local spillover is removed by subtraction, and wherein combining a spillover cancellation signal into a received signal path subtracts transmitter interference from the signal path.

10. The MIMO radar system of claim **9** further comprising second combiners associated with the spillover cancellation unit, wherein the second combiners are configured to combine back into the received signal path of each receiver, at a point after a down-converter and an analog-to-digital converter down-converts and digitizes the received signal, respectively, signals substantially equivalent to the signals subtracted by the first combiners.

11. The MIMO radar system of claim **9**, wherein the local spillover comprises components of different delays due to on-chip transmit-receive coupling, antenna-to-antenna transmit-receive coupling, and transmit-receive coupling due to reflections of transmitted signals from a nearby part of the radar system, and wherein the signal generator produces a spillover cancellation signal for each receiver approximating the sum of all of the components from all of the transmitters.

12. The MIMO radar system of claim **9**, wherein a bit rate of the digital symbol sequence bears a constant ratio to the carrier frequency, and wherein a back-end processor translates object echo delays measured in chips to object distances using the bit rate.

13. A method for preventing receivers of a continuous wave multiple-input, multiple-output (MIMO) radar system from being saturated by local spillover from transmitters of the MIMO radar system, the method comprising:

operating a plurality of receivers of the MIMO radar system during a system calibration phase with only one of a plurality of transmitters of the MIMO radar system operating at a time;

via monitoring an output signal of each receiver of the plurality of receivers, determining a recipe for each receiver for forming a cancellation signal based on knowledge of a modulation of the only one operating transmitter which, when the cancellation signal is combined with the received signal in the receive path, minimizes a determined output due to the only one operating transmitter;

via continued monitoring of the output signal of each receiver of the plurality of receivers, determining individual outputs due to each transmitter of the plurality of transmitters as each transmitter is operated in turn as the only operating transmitter to obtain recipes for forming a cancellation signal for each combination of a receiver and a transmitter; and

combining the recipes for all transmitters for a given receiver to form a cancellation signal generation recipe for the given receiver that will cancel the local spillover due to all transmitters at the given receiver when all transmitters are operated at once, and repeating for all receivers to determine a cancellation signal generation recipe for each receiver.

14. The method of claim **13**, wherein determining a recipe for each receiver for forming a cancellation signal based on knowledge of a modulation of the only one operating transmitter comprises determining the contents of at least one waveform memory to be addressed by a modulation bit stream of the only one operating transmitter that will produce the cancellation signal for any transmitter modulation bit sequence that is based upon the contents of the at least one waveform memory.

15. The method of claim **14**, wherein the local spillover comprises a plurality of independent spillover interference paths, and wherein the at least one waveform memory comprises a separate waveform memory for each independent spillover interference path of the plurality of independent spillover interference paths, the plurality of independent spillover interference paths comprising any or all of an on-chip transmitter to receiver coupling path, a transmit antenna to receive antenna coupling path, and a transmitter to receiver reflection path from a nearby radome or protective cover.

16. The method of claim **14**, wherein the at least one waveform memory comprises one waveform memory for each given transmitter that stores the sum of cancellation waveforms needed to cancel the spillover from the given transmitter to a given receiver through multiple spillover paths comprising any or all of an on-chip transmitter to receiver coupling path, a transmit antenna to receive antenna coupling path, and a transmitter to receiver reflection path from a nearby radome or protective cover.

17. The method of claim **14**, wherein the waveform memory stores cancellation signal samples at an oversampling factor of 4, 8, or 16 samples per modulating bit or chip period.

18. The method of claim **14**, wherein the waveform memory stores cancellation signal samples at an oversampling factor of 4, 8, or 16 samples per modulating bit or chip period, and wherein samples extracted at a given instant from the at least one memory associated with the given receiver are combined to obtain a composite sample value of a cancellation signal that will cancel spillover interference from all transmitters to the given receiver.

19. The method of claim **14**, wherein the waveform memory stores cancellation signal samples at an oversampling factor of 4, 8, or 16 samples per modulating bit or chip period, and wherein samples extracted at a given instant from the at least one memory associated with the given receiver are combined to obtain a composite sample value of a cancellation signal that will cancel spillover interference from all transmitters to the given receiver, and wherein successive ones of the composite sample are applied to a digital-to-analog converter to obtain a continuous, analog cancellation waveform for the given receiver.

20. The method of claim **14**, wherein the waveform memory stores cancellation signal samples at an oversampling factor of 4, 8 or 16 samples per modulating bit or chip period, wherein samples extracted at a given instant from the at least one memory associated with the given receiver are combined to obtain a composite sample value of a cancellation signal that will cancel spillover interference from all transmitters to the given receiver, wherein successive ones of the composite sample are applied to a digital-to-analog converter to obtain a continuous, analog cancellation waveform for the given receiver, and wherein the continuous waveform is combined with the analog signal output of a first RF preamplifier stage after the receive antenna such as to cancel the spillover interference before the spillover interference can saturate later preamplifier stages or other functions later in the receiver signal processing chain.

* * * * *